ACTA PROTOZOOLOGICA

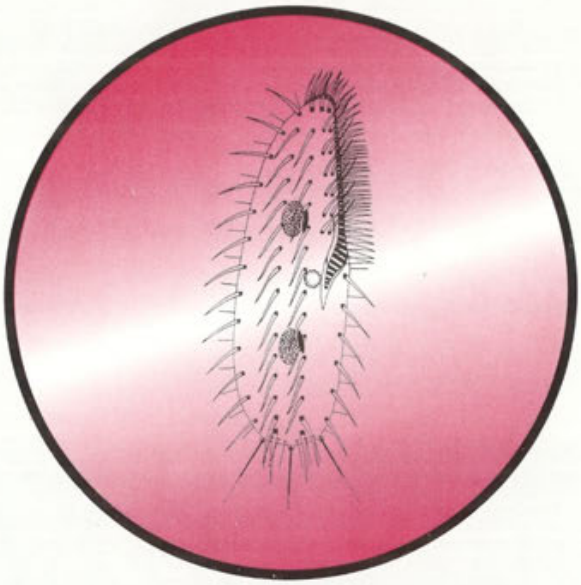

NENCKI INSTITUTE OF EXPERIMENTAL BIOLOGY
WARSAW, POLAND
1995
VOLUME 34 NUMBER 1
ISSN 0065-1583

Polish Academy of Sciences
Nencki Institute of Experimental Biology

ACTA PROTOZOOLOGICA

International Journal on Protistology

ACTA PROTOZOOLOGICA appears quarterly.

Printed at the MARBIS, 60 Kombatantów Str., 05-070 Sulejówek, Poland

Front cover: *Wallackia schiffmanni*. In : W. Foissner (1976) *Wallackia schiffmanni* nov. gen., nov. spec. (Ciliophora, Hypotrichida) ein alpiner hypotricher Ciliat. *Acta Protozool.* 15: 387-392

ACTA
PROTOZOOLOGICA

Acta Protozoologica (1995) 34: 1 - 11

Review article

Phototransduction in *Blepharisma* and *Stentor*

Stanisław FABCZAK and Hanna FABCZAK

Department of Cell Biology, Nencki Institute of Experimental Biology, Warszawa, Poland

Summary. The ciliates *Blepharisma* and *Stentor* exhibit distinct light-avoiding behavior (photophobic response). This cell behavior is attributed to photoexcitation of receptor chromoproteins located in cell organelles (pigment granules). The photochemical process in the receptors of both these ciliates, considered as a primary reaction to light, initiates the sensory transduction chain leading to delayed generation of membrane photoreceptor potential. The photoreceptor potential is coupled to the photophobic response (ciliary reversal) through an action potential which is elicited by receptor potential when its amplitude exceeds the membrane excitation threshold. The direct relationship between photoelectrical transduction and electromotor events is evidenced by a close temporal correlation observed in *Blepharisma* and *Stentor* between the latency periods of the action potential and of the cell stop response (receptor/action potentials appear to be instrumental in initiation of ciliary reversal). The photoreceptor potentials in *Blepharisma* are generated by transient changes in membrane conductance for Ca^{2+} ions. In *Stentor* the ionic nature of light-dependent membrane depolarization has not been fully elucidated. The action potentials in both *Blepharisma* and *Stentor* ciliates are produced by any suprathreshold depolarization, such as a photoreceptor potential, in the consequence of the Ca^{2+} channel and, after a delay, the K^+ channel activations.

Key words. Photoreceptor potential, action potential, photophobic response, *Blepharisma*, *Stentor*, sensory transduction.

INTRODUCTION

The pink *Blepharisma japonicum* and related blue-green *Stentor coeruleus* ciliates are known to respond to changes in environmental illumination. In an unevenly illuminated container these cells swim predominantly towards shady or darker areas, away from the light source (photodispersal) (Jennings 1906, Mast 1906, Giese 1973, Diehn et al. 1977). Both these protozoa display distinct sensitivity to light since, unlike most other ciliates, they possess specific pigments (photoreceptors) enclosed in membrane-vesicle granules of about 0.3-0.7 μm in diameter. The pigment granules are located in the vicinity of ciliary basal bodies, directly under the cell pellicle. They are distributed in regular pigmented rows, alternating with clear rows of kineties over the cell body surface (Huang and Pitelka 1957, Randall and Jackson 1958, Tartar 1961, Kennedy 1965, Giese 1973, Newman 1974). Spectrophotometric analysis of the pigment structure of *Stentor* cells showed that the pigment identified as stentorin belongs to *meso*-naphthodianthrone class of compounds (Lankester 1973, Moller 1962, Walker et al. 1979, Tao et al. 1994). The structure of the pigment in *Blepharisma*, called blepharismin, has not been fully elucidated yet. According to Sevenants (1965) blepharismin presumably is also a derivative of hypericin.

Address for correspondence: S. Fabczak, Department of Cell Biology, Nencki Institute of Experimental Biology, ul. Pasteura 3, PL-02-093 Warszawa, Poland; Fax: (4822) 225342; E-mail: sfabczak@plearn.edu.pl

Recent experiments on aqueous preparations of pigment granules from *Blepharisma* and *Stentor* provide some data indicating that the absorption of light energy by cellular pigments is accompanied by a release of H^+ ions and acidification of the solution (Walker et al. 1981, Matsuoka et al. 1992). The changes in the cytoplasm pH of intact *Stentor* cells under steady-state photic stimulation have also been shown to occur (Song 1981, Song et al. 1981). Based on these data, it has been proposed that the observed rapid proton release from the pigment into cell cytoplasm is an initial signal triggering the photosensory transduction chain which results in photodispersal of *Blepharisma* and *Stentor* cells (Song 1981, 1983; Passarelli et al. 1984; Ghetti 1991).

LIGHT-DEPENDENT MOTILE RESPONSES

Photophobic response

The photodispersal in *Blepharisma* and *Stentor* ciliates is a behavioral consequence of different specific light-avoiding responses such as negative phototaxis, positive photokinesis and step-up photophobic responses. The negative phototaxis is displayed by *Stentor* when a light beam is applied from a particular direction. On such illumination, the cells tend to turn and swim away from the light source in a direction parallel to the direction of light propagation, both in region where the beam is converging and were it is diverging (Song et al. 1980b). The mechanism of cell phototactic response has not been elucidated in detail but it is supposed to consist of a series of consecutive and rapid ciliary reversals (Song 1989). Both in *Blepharisma* and *Stentor* there is a distinct dependence of the velocity of their movement upon light intensity (photokinesis); the stronger is the intensity of illumination of the cells, the greater is the speed of their swimming (Kraml and Marwan 1983, Matsuoka 1983b, Iwatsuki 1991, Fabczak S. et al. 1993b). Moreover, in *Blepharisma*, the changes in body length in the order of 50% were reported upon steady-state illumination (Matsuoka 1983b, Matsuoka and Shigenaka 1985).

Most studies on behavioral photoresponses in *Blepharisma* and *Stentor* cells were devoted to the analysis of the motile response to the increase of light intensity in the environment (step-up photophobic response) (Wood 1975, 1976; Song et al. 1980a; Kraml and Marwan 1983; Matsuoka 1983a; Fabczak S. et al. 1993a, b). The step-up photophobic response consists of cessation of forward swimming of the cell (stop response) followed by a period of backward swimming (ciliary reversal) (Fig. 1). *Stentor* moves backwards in a more or less straight line (Figs. 1b,c) while *Blepharisma* mostly moves backwards along a semicircular pathway (Figs. 1e,f). After a period of ciliary reversal the cell stops its movement before resuming a forward movement. Between the onset of the applied light stimulus and the beginning of the cell stop response there is a lag-time the length of which is inversely proportional to the light intensity (Kraml and Marwan 1983; Scevoli et al. 1987; Iwatsuki and Kobayashi 1991; Fabczak S. et al. 1993a, b). The delay of response in *Stentor* cells is of 0.1-0.2 s (Wood 1976, Iwatsuki and Kobayashi 1991, Fabczak S. et al. 1993a), and in *Blepharisma* this delay is longer and is about 1 s (Kraml and Marwan 1983, Ghetti 1991, Fabczak S. et al. 1993b). The overall result of the photophobic response in *Blepharisma* and *Stentor* is the change of the forward movement direction and escape from the lighted area.

The sensitivity of the surface of the cell body to light in *Blepharisma* as well as in *Stentor* is not uniform. On light stimulation of different regions of *Blepharisma* body the photophobic response could be more readily elicited by illuminating the anterior part of the cell. Illumination of the posterior part of the cell did not evoke the photophobic response. In contrast, the acceleration of swimming (photokinetic response) was elicited to the same extent irrespective which part of the *Blepharisma* was subjected to illumination (Kraml and Marwan 1983, Matsuoka 1983b). A similar morphological difference has been reported in the ciliate *Stentor* where the anterior part of the cell is more sensitive to light stimulation than the posterior one (Wood and Martinelli 1990). These differences in responses, similarly as the recent spectroscopic evidence provided for *Stentor* (Iwatsuki 1991), suggest that the photoreceptors initiating the photophobic response are different from those inducing the photokinetic effect.

The ciliary reversal which is observed during the photophobic response is quite typical and can be evoked in many ciliates by a variety of stimuli. However, the overall photophobic response in *Blepharisma* and *Stentor* differs from their response, for instance, to a mechanical stimulus by the magnitude of the delay after which the ciliary reversal does appear. In *Blepharisma* and *Stentor*, similarly as in those ciliates which do not exhibit photoreception (e.g. *Paramecium*, *Stylonychia*), the ciliary reversal elicited by mechanical stimulation

Fig. 1. Pictures of *Stentor* (a,b) and *Blepharisma* (d,e) swimming in the dark (a,d) and exhibiting a phobic response (b,e) to light. Photophobic response in *Stentor* (c) and *Blepharisma* (f) consists of stop of forward movement with some delay (t_{CRL}), ciliary reversal period (t_{BSD}), stop of backward movement and resumption of forward swimming, in a new direction

appears as early as within a few milliseconds (Eckert et al. 1972; Peyer and Machemer 1978; Wood 1982, 1991; Fabczak S. 1992, unpublished results) whereas the delay of the light-evoked response is several times longer. Despite the same final response of the cells (ciliary reversal) to the different stimuli the evident difference in the latency period between the light-induced response and that evoked by a mechanical stimulus indicates that separate processes are involved in the photo- and mechanotransduction chains.

Action spectrum of photophobic response

The action spectrum determined in *Stentor* in relation to the amount of phobically responding cells has the peaks at 570 and 610 nm (Song 1989, Fabczak S. 1993a) (Fig. 2b). This action spectrum shows a close resemblance to the optical absorption spectrum of stentorin, of pigment extracted from *Stentor* (Kim et al. 1984). An analogous correlation was observed for *Blepharisma* cells between the action spectra for the photophobic responses (Fig. 3b) and the absorption spectrum of blepharismin (Gualtieri et al. 1989, Scevoli et al. 1987, Fabczak S. et al. 1993b). These data are consistent with the identification of blepharismin and stentorin as the photoreceptor which triggers the photophobic response of *Blepharisma* and *Stentor* cells, respectively (Song 1981; Ghetti 1991; Wood 1991; Fabczak S. et al. 1993a, b).

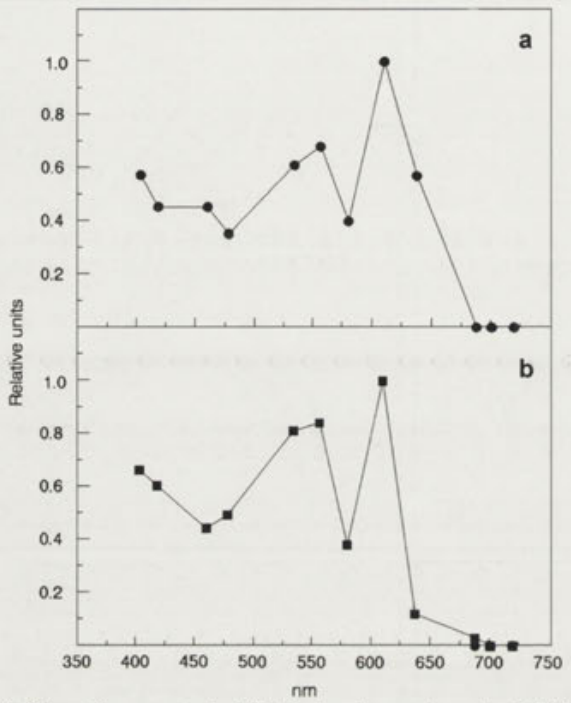

Fig. 2. The action spectra for light-induced receptor potential (a) and step-up photophobic response (b) in *Stentor* cell. The spectra display the same maxima at 610 and 570 nm

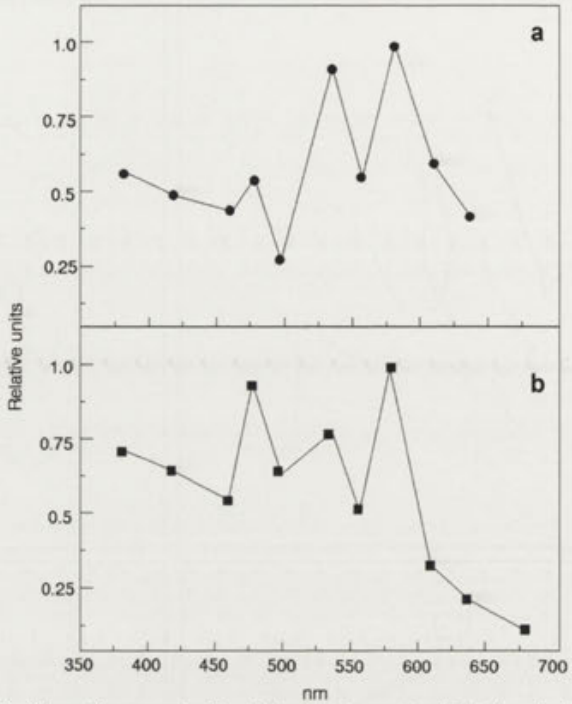

Fig. 3. The action spectra for photoreceptor potential (a) and phobic response to light stimulation (b) in *Blepharisma* ciliates. The spectra show the maxima at 460, 530 and 580 nm

Modification of photophobic responses by external agents

Whereas the involvement of blepharismin and stentorin as photoreceptor pigments in the photophobic response seems to be well established, at present the signal transduction scheme in both *Blepharisma* and *Stentor* cells are incompletely known. In a series of studies it has been demonstrated that Ca^{2+} channel-blockers including ruthenium red, pimozide, diltiazem, or La^{3+} ions specifically reduce the photophobic response and prolong the delay of the cell stop response without affecting significantly the swimming pattern of the cells unstimulated by light (Song 1983, Kim et al. 1984, Prusti at al. 1984, Fabczak S. et al. 1994a). Low concentrations of external Ca^{2+} ions (Fig. 4) or increased level of K^+ ions in the external solutions inhibit the light-dependent response as well (Colombetti et al. 1982, Iwatsuki and Song 1989, Fabczak S. et al. 1994a). In contrast, both caffeine and phosphatidic acid enhance the photophobic response and shorten the stop response time (Kim et al. 1984, Prusti et al. 1984). Thus, in *Blepharisma* and *Stentor* ciliates, as in a variety of other ciliates, the ciliary reversal that ends the signal transduction chain seems to be promoted by increasing the intracellular concentration of Ca^{2+} ions (Song 1981, Ghetti 1991).

Moreover, protonophores such as FCCP, CCCP and $TPMP^+$ inhibits strongly the photoresponses in both ciliates (Song et al. 1980a; Song 1981, 1989; Passarelli et al. 1984; Fabczak H. et al. 1993a). Thus the results seem to confirm the earlier suggestion that deprotonation of the pigment is the initial step of cell transduction of the light signal leading to the photophobic response (Passarelli et al. 1984; Song 1981; Ghetti 1991; Fabczak S. et al. 1993a, b).

According to the recent experiments, the cyclic GMP nucleotide seems to be involved in the photophobic response of *Stentor*. Light stimulation, as it has been demonstrated, induce a transient decrease in the level of cytoplasmic cGMP in the cell (Fabczak H. et al. 1994). Furthermore, the incubation of the *Blepharisma* and *Stentor* cells in solutions containing 8-bromo-cGMP, a membrane permeating analog of cGMP, or IBMX, a cGMP phosphodiesterase inhibitor, that is the agents raising the concentration of intracellular cGMP, inhibit significantly the photophobic response (Fabczak H. et al. 1993b,c). These findings, together with the demonstrated existence of a protein homologous to transducin, suggest that the changes of cGMP level in cell cytoplasm during illumination might be regulated with participation, at least in *Stentor* cells, of G-protein, that is in a way analogous to light signal transduction in

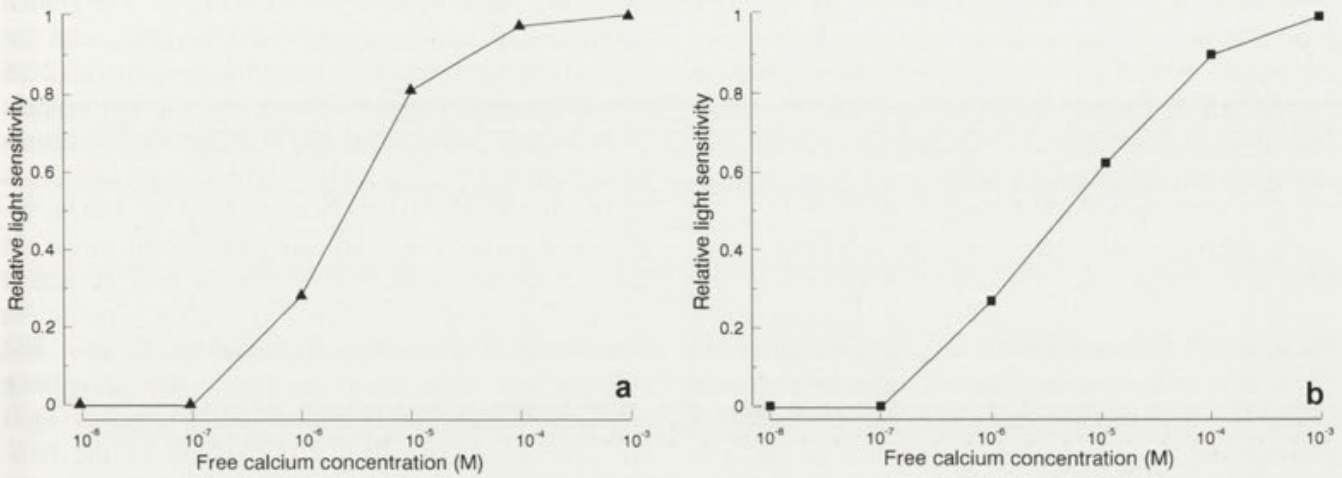

Fig. 4. Inhibition of phobic response in *Stentor* (a) and *Blepharisma* (b) cells to constant light stimulation by decreasing external free Ca^{2+} ion concentration

photoreceptor cells of higher organisms (Rayer et al. 1990, Yarfitz and Hurley 1994).

PHOTOELECTRICAL MEMBRANE RESPONSES

Resting, receptor and action potentials

In the first attempts at studying the electrical changes occurring in protozoan cell membranes in the course of the photophobic response, *Stentor* cells were used. The internal recordings were performed with the conventional glass microelectrodes introduced into the large vacuole containing cannibalized another *Stentor* cell (Wood 1975, 1976). The intense regenerative processes which occur in the cell cause a rapid loss of contact of the electrode tip with the cytoplasm and deform to a significant extent, or even preclude, the recording of membrane potential in these cells. These intravacuolar recordings from cells in swimming form (pear-shaped) demonstrated generation of a depolarizing membrane response upon a photic stimulation (receptor and regenerative potentials). Since the initial deflection and the peak of the receptor potential are surmounted by the regenerative response, it was rather difficult to achieve temporal quantification of the receptor potential. The long lasting stimulus of high intensity applied to the extended sessile form of the cell could evoke a positive-going irregular receptor potential triggering an action potential and cell body contraction (Wood 1976).

The resting membrane potentials were also measured in *Blepharisma* cells but the accuracy of these measurements was insufficient due to same reasons as in the case of *Stentor* cells. In fact, they were even less reliable because of cytoplasm vacuolization during the measurement (Colombetti et al. 1987). To overcome these difficulties with membrane potential recordings some attempts were made to estimate the membrane potential in *Blepharisma* indirectly, on the basis of distribution of tetraphenylphosphonium ions (TPP^+) across the cell membrane (Ishida et al. 1990). TPP^+ ions readily penetrate the membrane and their distribution follows the Nernst equation (Kamo et al. 1979). Changes in the level of this cation in the medium were measured with the external TPP^+-sensitive electrode. This method, however, proved to be inadequate for studying protozoan cells. The value of the resting potential of the *Blepharisma* cell membrane calculated from such experiments (about -140 mV) was markedly overestimated and the recorded changes seem to be too slow. As it follows from conventional electrophysiological measurements, the resting membrane potential in *Blepharisma* does not exceed, under typical experimental conditions, -60 mV (Fabczak S. 1990; Fabczak S. et al. 1993b, 1994b).

Satisfactory recordings of the light-induced changes in the membrane potential in both protozoan organisms, *Blepharisma* and *Stentor*, have been only recently obtained by taking advantage of intracellular microelectrodes introduced directly into cell cytoplasm (Fabczak S. et al. 1993a, b, 1994b). It was possible to obtain reproducible recordings this case because the recording chamber containing the cells was cooled and/or a calcium-chelating agent like EGTA or EDTA was added to the microelectrode-filling solution. Such procedures fully prevented the tip of the penetrating

microelectrode from encapsulation within the cell. Moreover, at lower temperature the cell motile responses are greatly slowed down which significantly facilitates microscope observations or cell video recordings. Successful membrane potential measurements were also attained when the recording microelectrode tip was exposed to mechanical microvibration (buzz).

By applying these methodical improvements it has been demonstrated that the ciliates *Blepharisma* and *Stentor*, under standard conditions (culture medium, pH 7; 8-12°C), have a similar resting potential of -45 to -55 mV. An increase in the light intensity evokes in swimming *Blepharisma* and pear-shaped *Stentor* a transient depolarization of the membrane, i.e. the cells generate a photoreceptor potential (Fig. 5). The graded amplitude of the receptor potential increases with the intensity of the stimulus to a maximum value of 12-25 mV. The potential appears after a lag time with respect to the onset of stimulation and is, under the conditions studied, about 0.5-0.7 s (10°C) for *Stentor* and 2-5 s (12°C) for *Blepharisma* (Fabczak S. et al. 1993a, b). The receptor potential exceeding the electric threshold for membrane excitation, evokes a typical action potential of all-or-none type. The latency period in generation of the action potential in *Stentor* and *Blepharisma* cells decreases with the increasing stimulus intensity. When a short-lasting stimulus (light pulse) is applied to cells of either protozoan, the dura-

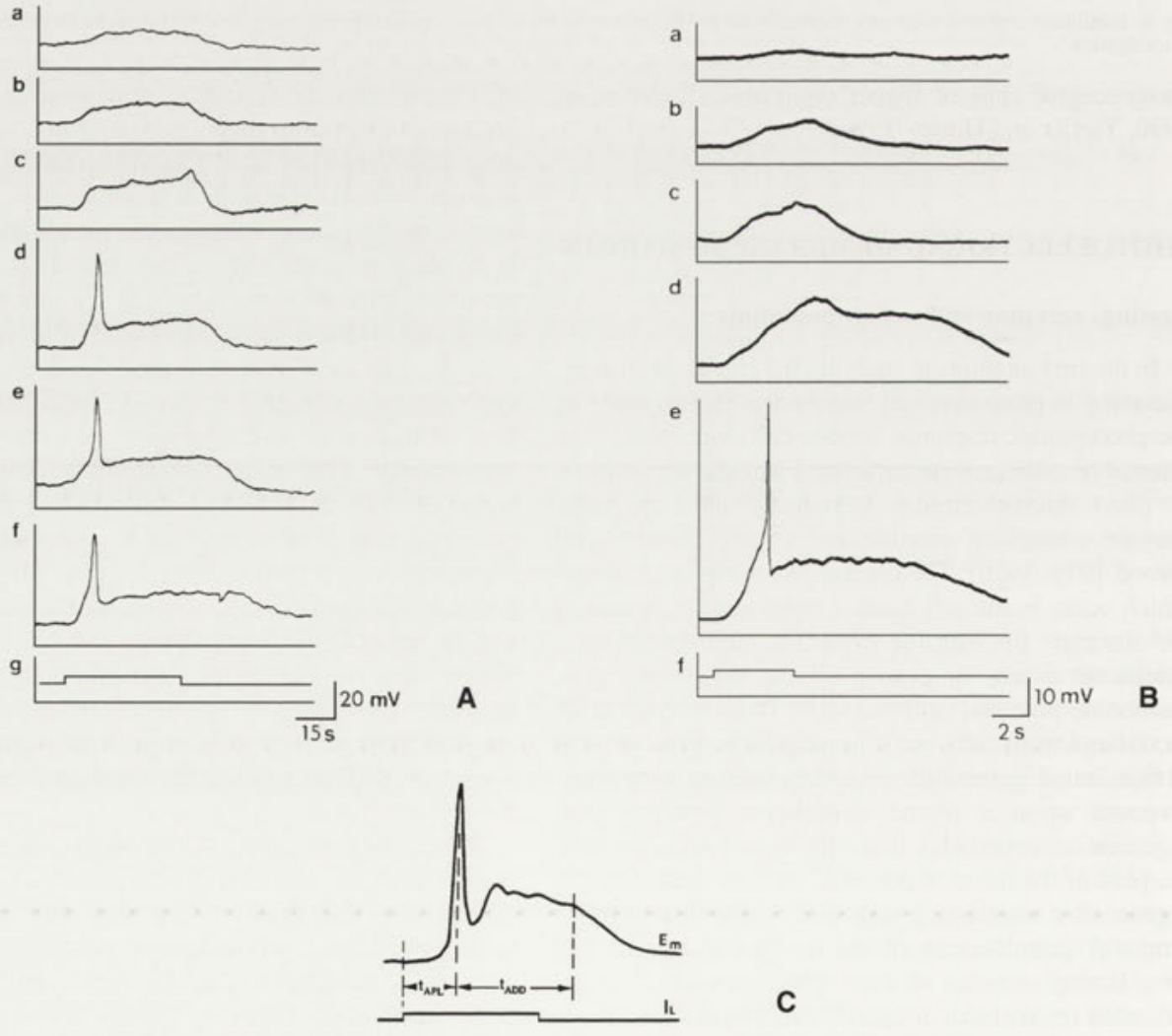

Fig. 5. Examples of transient membrane depolarizations in *Blepharisma* (A) and *Stentor* (B) cells to photic stimulation. (A) graded receptor potentials alone (a-c) and surmounted by action potentials (d-f) in response to 556 nm light pulses of following intensity (in 10^{18} photons m^{-2} s^{-1}) of (a) 1.4, (b) 2.1, (c) 3.6, (d) 6.7, (e) 10.4, (f) 15.4 and (g) 45 s duration; (B) receptor potentials (a-d) and receptor potential superimposed upon action potential (e) in response to 610 nm light pulses of intensities (in 10^{18} photons $m^{-2}s^{-1}$) of (a) 0.3, (b) 0.7, (c) 1.1, (d) 1.7, (e) 3.2 and (f) 4 s duration; (C) schematic illustration of receptor potential superimposed upon action potential (E_m) elicited by light pulse (I_L): t_{APL}- represents latency of action potential generation; t_{ADD}- duration of after-peak depolarization

tion of the receptor potential is short as well and generation of an action potential is followed by rapid repolarization to the level of the resting potential. The stimuli acting for a longer time elicit a prolonged receptor potential and the action potential in this case is followed by long-lasting depolarization of the membrane (after-peak depolarization). The delayed depolarization seems to represent, as it follows from a comparison of membrane responses including the receptor potential alone and the photic receptor potential superimposed upon action potential, a persisting photoreceptor potential (Fabczak S. et al. 1993a, b). The electrical responses of the membrane to stimulation of cells with constant light are similar to those observed with long-lasting stimuli; however, the amplitude of the receptor potential or after-peak depolarization decreased with time (Fabczak S. et al. 1993b). This finding is probably related to the cell adaptation to light, as it has also been observed for vertebrate and invertebrate photoreceptor cells (Rayer et al. 1990).

Action spectrum of receptor potential

The action spectra determined in *Blepharisma* and *Stentor* cells for the receptor potential at fluence rates of the same order as those effective around 600 nm, show a close similarity to that of the photophobic response. In *Stentor* spectra there is a sharp and highest peak at approximately 610 nm followed by distinct decrease at longer wavelengths. Another smaller peak is at 570 nm and a marked increase below 520 nm (Fig. 2a). Like the action spectrum for the photophobic response in *Blepharisma* cells, the action spectrum for the receptor potential has three marked peaks, at 460, 530 and 580 nm (Fig. 3a).

Ionic specificity of photoelectrical responses

In earlier experiments on a photophobic behavior in *Blepharisma* and *Stentor* cells it has been demonstrated that their responses can be significantly modified by changes in the level of some ions in the external solution, including K^+ and Ca^{2+} ions (Colombetti el al. 1982, Fabczak S. et al. 1994b). This indicates that motile responses to light stimuli in these cells, like in some other ciliates, may arise from changes in membrane potentials. To verify this supposition, electrophysiological experiments with the use of the ion substitution method were undertaken.

The recent microelectrode recordings in *Blepharisma* show that the membrane potential undergoes

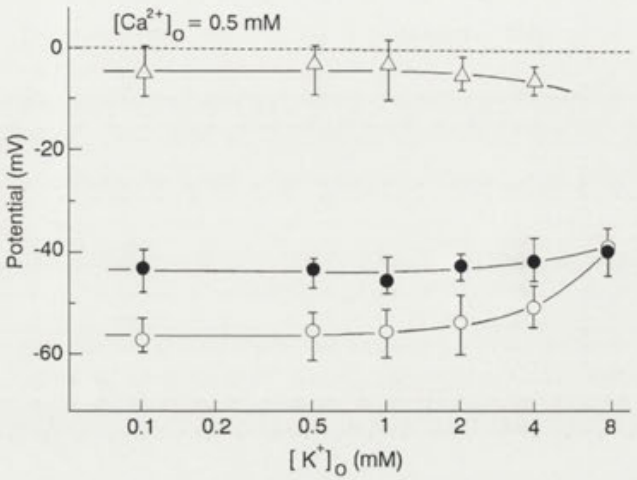

Fig. 6. Resting (open circles), receptor (black circles) and action potentials (triangles) as a functions of external potassium concentrations at a constant external Ca^{2+} concentration of 0.5 mM. The generation of action potential at 8 mM of K^+ or higher concentrations is inhibited

depolarization when the level of K^+ ions, at a constant content of other ions in external solution, is increased to 2 mM or more (Fabczak S. et al. 1994b,c) (Fig. 6). A similar depolarization of the membrane occurs in *Stentor* cells when the extracellular K^+ concentration becomes increased (Wood 1982). This depolarizing influence of K^+ ions is especially evident at higher concentrations of these ions in medium. At external K^+ concentration higher than 4 mM the membrane potential is shifted by about 54 mV when the level of K^+ is changed by one order of magnitude, i.e. the potential changes closely approach the theoretical value predicted by the Nernst equation (about 55 mV/10-fold change at the temperature of 10-12° C used in these recordings). The dependence of the membrane potential on K^+ concentration is not linear over the whole range of concentrations tested. At K^+ concentration of 0.5 mM or lower the membrane potential is almost independent of external K^+ level. This testifies to a considerable membrane permeability of the resting *Blepharisma* and *Stentor* cells also to other ions present in the medium. These observations have been confirmed by marked membrane depolarization, both in *Blepharisma* and *Stentor* cells, produced by an increase in concentration of external Ca^{2+} (Fig. 7). Chloride ions present in the medium do not seem to exert any detectable effect on membrane potential as on substituting NO_3- ion for Cl^-, or on addition of choline chloride to solution, no changes of the potential were observed (Wood 1982; Fabczak S. et al. 1994b, c).

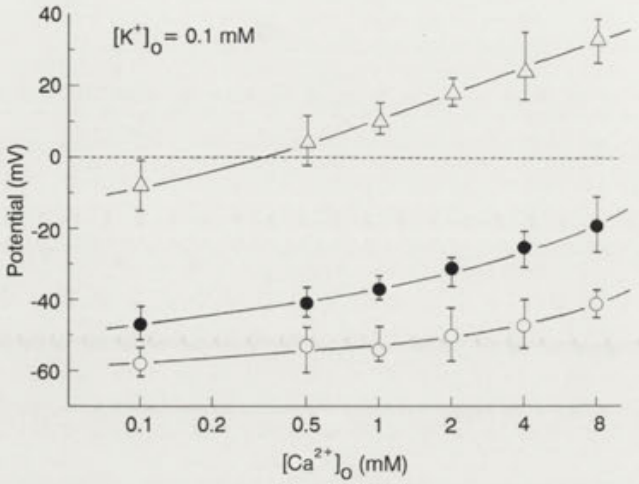

Fig. 7. Resting (open circles), receptor (black circles) and action (triangles) potentials as a function of concentration of external calcium ions at constant level of external K^+ concentration (0.1 mM)

The light stimuli of a higher intensity induce in both ciliates besides a receptor potential also an action potential the amplitude of which in standard experimental conditions is 50 to 55 mV (Fig. 6 and 7). The time duration of action potential in *Blepharisma* and *Stentor* differs substantially. *Stentor* ciliates represent "fast" organisms as the increasing phase of action potential is completed in about 0.3 s (Fabczak S. et al. 1993a, 1994b), while in *Blepharisma* the depolarizing phase lasts longer, from 2 to 2.5 s (Fabczak S. et al. 1993b). In *Stentor* the peak of action potential is influenced by changes in concentration of extracellular Ca^{2+} ions more than by those of K^+ ions (Wood 1982). However, the estimated slope of this dependence is about 12 mV/10-fold change in Ca^{2+} concentration between 0.1 and 2.5 mM and steeper at higher concentrations. The dependence of the peak of action potential in the related *Blepharisma* is higher; a 10-fold change in extracellular Ca^{2+} concentration elicits the shift in membrane peak potential by about 28 mV (Fabczak S. et al. 1994b). Photostimulation of the cells when the medium contained K^+ ions at 8 mM or higher concentration, did not elicit any action potential although the receptor potential continued to be evoked. The action potential does not appear under those conditions presumably due to high depolarization of the cell membrane which increases membrane permeability to K^+ ions and inactivates the mechanism responsible for generation of the action potential (Wood 1982, Fabczak S. et al. 1994b). These observations probably explain the reported inhibitory effect of high K^+ ion level on the photophobic response in *Stentor* (Colombetti et al. 1982).

The data obtained from direct measurements of ion fluxes across cellular membranes in *Stentor* cells under conditions of voltage-clamp, show that the depolarizing phase of the action potential is generated mainly by Ca^{2+} ion influx into the cell, whereas the delayed efflux of K^+ ions is responsible for the cell membrane repolarization (Wood 1982). The measurements of ion fluxes in the *Blepharisma* membrane during generation of the action potential gave results identical to those observed in *Stentor* (Fabczak S. 1993, unpublished results).

Stimulation of *Blepharisma* or *Stentor* cells with light pulses of a moderate intensity results in generation of a depolarizing receptor potential alone. In cells of *Blepharisma* the receptor potential is dependent, like the action potential, on the level of Ca^{2+} ions in the medium, although its dependence is lower, since the peak of receptor potential at Ca^{2+} concentration higher then 2 mM is altered only by 20-22 mV on changing Ca^{2+} concentration by one order of magnitude (Fabczak S. et al. 1994b,c). Changes in the level of other ions, e.g. K^+ or Cl^- in the external solution have no significant effect on the receptor potential peak. A depolarization of the membrane potential of *Blepharisma*, due to current injection, decreases the amplitude of the receptor potential produced by the light stimulus, whereas hyperpolarization increases the amplitude. These observations suggest that the receptor potentials in *Blepharisma* elicited by increase in light intensity are generated primarily by a transient increase in the membrane conductance for Ca^{2+} ions, similarly to the receptor potential in *Paramecium* which appears in response to mechanical stimulation of the anterior part of the cell (Eckert et al. 1972). The reversal of polarity of the receptor potential is not observed on membrane depolarization, presumably because a micromolar level of free Ca^{2+} in cell cytoplasm prevents efflux of these ions from the cell, irrespective of increased membrane conductance for Ca^{2+} (Fabczak S. et al. 1994b). The involvement of the membrane permeability to Na^+ or K^+ ions in the receptor potential changes can be excluded, since the intracellular concentrations of these ions are greater than their level in external solution, and the electrochemical equilibrium potential for Na^+ or K^+ ion is negative and below the resting membrane potential under the experimental conditions used (Hilden 1970, Fabczak S. 1990, Fabczak S. et al. 1994b).

Among other ciliate protozoa, similar depolarizing responses of membrane to light stimulation have been

reported for chlorella-free *Paramecium bursaria* only (Nakaoka et al. 1987). The photoreceptor potential in these cells is exclusively caused, as in the case of *Blepharisma* ciliates, by a transient increase in the membrane conductance to Ca^{2+} ions. In a variety of vertebrate photoreceptor cells, the hyperpolarizing receptor potential results mainly from the inhibition of the influx of Na^+ and Ca^{2+} ions by light (Detwiler and Gray Keller 1992, Lagnado and Baylor 1992). Light stimulation of the photoreceptors in invertebrate, similarly as in protozoan ciliate cell, depolarizes the plasma membrane (Rayer et al. 1990).

It is difficult, on the basis of the existing data, to define the nature of the photoreceptor potential in *Stentor* cells. Some reports show that photostimulation in these cells generates a current directed towards the interior of the cells, maximally of the order of 1 nA, whereas mechanical stimulation, for comparison, generated a current of as much as 40 nA. Such a low current intensity observed on photoreception cannot explain the rather high value of the photoreceptor potential observed. Thus it seems reasonable to suggest that the light-induced receptor potential can be generated *via* stimulation of an active ion-transport mechanism. This mechanism would consist in the exchange of one H^+ ion released during chromophore activation for one Ca^{2+} ion derived from the environment. Such ion fluxes would generate a resultant ion current directed towards the interior of the cell, and lead thereby to depolarization of the cell membrane (Wood 1991). Further detailed studies which would provide more experimental data are needed to elucidate the process of photoreceptor potential generation in *Stentor* cells.

SENSORY TRANSDUCTION AND ELECTROMOTOR COUPLING

Analysis of the time-course of the photophobic response in the *Stentor* and *Blepharisma* cells studied at the same experimental conditions at which electrophysiological experiments were performed, permitted to demonstrate a close relationship between generation of the action potential and ciliary beat reversal. It appears that the delay in generation of the action potential, and the latency period of the cell stop movement are similar; both the latency of an action potential and cell stop response decreases in the same manner with the increase in stimulus intensity (Fabczak S. et al. 1993a, b). The coupling between action potential generation and cell movement is evident also when the internal recordings were made on a *Blepharisma* cell with one recording microelectrode (i.e. without the use of a second stimulating electrode or suction micropipette), and the cell had the possibility of performing partial rotations around the microelectrode. Simultaneous videorecording of the cell behavior under such conditions revealed that the onset of the cell movement (ciliary reversal) was initiated at the end of the depolarization phase of an action potential (Fabczak S. et al. 1994b). Thus in both ciliates, *Stentor* and *Blepharisma*, there exists the same relationship between the membrane potential changes and the cell motile response elicited by light stimulation as reported for other ciliates (Machemer and Dietmer 1985).

CONCLUDING REMARKS

The transduction of light signals in the ciliates *Blepharisma* and *Stentor* initiated by cell photoreceptor activation leads, like in the photoreceptor cells of invertebrates, to a transient membrane depolarization, that is to generation of the receptor potential. The step-up photophobic response occurs only when resultant amplitude of the receptor potential triggers the action potential which in turn elicits the ciliary reversal. The cells exposed to light stimulation eliciting the receptor potential alone, i.e. without an action potential, display distinct acceleration of the forward movement, i.e. under these conditions the photokinetic effect is observed (Fabczak S. et al. 1993a).

On the basis of the presented results and other literature data it can be assumed that the light signal transduction, in the ciliates studied, proceeds in the following way:

(1) light absorption by photoreceptor molecules contained in the cell pigment granules leads to a rapid photochemical process within the chromophore (photoexcitation);

(2) the photoexcited chromophore triggers some time-consuming biochemical process with participation, at least in *Stentor*, of G-protein (the duration of which corresponds to the delay in generation of the receptor potential);

(3) this leads to generation of the receptor potential as a result of:

(a) in *Blepharisma*, transient increase of the cell membrane permeability to Ca^{2+} ions,

(b) in *Stentor*, transient activation of the ion exchange mechanism (e.g. of H^+ for Ca^{2+});

(4) the receptor potential, when its amplitude is sufficiently large, elicits the typical calcium response (an action potential);

(5) the increase of Ca^{2+} concentration within the cytoplasmic or intraciliary spaces is accompanied by ciliary reversal;

(6) this is followed by a subsequent stop of the cell backing and renewal of ciliary beating (the cell swims forward again in a new direction).

The above-presented scheme of the phototransduction process in the protozoa studied, although it is much simplified due to scarcity of relevant experimental data, seems nevertheless to form a useful basis for further detailed investigations.

REFERENCES

Colombetti G., Lenci F., Song P.-S. (1982) Effect of K^+ and Ca^{2+} ions on motility and photosensory responses of *Stentor coeruleus*. *Photochem. Photobiol.* **36**: 609-611

Colombetti G., Fiore L., Santangelo G., Spedale N. (1987) Photosensitivity of a ciliated protozoan. Abstr. 6th European Conf. Ciliate Biology, Denmark, 32

Detwiler P. B., Gray Keller M. P. (1992) Some unresolved issues in the physiology and biochemistry of phototransduction. *Curr. Opin. Neur.* **2:** 433-438

Diehn B., Feinleib M. E., Haupt W., Hildebrand E., Lenci F., Nultsch W. (1977) Terminology of behavioral responses of motile organisms. *Photochem. Photobiol.* **26:** 559-560

Eckert R., Naitoh Y., Friedman K. (1972) Sensory mechanism in *Paramecium*. I. Two components of the electric response to mechanical stimulation of the anterior surface. *J. Exp. Biol.* **561:** 683-694

Fabczak H., Fabczak S., Song P.-S., Checcucci G., Ghetti F., Lenci F. (1993a) Photosensory transduction in ciliate: The role of intracellular pH and comparison between *Stentor coeruleus* and *Blepharisma japonicum*. *J Photochem. Photobiol.* **21:** 47-52

Fabczak H., Park P. B., Fabczak S., Song P.-S. (1993b) Photosensory transduction in ciliates. II. Possible role of G-protein and cGMP in *Stentor coeruleus*. *Photochem. Photobiol.* **57:** 702-706

Fabczak H., Tao N., Fabczak S., Song P.-S. (1993c) Photosensory transduction in ciliates. IV. Modulation of the photomovement response of *Blepharisma japonicum* by cGMP. *Photochem. Photobiol.* **57:** 889-892

Fabczak H., Walerczyk M., Fabczak S., Song P.-S. (1994) Light-induced changes of cGMP in *Stentor* cells. *Cell Biol. Int.* **18:** 445

Fabczak S. (1990) Free potassium and membrane potentials in cells of *Blepharisma japonicum*. *Acta Protozool.* **29:** 179-185

Fabczak S., Fabczak H., Tao N., Song P.-S. (1993a) Photosensory transduction in ciliates. I. An analysis of light-induced electrical and motile responses in *Stentor coeruleus*. *Photochem. Photobiol.* **57:** 696-701

Fabczak S., Fabczak H., Song P.-S. (1993b) Photosensory transduction in ciliates. II. The temporal relation between membrane potentials and photomotile responses in *Blepharisma japonicum*. *Photochem. Photobiol.* **57:** 872-876

Fabczak S., Fabczak H., Song P.-S. (1994a) Ca^{2+} ions mediate the photophobic response in *Blepharisma* and *Stentor*. *Acta Protozol.* **33:** 93-100

Fabczak S., Fabczak H., Song P.-S. (1994b) Photoreceptor and action potentials in *Blepharisma japonicum*. *J. Photochem. Photobiol.* (in press)

Fabczak S, Fabczak H., Song P.-S. (1994c) Ca^{2+} mediate the photoresponses of *Blepharisma* cells. *Cell Biol. Int.* **18:** 409

Ghetti F. (1991) Photoreception and photomovements in *Blepharisma japonicum*. In: Biophysics of Photoreceptors and Photomovements in Microorganisms. (Ed. F. Lenci et al.), Plenum Press, New York 257-265

Giese A.C. (1973) The biology of a light-sensitive Protozoan. Stanford University Press, Stanford

Gualtieri P., Passarelli V., Barsanti L. (1989) *In vivo* microspectrophotometric investigation of *Blepharisma japonicum*. *J. Photochem. Photobiol.* B. **3:** 379-383

Hilden S. (1970) Sodium and potassium levels in *Blepharisma intermedium*. *Exp. Cell Res.* **61:** 246-254

Huang B., Pitelka D.R. (1957) The contractile process in the ciliate *Stentor coeruleus*. I. The role of microtubules and filaments. *J. Cell. Biol.* **57:** 704-728

Ishida M., Utsumi K., Suzaki T., Shigenaka Y. (1990) Studies on the mechanism of cell elongation in *Blepharisma japonicum*. II: Changes of the membrane potential measured by an electrode sensitive to tetraphenyl phosphonium. *Cell Struct. Funct.* **15:** 251-256

Iwatsuki K. (1991) *Stentor coeruleus* shows positive photokinesis. *Photochem. Photobiol.* **55:** 469-471

Iwatsuki K., Kobayashi Y. (1991) The latency of the photophobic response in *Stentor coeruleus* depends upon the ratio of extracellular Ca to K ions. *Comp. Biochem. Physiol.* **100:** 101-106

Iwatsuki K., Song P.-S. (1989) The ratio of extracellular Ca^{2+} to K^+ ions affects the photoresponses in *Stentor coeruleus*. *Comp. Biochem. Physiol.* **92A:** 101-106

Jennings H. (1906) Contributions to the Study of the Behavior of Lower Organisms. Reactions to light in ciliates and flagellates. Carnegie Inst. Washington, 31-48

Kamo M., Muratsugu M., Hongoh R., Kobatake Y. (1979) Membrane potential of mitochondria measured with an electrode sensitive to tetraphenyl phosphonium and relationship between proton electrochemical potential and phosphorylation potential in steady state. *J. Membrane Biol.* **49:** 105-121

Kennedy J. R. (1965) The morphology of *Blepharisma undulans* Stein. *J. Protozool.* **12:** 542-561

Kim I.-H., Prusti R. K., Song P.-S., Häder D.-P. (1984) Phototaxis and photophobic responses in *Stentor coeruleus*: Action spectrum and role of Ca^{2+} fluxes. *Biochim. Biophys. Acta* **799:** 298-304

Kraml M., Marwan W. (1983) Photomovement responses of the heterotrichous ciliate *Blepharisma japonicum*. *Photochem. Photobiol.* **37:** 313-319

Lagnado L., Baylor D. (1992) Signal flow in visual transduction. *Neuron* **8:** 995-1002

Lankester E. R. (1973) Blue stentorin, the coloring matter of *Stentor coeruleus*. *Quart. J. Microsc. Sci.* **13:** 139-142

Machemer H., Deitmer J. W. (1985) Mechanoreception in ciliates. *Progr. in Sensory Physiol.* **5:** 81-118

Mast S. O. (1906) Light reactions in lower organisms. I. *Stentor coeruleus*. *J. Exp. Biol.* **3:** 359-399

Matsuoka T. (1983a) Distribution of photoreceptors inducing ciliary reversal and swimming acceleration in *Blepharisma japonicum*. *J. Exp. Zool.* **225:** 337-340

Matsuoka T. (1983b) Negative phototaxis in *Blepharisma japonicum*. *J. Protozool.* **30:** 409-414

Matsuoka T., Shigenaka Y. (1985) Mechanism of cell elongation in *Blepharisma japonicum*,with special reference to the role of cytoplasmic microtubules. *Cytobios* **42:** 215-226

Matsuoka T., Murakami Y., Furukohri T., Ishida M., Taneda K. (1992) Photoreceptor pigment in *Blepharisma*: H^+ release from red pigment. *Photochem. Photobiol.* **56:** 399-402

Moller K. M. (1962) On the nature of stentorin. *Comp. Rend. Trav. Lab. Carlsberg*. **32:** 471-497

Nakaoka Y., Kinugawa K., Kurotani T. (1987) Ca^{2+}-dependent photoreceptor potential in *Paramecium bursaria*. *J. Exp. Biol.* **131:** 107-115

Newman E. (1974) Scanning electron microscopy of the cortex of the ciliate *Stentor coeruleus*. A view from the inside. *J. Protozool.* **21:** 729-737

Passarelli V., Lenci F., Colombetti G., Barone E., Nobili R. (1984) The possible role of H and Ca in photobehavior of *Blepharisma japonicum*. In: Blue Light Effects in Biological Systems. (Ed. H. Senge), Springer-Verlag, Berlin, Heidelberg, 480-483

Peyer J. de, Machemer H. (1978) Hyperpolarizing and depolarizing mechanoreceptor potentials in *Stylonychia*. *J Comp. Physiol.* **127:** 255-266

Prusti R.K., Song P.-S., Häder D. T., Häder M. (1984) Caffeine-enhanced photomovemnt in the ciliate, *Stentor coeruleus*. *Photochem. Photobiol.* **40**: 369-375

Randall J.T., Jackson S. (1958) Fine structure and function in *Stentor polimorphus*. *J. Biophys. Biochem. Cytol.* **4:** 807-830

Rayer B., Naynert M., Stieve H. (1990) Phototransduction; Different mechanisms in vertebrates and inveretebrates. *J. Photochem. Photobiol.* B. **7:** 107-148

Scevoli P., Bisi G., Colombetti G., Barone E., Nobili R. (1987) Photomotile responses of *Blepharisma japonicum*. I. Action spectra determination and time-resolved fluorescence of photoreceptor pigments. *J. Photochem. Photobiol.* B. **1:** 75-84

Sevenants M. R. (1965) Pigments of *Blepharisma undulans* compared with hypericin. *J. Protozool.* **12:** 75-84

Song P.-S. (1981) Photosensory transduction in *Stentor coeruleus* and related organisms. *Biochim. Biophys. Acta* **639:** 1-29

Song P.-S. (1983) Protozoan and related photoreceptors. Molecular aspects. *Annu. Rev. Biophys. Bioeng.* **12:** 35-68

Song P.-S. (1989) Photomovement. In: The Science of Photobiology. (Ed. K. C. Smith), Plenum Publ. Co., 305-346

Song P.-S., Häder D.-P., Poff K. L. (1980a) Step-up photophobic response in the ciliate *Stentor coeruleus*. *Arch. Microbiol.* **126:** 181-186

Song P.-S., Häder D.-P., Poff K. L. (1980b) Phototactic orientation by the ciliate *Stentor coeruleus*. *Photochem. Photobiol.* **32:** 781-786

Song P.-S., Walker E. B., Auerbach R. A., Robinson G. W. (1981) Proton release from *Stentor* photoreceptors in the excited states. *Biophys. J.* **35:** 551-555

Tao N., Deforce L., Romanowski M., Meza-Keuthen S., Song P.-S., Furuya M. (1994) *Stentor* and *Blepharisma* photoreceptors: Structure and function. *Acta Protozool.* **33:** 199-211

Tartar V. (1961) The biology of *Stentor*. Pergamon Press

Walker E. B., Lee T. Y., Song P.-S. (1979) Spectroscopic characterization of the *Stentor* photoreceptor. *Biochim. Biophys Acta.* **586:** 129-144

Walker E. B., Yoon M., Song P.-S. (1981) The pH dependence of photosensory responses in *Stentor coeruleus* and model system. *Biochim. Biophys. Acta* **634:** 298-308

Wood D. C. (1975) Protozoa as models of stimulus transduction. In: Aneural Systems in Neurobiology. (Ed. E. Eisenstein), Plenum Press, New York, 5-23

Wood D. C. (1976) Action spectrum and electrophysiological responses correlated with the photophobic response of *Stentor coeruleus*. *Photochem. Photobiol.* **24:** 261-266

Wood D. C. (1982) Membrane permeabilities determining resting, action and mechanoreceptor potentials in *Stentor coeruleus*. *J. Comp. Physiol.* **146:** 537-550

Wood D. C. (1991) Electrophysiology and Photomovement of *Stentor*. In: Biophysics of Photoreceptors and Photomovements in Microorganisms. (Ed. F. Lenci et al.), Plenum Press, New York 281-291

Wood D. C., Martinelli R. (1990) Doublet *Stentor* do not display photodispersal. *Photochem. Photobiol.* **55:** 572-580

Yarfitz S., Hurley J. B. (1994) Transduction mechanisms of vertebrate and invertebrate photoreceptors. *J. Biol. Chem.* **269:** 14329-14332

Received on 30th December, 1994

Acta Protozoologica (1995) 34: 13 - 20

ACTA
PROTOZOOLOGICA

Effects of Artificial UV-B and Simulated Solar Radiation on the Flagellate *Euglena gracilis*: Physiological, Spectroscopical and Biochemical Investigations

Sabine GERBER and Donat-P. HÄDER

Institut für Botanik und Pharmazeutische Biologie, Friedrich-Alexander-Universität, Erlangen, Germany

Summary. The effects of enhanced artificial UV-B radiation and simulated solar radiation on cell shape, motility, pigmentation, photosynthetic oxygen production, protein pattern and content of the D1 protein have been investigated in the flagellate *Euglena gracilis*. The experiments showed that a spherical cell shape, vacuolization and the impairment of motility occurred much earlier when the cells were irradiated with enhanced UV-B radiation, while photobleaching of photosynthetic pigments occurred earlier when the cells had been exposed to simulated solar radiation. The inhibition of photosynthetic oxygen production was reversible under simulated solar radiation and irreversible (after 60 h of recovery) after exposure to enhanced UV-B radiation. There was an initial increase in chlorophyll *a* fluorescence emission after irradiation with enhanced UV-B radiation which did not occur after irradiation with simulated solar radiation. The protein pattern did not change significantly after irradiation but the content of D1 protein decreased after short exposure times to both radiation sources.

Key words. Absorption spectroscopy, artificial UV-B radiation, D1 protein, *Euglena gracilis*, fluorescence spectroscopy, gel electrophoresis, photosynthetic oxygen production, protein composition, phytoplankton, simulated solar radiation.

INTRODUCTION

Ozone depletion has been reported since the late sixties; an ozone hole over Antarctica was discovered in the eighties (Farman et al. 1985), and in the last years decreased levels of stratospheric ozone have occurred over the Northern hemisphere as well (Gleason et al. 1993, Kerr 1993, Stone 1993). Even with strict international controls on the use of CFCs, ozone depletion is predicted to continue well into the next century (NASA Reference Publication 1990). In this context investigations on effects of enhanced UV-B radiation (due to ozone depletion) on individual organisms, populations and whole ecosystems appear to be of great importance.

Marine and freshwater phytoplankton produce about half of the Earth's biomass (Houghton and Woodwell 1989) and form the basis of aquatic food webs. *Euglena gracilis* is a green colored, unicellular flagellate found in eutrophic freshwater habitats. Photosynthetic phytoplankton organisms are faced with the dilemma that on the one hand they need to be close to the water surface in order to receive enough solar radiation for photosynthesis (Ignatiades 1990), but on the other hand

Address for correspondence: D-P. Häder, Institut für Botanik und Pharmazeutische Biologie, Friedrich-Alexander-Universität, Staudtstr. 5, D-91058 Erlangen, Germany; FAX+499131 858215; E-mail: haeder@botanikl-pc. biologie. uni-erlangen.de

most species cannot tolerate the high visible and ultraviolet radiation found at the water surface (Häder et al. 1991, Raven 1991). Therefore many motile phytoplankton organisms accumulate at specific depths in the water column where they find favorable conditions for their growth and survival.

The basis for this vertical distribution is active movement powered by flagella or cilia in swimming organisms and changes in buoyancy in others. The organisms are guided by external stimuli, the most important of which are light and gravity (Häder 1988). At its vertical position within the water column phytoplankton is exposed to considerable levels of solar UV-B radiation which has been shown to affect the percentage of motile organisms, the swimming velocity as well as photo- and gravitaxis (e.g. Häder and Häder 1990, Häder and Liu 1990). Furthermore, important enzymatic reactions are impaired including nitrogen incorporation (Döhler and Alt 1989), and also photosynthetic capacity has been found to be reduced by UV-B radiation (e.g. Calkins and Thordardottir 1980).

Field studies can be used to study the effects of naturally enhanced UV radiation (at higher altitudes or lower latitudes) as compared with ambient levels of UV radiation (Gerber and Häder 1993, Häder and Liu 1990). In contrast, laboratory studies with artificial radiation sources allow to investigate mechanisms of inhibition under quantitative conditions. The aim of the present study is to investigate the effects of artificial UV-B and simulated solar radiation on *Euglena gracilis*, in order to determine which effects are caused by UV-B alone and which by UV-B in combination with UV-A and visible radiation.

Abbreviations

BSA	Bovine serum albumin
BCIP	5-Br-4-Cl-3-indolylphosphate
CAPS	3-[Cyclohexylamino]-1-propanesulfone acid
NBT	Nitrobluetetrazolium
PS II	Photosystem II
SDS	Sodium dodecyl sulfate
TBS	Tris-buffered saline

MATERIALS AND METHODS

Organisms and culture conditions

The flagellate *Euglena gracilis* Klebs, strain Z, was cultivated in an organic medium (Starr 1964). For the experiments the cells were harvested by centrifugation (100 x g, 5 min, 20°C) and transferred to a mineral medium (Checcucci et al. 1976). The cells were grown in static cultures at 20°C in continuous white light (12 W m^{-2}) from mixed daylight and warm tone fluorescent lamps (Osram L36 W/19 daylight 5000 de luxe and Osram L36 W/3L warm white de luxe). The illuminance was measured with an RM-10 integrating filter meter (Gröbel, Karlsruhe, FRG).

Exposure to radiation

The organisms were exposed either to artificial UV-B radiation produced from a transilluminator (Bachhofer, Reutlingen, FRG) or to simulated solar radiation from a solar lamp (Dr. Hönle GmbH, Martinsried, FRG). The spectral irradiance was measured with a spectroradiometer (Optronic model 752, Optronic Laboratories Inc., Orlando, FL, USA). The emission spectra of both radiation sources in comparison to solar radiation are shown in Fig. 1 and integrated irradiance data are listed in Table 1. In addition to the pronounced peak at 540 nm, simulated solar radiation deviates from natural solar radiation by having a higher UV-A component.

When the cells were exposed to simulated solar radiation the temperature was kept at 20°C in a thermostated room; there was no need to control the temperature when the cells were exposed to artificial UV-B radiation as the transilluminator does not emit in the infrared and hardly at visible wavelengths.

In the experiments on cell motility the cells were exposed in glass Petri dishes (5 cm diameter) which could be covered with cut-off filters (WG and GG series, Schott & Gen., Mainz, FRG). The cell concentration was 0.6 x 10^6 cells/ml and the volume was 10 ml. In order to compensate for energy losses due to the filter characteristics the samples were exposed at variable distances (45 to 60 cm) from the solar lamp, which had an irradiance of about 425 W m^{-2} (280-700 nm). In all other experiments, the distance to the lamps (60 cm for the solar lamp, 22 cm for the transilluminator), the optical density (0.9 O.D. at 674 nm) and the volume of the cell suspensions (200 ml) were kept constant, in order to be able to compare the kinetics of the different parameters, which strongly depend on irradiance, optical density and volume of the cell suspensions. The cells were exposed in large Petri dishes (20 cm diameter) and samples were taken at regular intervals for determination of spectra, microscopical investigations and biochemistry. For photosynthesis measurements, the cells were exposed for a predetermined time interval, then photosynthetic oxygen production was measured which took about 30 min, and then the samples were exposed again.

Determination of cell number, motility and shape

The cell number as well as the percentage of moving cells were determined microscopically with a hematocytometer (Brand, Wertheim, FRG) at a magnification of 160 x. Cell shape and vacuolization were determined visually at a magnification of 400 x.

Absorption and fluorescence spectroscopy

In vivo absorption spectra were measured with a DU 70 spectrophotometer (Beckman, Palo Alto, CA, USA) supplied with a miniature Ulbricht sphere, which allows to measure absorption spectra of cell suspensions. Fluorescence emission spectra were measured with a Shimadzu RF 5000 spectrofluorometer (Shimadzu, Kyoto, Japan). The excitation wavelength was 434 nm (the *in vivo* Soret absorption

maximum of chlorophyll *a*). For the spectroscopical measurements the cells were transferred into optical glass cuvettes with an optical path length of 10 mm (Hellma, Mühlheim, FRG).

Photosynthetic oxygen production

Photosynthetic oxygen production was determined in a custom made Plexiglas cylinder with 20 mm inner diameter inside a water jacket which was connected to a thermostat (RMT6, Dr. Wobser GmbH, Lauda-Königshofen, FRG). Temperature was kept constant at 20°C. Aliquots of 7 ml cell suspension were filled into the Plexiglas cylinder and agitated with a magnetic stirrer during oxygen determination. A Clark electrode (EOT 196, WTW Weilheim, FRG) was inserted, taking care not to introduce air bubbles into the cell suspension and connected to a microprocessor (OXI 96, WTW, Weilheim, FRG) attached to an XY plotter. The sample was irradiated with white light produced from a 250-W slide projector with a 24-V quartz halogen bulb (Kindermann Universal, Wetzlar, FRG). Irradiance was controlled by inserting neutral density filters (Schott & Gen., Mainz, FRG) into the slide projector and measured inside the Plexiglas cylinder with a pindiode connected to a microvoltmeter (Keithley, type 155). The pindiode was calibrated against the filter radiometer.

For photosynthesis measurements the cells were kept in the dark for 10 min, then photosynthetic oxygen production was measured at 4 different irradiances for 5 min each. For evaluation only the illuminance (18 klx) was used which was most effective as determined by previously measured fluence rate-response curves. When photosynthetic oxygen production had ceased after about 20 min of irradiation, the cells were kept under culture conditions and photosynthesis was measured again to study recovery.

Gel electrophoresis

For gel electrophoresis samples of 2 ml were taken, the cell number was determined, the cells were pelleted (5 min, 48 x g, 20°C), resuspended in 0.5 ml of the supernatant and mixed with 0.5 ml Laemmli buffer (containing 6 % SDS, 10 % 2-mercaptoethanol, 20 % glycerol in a 150 mM Tris buffer at a pH of 6.8). These samples were applied to the gel, the concentration was adjusted to an equivalent of 3.1×10^5 cells/slot in all samples.

SDS polyacrylamid gel electrophoresis was carried out in a vertical system (2001, LKB Pharmacia, Uppsala, Sweden) according to Laemmli (1970) with a resolving gel of 5-15 % acrylamide. The gels were Laeither silver stained (Merril et al. 1981, Görg et al. 1988) or used for Western blotting. The gel size was 140 x 110 x 2 mm.

Western blotting and immunostaining

The gels were blotted for 3 h at 200 mA and 4°C on nitrocellulose using a semidry blotting technique (anode buffer: 50 mM CAPS, pH 10.0; cathode buffer: 50 mM CAPS, 0.1 % SDS, pH 5.5).

After saturation with 5 % BSA (peroxidase free) in TBS over night, the primary antibody was allowed to react in TBS/BSA for 1 h at room temperature. Then the blot was washed with TBS and TBS/Triton and the secondary antibody (alkaline phosphatase-conjugated) in TBS/BSA was allowed to react for 1 h. After washing with TBS and TBS/Triton the color was developed using NBT and BCIP.

The primary antibody against the D1 protein was kindly supplied by Dr. U. Johanningmeier (Johanningmeier 1987).

RESULTS

Motility, cell shape and vacuolization

After 10-15 min of exposure to enhanced artificial UV-B radiation from the transilluminator the percentage of motile cells decreased significantly; after 30-40 min of exposure all cells were immotile. The cells began to assume a round shape after 15 min of exposure; after 20 min most of the organisms were spherical and had lost motility. Vacuolization occurred after 25 min, after 50 min most of the cells had large additional vacuoles (Table 2).

When the algae had been exposed to simulated solar radiation they remained motile for a much longer time of irradiation: up to about 60 min there was no significant decrease in the percentage of motile cells; then, however, motility decreased rather rapidly, and all cells were immotile after 80 min. The cells became spherical after about 60 min of exposure, after 120 min of exposure time nearly all cells had a round shape. Vacuolization occurred later compared to the samples irradiated with simulated solar radiation: small vacuoles occurred after 60 min in immotile cells; after 120 min all cells had large additional vacuoles (Table 2).

Figure 2 shows the kinetics of the inhibition of motility in dependence of exposure time. In these experiments the samples had been covered with different cut-off filters, in order to determine the significance of different wavelength bands (at a constant total irradiance) for the inhibition of motility.

In the samples which were covered with a WG225 (and served as a control) motility decreased fastest; after 50 min there was no more motility. A WG320 filter, which removes about 2/3 of the UV-B radiation

Table 1

Integrated irradiance [in W m^{-2}] in the UV-B, UV-A and visible regions of the spectrum of the two radiation sources and the solar lamp with the cut-off filters

Radiation source	**280 - 315 nm**	**315 - 400 nm**	**400 - 700 nm**
Transilluminator	8.52	8.89	0
Hönle lamp	1.48	95.76	372.71
Solar spectrum	1.02	50.66	485.36
Filter (Hönle lamp)	**280 - 315 nm**	**315 - 400 nm**	**400 - 700 nm**
WG 225	1.33	88.12	346.75
WG 320	0.46	87.41	344.57
WG 345	0.38	67.54	320.65
GG400	0	1.61	455.85
GG420	0	0	409.83

(Table 1), delays the impairment of motility: complete immotility of the cells occurred only after 90 min of irradiation. Under a WG345 filter, which cuts off most of the UV-B and about 20 % of the UV-A radiation the occurrence of complete immotility (120 min) was further delayed. When the samples were covered with a GG400 filter (which cuts off all of the UV-B and most of the UV-A) the percentage of motile cells decreased during the first 50 min of irradiation and then increased again. The samples covered with a GG420 filter (which removes the whole UV-band) showed about the same percentage of motile cells before and after 120 min of irradiation.

Absorption spectroscopy

A slight decrease in chlorophyll *a* absorption occurred after 60 min of exposure to enhanced artificial UV-B radiation (Fig. 3), after 360 min there was still about 80 % (0.7 O.D.) of the initial absorption and after 600 min about 60 % (0.5 O.D.). The suspension was still green, although the color had changed from light green to olive. When the cells were irradiated with simulated solar radiation photobleaching occurred much earlier: after 120 min the absorption had decreased to 50 % (0.4 O.D.) of the initial value. After 300 min there was no more absorption of chlorophyll *a*, and the cell suspension was white.

Fluorescence spectroscopy

In the suspensions which had been exposed to enhanced artificial UV-B radiation (Fig. 4A) there was an increase of chlorophyll *a* fluorescence at 690 nm after the first 30 min of exposure, then fluorescence decreased. After 90 min of exposure the relative fluorescence was lower than the initial value. After 240 min of exposure a shoulder at a shorter wavelength occurred which became a peak at 673 nm after 360 min of exposure.

In contrast, there was no fluorescence increase in the samples which had been exposed to simulated solar radiation (Fig. 4B); even after 5 min of exposure fluorescence was lower than in the control. Up to 120 min of exposure the chlorophyll *a* fluorescence maximum was at 690 nm, then it shifted to 673 nm and decreased further. After 360 min of exposure, when there was nearly no chlorophyll *a* (or any other) absorption, new peaks at 690 and 712 nm occurred.

Summarizing one can say that in the samples irradiated with UV-B alone as well as in the samples irradiated with simulated solar radiation chlorophyll *a* fluorescence changed before absorption changed. After irradiation the initial chlorophyll *a* fluorescence decreased and the

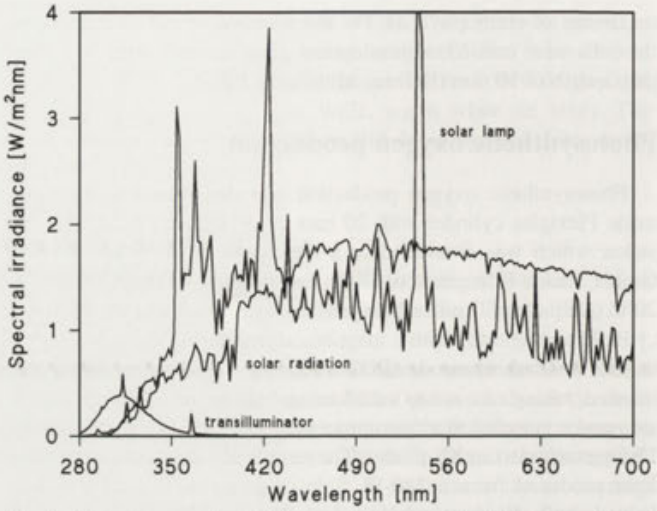

Fig. 1. Emission spectra of the sun (measured in Erlangen at local noon on 28 May 1993), a solar simulator lamp (Hönle) and a transilluminator as measured with an Optronic spectroradiometer

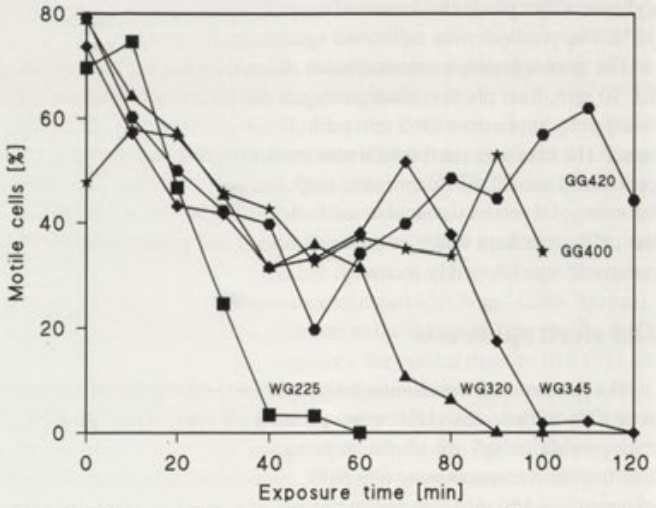

Fig. 2. Effects of filtered (WG225: squares, WG320: triangles, WG345: diamonds, GG400: stars, GG420: hexagons) simulated solar radiation on the motility (percentage of motile cells) of *Euglena gracilis* in dependance of the exposure time

fluorescence maximum shifted from 690 nm to 673 nm. After extensive times of irradiation an additional peak at 712 nm occurred, which lates vanished in the samples irradiated with simulated solar radiation. An initial increase of chlorophyll *a* fluorescence occurred only in the samples irradiated with artificial UV-B radiation alone.

Photosynthetic oxygen production

After 20 min of irradiation both with enhanced UV-B and with simulated solar radiation, photosynthetic oxygen production had ceased (Fig. 5). Oxygen production was slightly lower in the samples irradiated with enhanced UV-B radiation. Recovery, however, differed very much: there was no recovery even after 60 h in the

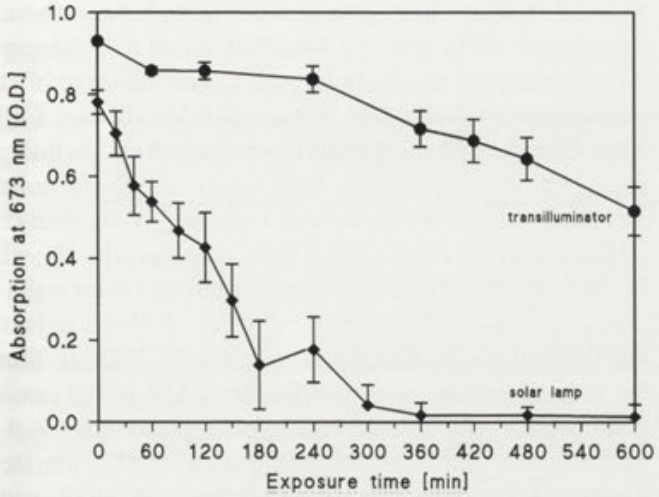

Fig. 3. Absorption of chlorophyll *a* at 673 nm after various times of exposure to enhanced UV-B radiation (circles) and simulated solar radiation (diamonds)

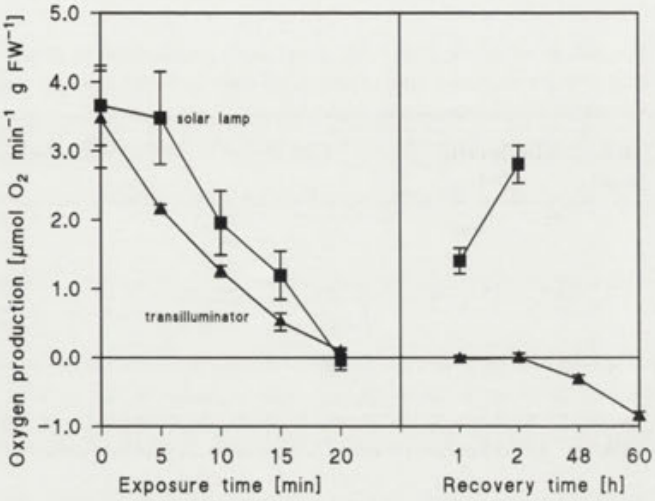

Fig. 5. Photosynthetic oxygen production of *E. gracilis* after different times of exposure to simulated solar radiation (squares) and enhanced UV-B radiation (triangles) and after recovery in dim light

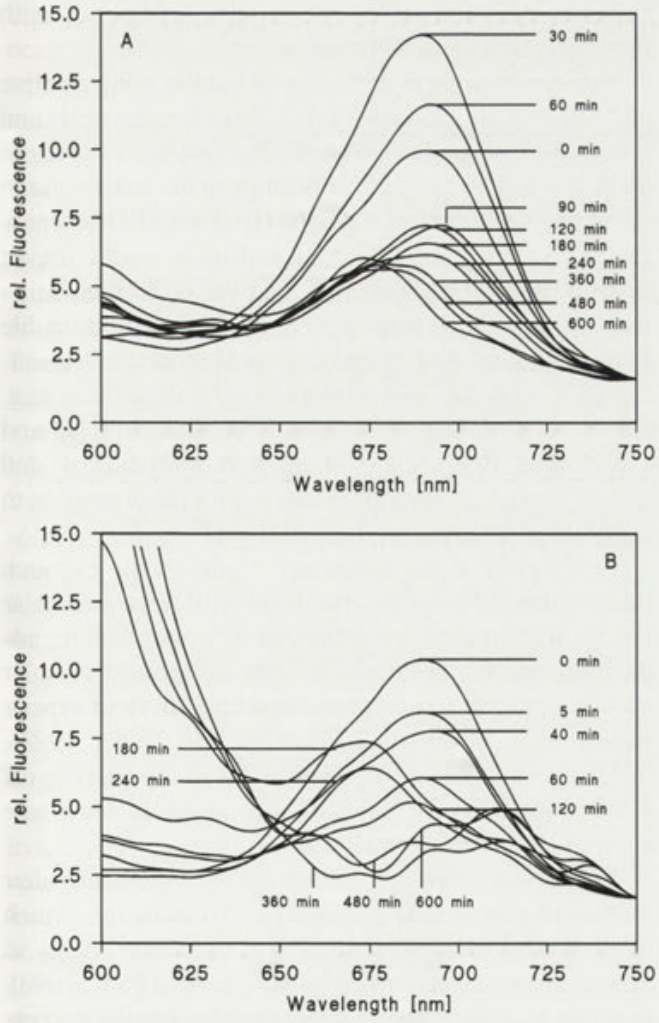

Fig. 4. Fluorescence emission spectra of chlorophyll *a* (excitation at 434 nm) after different times of exposure to enhanced UV-B radiation (A) and simulated solar radiation (B)

samples which had previously been irradiated with enhanced UV-B radiation, in contrast to the samples which had been irradiated with simulated solar radiation which recovered partially after 1 h and almost completely after 2 h under culture conditions.

Biochemistry

The protein pattern of the samples which had been irradiated with enhanced UV-B radiation did not change much during exposure (Fig. 6). In the samples which had been irradiated with simulated solar radiation the protein pattern did not change, but unspecific protein destruction occurred after 4 h of exposure.

The Western blots (Fig. 7) which had been immuno stained with a polyclonal antibody against the D1 protein however showed a reduction of the binding of the D1 protein after 30 min of irradiation with either artificial UV-B radiation or simulated solar radiation. After 4 h of irradiation there was little D1 protein left, a faint band was still visible.

DISCUSSION

In the present study it is shown that the cell shape of *Euglena gracilis* alters from spindle shaped to spherical after the cells had been irradiated either with enhanced artificial UV-B radiation or with simulated solar radiation. Simultaneously, vacuoles occur in the cells which possibly indicate changes in the permeability of the cytoplasmic membrane which lead to an influx of water into the cells.

Table 2

Percentage of motile cells, cell shape and vacuolization in dependence of the exposure time to simulated solar radiation (Hönle) and enhanced UV-B radiation (transilluminator)

E.t. (min)	Motile cells [%]		Cell shape		Vacuoles	
	TI	Hönle	TI	Hönle	TI	Hönle
0	64.8	55 ± 20	spindle shaped	spindle shaped	–	–
5	70.0	48 ± 10	spindle shaped	spindle shaped	–	–
10	41.1	53 ± 23	spindle shaped	spindle shaped	–	–
15	20.5	52 ± 7	spindle shaped some rounded	spindle shaped	–	–
20	9.2	54 ± 11	round some spindle shaped	spindle shaped	–	–
25	3.6	57	round	spindle shaped	[1]	–
30	1.9	54 ± 4	round	spindle shaped		–
40	0	34 ± 16	round	spindle shaped		–
50	0	62 ± 10	round	spindle shaped	+[2]	–
60	0	40 ± 5	round	spindle shaped some rounded	+	[3]
70	0	11 ± 6	round	few spindle shaped many round	+	+[4]
80	0	1 ± 1	round	few spindle shaped many round	+	+
90	0	0	round	few spindle shaped most round	+	+
120	0	0	round	most round	+	+
>120	0	0	round	round	+	+

E.t.- Exposure time
[1] - very small vacuoles
[2] - in most cells
[3] - small vacuoles in immotile cells
[4] - in immotile cells

Murphy (1983) has shown that non-photosynthetic membranes are targets of UV-radiation and that changes in the transport across membranes occur quickly after exposure to a relative low fluence of UV-radiation. Cell shape changes and vacuolization occur much earlier under enhanced UV-B radiation than under simulated solar radiation, indicating that these are mainly UV-B effects.

Enhanced UV-B radiation from the transilluminator impairs motility much faster than simulated solar radiation, and reducing UV radiation by cut-off filters delays the inhibition significantly. These results indicate that the impairment of motility is mainly a UV-B and not a white light effect. Similar results are reported for *Cryptomonas maculata* (Häder and Häder 1991), marine dinoflagellates (Ekelund 1991, Schäfer et al. 1993) and marine diatoms (Ekelund 1990). Ekelund (1991) discusses cytoskeletal proteins as possible targets responsible for the inhibition of motility since the maximum of the response occurred at 280 nm which corresponds with the absorption of most proteins.

Euglena gracilis orientates in its habitat using positive and negative phototaxis as well as negative gravitaxis and accumulates at bands of moderate light intensities of about 30 W m^{-2} which change their position in the water column according to changing daylight (Häder and Griebenow 1988). An increase of UV-B radiation would impair motility in *Euglena*, thus affecting the cells' orientation mechanisms which help them to escape from unsuitable light conditions. As *Euglena* does not produce sunscreening pigments (data not shown) like dinoflagellates (e.g. Carreto et al. 1990) or cyanobacteria (Garcia-Pichel and Castenholz 1991) their orientation mechanisms and motility are a very important strategy for the organisms to escape from deleterious (UV) radiation.

Chlorophyll *a* absorption at 673 nm decreases much faster when the cells are irradiated with simulated solar radiation compared to enhanced UV-B radiation, indicating that UV-B is not the only component of solar radiation, which causes photobleaching. In field experiments with cut-off filters (Gerber and Häder 1993), however, photobleaching was delayed by cutting-off UV-B radiation, so UV-B seems to be at least one component involved in photobleaching.

There is an increase in chlorophyll *a* fluorescence after 30 min of exposure to enhanced UV-B radiation, which might be due to an accumulation of excitation energy in the antenna pigments caused by a decrease of PS II activity (e.g. Lawlor 1987). This increase of chlorophyll *a* fluorescence emission was not observed in the samples exposed to simulated solar radiation or in samples (of *Euglena* and

other phytoplankton organisms, data not published) exposed to natural solar radiation.

The decrease of fluorescence emission which takes place in both samples has to be correlated to quenching processes, as accumulated energy cannot be used for photochemistry (since photosynthetic oxygen production has ceased after only 25 min of irradiation) and it is not released by fluorescence (which decreases). A possible mechanism for relaxation is the xanthophyll cycle in which excess energy from chlorophyll *a* is transferred to carotenoids which relax radiationless by internal conversion (e.g. Tevini and Häder 1985). Barenyi and Krause (1985) reports a decrease of low-temperature fluorescence emission of PS II at 685 nm in photoinhibited broken spinach chloroplasts which she correlates to a decrease of variable fluorescence.

After longer irradiation times a fluorescence maximum at a shorter wavelength occurs in both samples (in the samples irradiated with simulated solar radiation the peak occurs earlier and is more pronounced). This shift seems to be due to a decrease of fluorescence of chlorophyll molecules which emit at longer wavelengths and an increase of fluorescence of species which emit at shorter wavelengths (e.g. the antenna pigments or pigments from the core complex).

Finally, peaks at wavelengths longer than 700 nm occurred in both samples, which are more pronounced in the samples irradiated with simulated solar radiation. The nature of the long wavelength species is unknown and currently under discussion.

Photosynthetic oxygen production was completely inhibited after 25 min of exposure to either radiation source. In the samples which had been irradiated with simulated solar radiation, an increase in photosynthetic oxygen production occurred after the cells had been kept in dim light for 1 h. This rather short recovery time indicates that the measured photoinhibition is caused by a degradation of the D1/D2 proteins to which the oxygen evolving system and the electron carriers of PS II are bound. The damage of the D1 protein which seems to be the major target is repaired by the "photoinhibition repair cycle" within hours (Andersson et al. 1992). In the samples irradiated with enhanced UV-B radiation, there was no recovery even after 60 h. Thus, simulated solar radiation leads to (reversible) photoinhibition which is assumed to be a protection mechanism (Trebst 1991, Krause and Weis 1991), while enhanced UV-B radiation leads to (irreversible) photodestruction.

The protein pattern of the crude extracts did not change significantly after irradiation of the cells, which is in

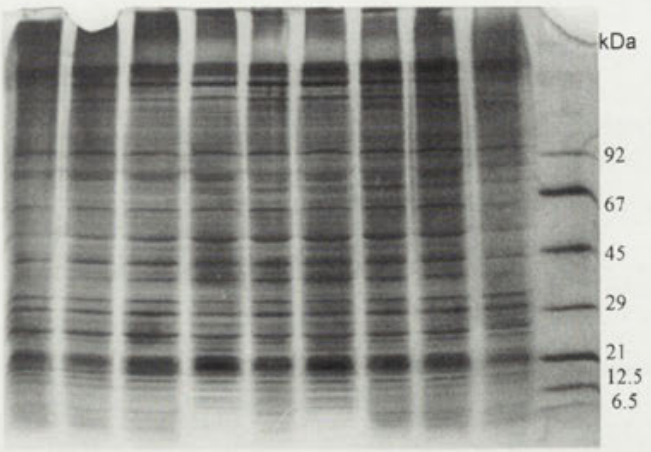

Fig. 6. Protein bands after SDS gel electrophoresis and silver staining of crude extracts of *Euglena gracilis* cells. From left to right: 4 h, 2 h, 1 h, 0.5 h of exposure to enhanced UV-B radiation, control, 0.5 h, 1 h, 2 h, 4 h of exposure to simulated solar radiation, marker

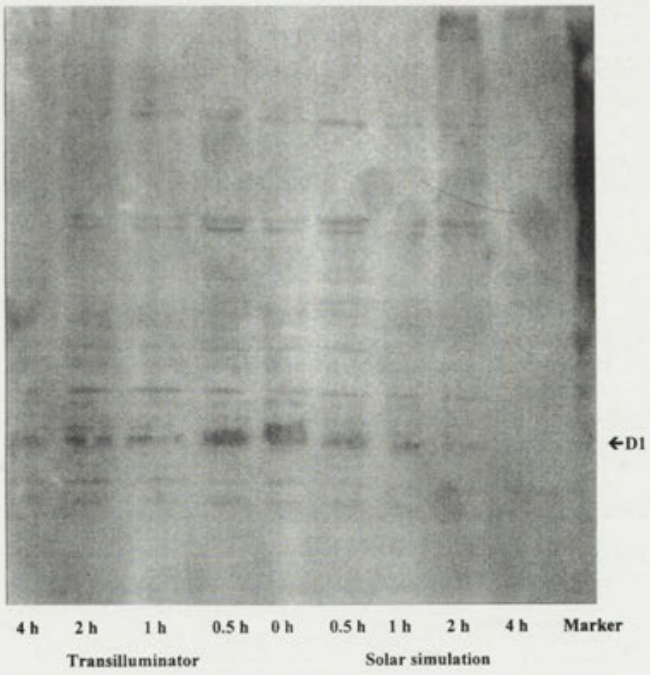

Fig. 7. Immunoblot with an antibody against the D1 protein after gel electrophoresis of the crude extract. From left to right: 4 h, 2 h, 1 h, 0.5 h of exposure to enhanced UV-B radiation, control, 0.5 h , 1 h, 2 h, 4 h of exposure to simulated solar radiation

accordance with the results obtained in spinach thylakoids (Renger et al. 1988, Trebst and Depka 1990), who found the polypeptide pattern hardly affected by UV-B radiation. The binding of the antibody against the D1 protein in both samples, however, decreased essentially after 30 min (when there was no longer photosynthetic oxygen production), indicating that photoinhibition (and photodestruction) lead to a decline of the D1 protein (for a recent review see Barber and Anderson 1992) in *Euglena* as well.

The loss of proteins in the sample which occurred after 4 h (simulated solar radiation) or 8-10 h (enhanced UV-B radiation, data not shown) in *E. gracilis* is consistent with the results reported by Döhler (1984) who measured a decrease in protein content with increasing UV dose and a simultaneous increase of free amino acids in the cells.

Summarizing it can be said that UV-B radiation (alone or in combination with UV-A and visible radiation) affects cell shape, vacuolization, motility, chlorophyll absorption and fluorescence, as well as photosynthetic oxygen production and the content of the D1 protein in *Euglena gracilis*. Some effects (inhibition of motility and destruction of the photosynthetic oxygen production) are predominantly or exclusively due to UV-B radiation, while other effects (photobleaching) are not or only partially due to UV-B radiation.

Acknowledgement. This work was supported by financial support from the State of Bavaria (BayFORKLIM, Projekt DIII/1), the Bundesminister für Forschung und Technologie (project KBF 57) and the European Community (EV5V-CT91-0026) to D.-P. H. We thank Dr. U. Johanningmeier (Lehrstuhl Biochemie der Pflanzen, Ruhr-Universität Bochum, Germany) for supplying the antibodies against the D1 protein and Thomas Schlenkrich for helpful discussions and critical reading of the manuscript.

REFERENCES

Andersson B., Salter A.H., Virgin I., Vass I., Styring S. (1992) Photodamage to photosystem II- primary and secondary events. *J. Photochem. Photobiol. B. Biol.* **15:** 15-31

Barber J., Andersson B. (1992) Too much of a good thing: light can be bad for photosynthesis. *Trends Biochem. Sci.* **17:** 61-66

Barenyi B., Krause G.H. (1985) Inhibition of photosynthetic reactions by light. *Planta* **163:** 218-226

Calkins J., Thordardottir T. (1980) The ecological significance of solar UV radiation on aquatic organisms. *Nature* **283:** 563-566

Carreto J.J., Carignana M.O., Daleo G., de Marco S.G. (1990) Occurrence of mycosporine-like amino acids in the red tide dinoflagellate *Alexandrium excavatum*. UV protective compounds. *J. Plankton Res.* **12:** 909-921

Checcucci A., Colombetti G., Ferrara R., Lenci, F. (1976) Action spectrum for photoaccumulation of green and colorless *Euglena*: evidence for identification of receptor pigments. *Photochem. Photobiol.* **23:** 51-54

Döhler G., (1984) Effect of UV-B radiation on biomass production, and protein content of marine diatoms. *Z. Naturforsch. Sect. C.* **39:** 634-638

Döhler G., Alt M.R. (1989) Assimilation of ^{15}N-ammonia during irradiance with ultraviolet-B and monochromatic light by *Thalassiosira rotula*. *Acad. Sci. Ser. D* **308:** 513-518

Ekelund N.G.A. (1990) Effects of UV-B radiation on growth and motility of four phytoplankton species. *Physiol. Plant.* **78:** 590-594

Ekelund N.G.A. (1991) The effects of UV-B radiation on Dinoflagellates. *J. Plant Physiol.* **138:** 274-278

Farman J.C., Gardiner B.G., Shanklin, J.D. (1985) Large losses of total ozone in Antarctica reveal seasonal ClO_x/NO_x interaction. *Nature* **315:** 207-210

Garcia-Pichel F., Castenholz R.W. (1991) Characterization and biological implications of scytonemin, a cyanobacterial sheath pigment. *J. Phycol.* **27:** 395-409

Gerber S., Häder D.-P. (1993) Effects of solar irradiation on motility and pigmentation of three species of phytoplankton. *Env. Exp. Bot.* **33:** 515-521

Gleason J.F., Bhartia P.K., Herman J.R., McPeters R., Newman P., Stolarski R.S., Flynn L., Labow G., Larko D., Seftor C., Wellemeyer C., Komhyr W.D., Miller A.J., Planet W. (1993) Record on global ozone in 1992. *Science* **260:** 523-526

Görg A., Postel W., Günther S. (1988) The current state of two-dimensional electrophoresis with immobilized pH gradients. *Electrophoresis* **9:** 531-546

Häder D.-P. (1988) Ecological consequences of photomovement in microorganisms. *J. Photochem. Photobiol. B: Biol.* **1:** 385-414

Häder D.-P., Griebenow K. (1988) Orientation of the green flagellate, *Euglena gracilis*, in a vertical column of water. *FEMS Microbiol. Ecol.* **53:** 159-167

Häder D.-P., Häder, M.A. (1990) Effects of UV radiation on motility, photoorientation and pigmentation in a freshwater *Cryptomonas*. *J. Photochem. Photobiol. B: Biol.* **5:** 105-114

Häder D.-P., Häder M.A. (1991) Effects of solar and artificial UV radiation on motility and pigmentation in the marine *Cryptomonas maculata*. *Env. Exp. Bot.* **31:** 33-41

Häder D.-P., Liu S.-M. (1990) Motility and gravitactic orientation in the flagellate *Euglena gracilis*, impaired by artificial and solar UV-B radiation. *Curr. Microbiol.* **21:** 161-168

Häder D.-P., Worrest R.C., Kumar, H.D. (1991) Aquatic ecosystems. *UNEP Environmental Effects Panel Report (Update 1991)*, 33-40.

Houghton R.A., Woodwell, G.M. (1989) Global climatic change. *Sci. Am.* **260:** 18-26

Ignatiades L. (1990) Photosynthetic capacity of the surface microlayer during the mixing period. *J. Plankton Res.* **12:** 851-860

Johanningmeier U. (1987) Expression of the *psbA* gene in *E. coli*. *Z. Naturforsch.* **42c:** 755-757

Kerr R.A. (1993) Ozone takes a nose dive after the eruption of Mt. Pinatubo. *Science* **260:** 490-491

Krause G.H, Weis E. (1991) Chlorophyll fluorescence and photosynthesis: the basics. *Ann. Rev. Plant. Physiol. Plant Mol. Biol.* **42:** 313-349

Laemmli U.K. (1970) Cleavage of structural proteins during the assembly of the head of bacteriophage T4. *Nature* **227:** 680-685

Lawlor D.W. (1987) Photosynthesis: metabolism, control and physiology, Longman Group UK Limited, London, p49f

Merril C.R., Goldman D., Sedman S.A., Ebert M.H. (1981) Ultrasensitive stain for proteins in polyacrylamide gels shows regional variation in cerebrospinal fluid proteins. *Science* **211:** 1437-1438

Murphy T.M. (1983) Membranes as targets of ultraviolet radiation. *Physiol. Plant.* **58:** 381-388

NASA Reference Publication 1242, September 1990, p.14

Raven J.A. (1991) Responses of aquatic photosynthetic organisms to increased solar UV-B. *J. Photochem. Photobiol. B: Biol.* **9:** 239-244

Renger G., Völker M., Eckert H.J., Fromme R., Hohm-Veit S., Gräber P. (1988) On the mechanism of photosystem II deterioration by UV-B radiation. *Photochem. Photobiol.* **49:** 97-105

Schäfer J., Sebastian C., Häder D.-P. (1993) Effects of solar radiation on motility, orientation, pigmentation and photosynthesis in a green dinoflagellate *Gymnodinium*. *Acta Protozool.* **33:** 59-65

Starr R.C. (1964) The culture collection of algae at Indiana University. *Am. J. Bot.* **51:** 1013-1044

Stone R. (1993) Ozone prediction hits it right on the nose. *Science* **261:** 290

Tevini M., Häder D.-P. (1985) Allgemeine Photobiologie. Georg Thieme Verlag, Stuttgart, New York

Trebst A. (1991) A contact site between the two reaction center polypeptides of photosystem II is involved in photoinhibition. *Z. Naturforsch.* **46:** 557-562

Trebst A., Depka B. (1990) Degradation of the D-1 protein subunit of photosystem II in isolated thylakoids by UV light. *Z. Naturforsch.* **45c**: 765-771

Received on 30th May, 1994; accepted on 4th August, 1994

Acta Protozoologica (1995) 34: 21 - 34

ACTA
PROTOZOOLOGICA

Fine Structure and Systematic Position of *Enchelyomorpha vermicularis* (Smith, 1899) Kahl, 1930, an Anaerobic Ciliate (Protozoa, Ciliophora) from Domestic Sewage

Wilhelm FOISSNER and Ilse FOISSNER

Universität Salzburg, Institute für Zoologie und Pflanzenphysiologie, Salzburg, Austria

Summary. *Enchelyomorpha vermicularis* is a pouch-like ciliate having not only a holotrichous ciliature but also many short, tentacle-like processes on the cell surface. Its systematic position thus varied, depending on the characters used, between the suctorians and the haptorid gymnostomes, and a recent investigation using refined light microscopic methods could also not clarify the situation. We thus examined some stages of the life cycle of *E. vermicularis* and studied its fine structure with the transmission electron microscope. The results definitely show that *E. vermicularis* is the swarmer of a small, globular suctorian with tentacles irregularly distributed on the anterior body half. The tentacles, which are not associated with barren basal bodies, contain the barrel-shaped haptocysts and the two concentric microtubule cores typical of "good" suctorians. Furthermore, the cortex possesses small pits and the fine structure of the somatic kinetids is also very similar to that known from other suctorian swarmers, although the kinetodesmal fibre is anchored to the epiplasm and subkinetal microtubules are probably absent. The kinetids are rotated 90 ° counter-clockwise with respect to the longitudinal body axis causing the ciliary rows to extend transversely. Usually, two swarmers are produced simultaneously by endogenous budding. *Enchelyomorpha vermicularis* lacks a scopuloid and mitochondria but possesses cytoplasmic inclusions resembling hydrogenosomes, indicating that it is a true anaerobic ciliate, which is in accordance with most faunistic data. The mode of swarmer production, the organization of the swarmer, and the fine structure of the tentacles show that *Enchelyomorpha* is an entotropid suctorian, belonging to the suborders Acinetina or Discophryina. Acinetid affinities are indicated by the fine structure of the tentacles and the general organization of the swarmer, whereas swarmer production resembles *Cyathodinium* in the suborder Discophryina. Obviously, *Enchelyomorpha* has a highly distinct combination of characters which suggests at least separation at family level, i.e. maintenance of the family Enchelyomorphidae Augustin and Foissner, 1992.

Key words. Anaerobic protists, Ciliophora, *Enchelyomorpha vermicularis*, sewage, Suctorida, ultrastructure.

INTRODUCTION

Enchelyomorpha vermicularis is a peculiar ciliate which has not only cilia but also many tentacle-like processes described by Smith (1899) as "fairly stout hispid setae". Smith (1899) assigned the organism to the genus *Enchelys* without , however, discussing his classification. In 1926 Kahl described the same organism as a "swarmer of an unknown suctorian". Later, Kahl (1930, 1931) recognized identity with *Enchelys vermicularis* Smith and put the species in a new genus, *Enchelyomorpha*, which he provisionally assigned to the family Actinobolinidae, together with *Actinobolina* and *Dactylochlamys*, which also possess tentacle-like struc-

Address for correspondence: W. Foissner, Universität Salzburg, Institut für Zoologie, Hellbrunnerstrasse 34, A - 5020 Salzburg, Austria; Tel. (0662) 8044-5615; FAX (0662) 8044-5698

tures on the cell surface. A few years later, Liebmann (1936) observed *E. vermicularis* feeding on bacteria by its anterior end, seemingly confirming the "simple apical oral aperture" mentioned by Smith (1899). More recently, Corliss (1979) definitely assigned *Enchelyomorpha* to the Actinobolinidae, a family of tentacle-bearing haptorids originally established by Kent (1881) and later nomenclaturally corrected by Kahl (1930). A light microscopic reinvestigation of *E. vermicularis* by Augustin and Foissner (1992) revealed sufficient details to establish a new family, Enchelyomorphidae, but could also not clarify its systematic position. We thus studied the fine structure of *E. vermicularis* with the transmission electron microscope and re-examined the protargol slides of Augustin and Foissner (1992) for developmental stages. The results definitely show that *E. vermicularis* is the swarmer of a globular suctorian with tentacles irregularly distributed on the anterior body half.

MATERIALS AND METHODS

The material used is the same as described in Augustin and Foissner (1992), viz. sewage from a trickling filter near Salzburg, where *E. vermicularis* was fairly abundant. Some sewage containing *E. vermicularis* was fixed *in toto* for the light and electron microscopical preparations. Most light microscopical data mentioned in this study are from Augustin and Foissner (1992), who used various light microscopical and silver impregnation techniques to reveal the infraciliature and other details. The protargol slides prepared at that time were re-examined for adult and budding stages. These were indeed found, but were difficult to recognize among the sludge masses which might explain why Augustin did not find them.

Transmission electron microscopy was performed as described in Foissner et al. (1988).

RESULTS

We shall show in our study that *Enchelyomorpha vermicularis* is the swarmer of a globular suctorian. This causes some problems with the orientation of the cell, which must thus be defined before the results are described and discussed. Generally, the orientation of suctorian swarmers is a complicated and controversial matter (Batisse 1994, Kormos and Kormos 1957), which has been almost completely ignored in the electron microscopic literature. It is, however, essential to understand the orientation of the kinetids and ciliary rows as well as the ontogeny and phylogeny of ciliates in general (Bardele 1989, Kormos and Kormos 1957).

Enchelyomorpha vermicularis has a distinct longitudinal body axis and swims with the narrowed end ahead (Figs. 1, 6). Thus, this end has been considered as anterior and the opposite one, which contains the contractile vacuole, as posterior (Augustin and Foissner 1992). However, the electron microscopic investigations indicate just the opposite, because the postciliary microtubules extend to the narrowed end. Thus, this region is very likely the morphologic posterior, as postciliary microtubules ususally extend rearward (Lynn 1981). Furthermore, the kinetid pattern suggests that the ciliary rows extend transversely, i.e. at right angles to the longitudinal body axis.

We thus use the following orientation in the description and figures: the broadened end of the cell is anterior, the narrowed is posterior; the right side of the kinetid is defined, as usual, by the kinetodesmal fibre, the posterior by the distal portion of the postciliary microtubules.

Light microscopic description of *E. vermicularis*

A detailed light microscopic characterization of *E. vermicularis* and a review of the older literature have been published by Augustin and Foissner (1992). Thus, only a brief description and some figures will be given here for orientation purposes.

Size *in vivo* 25-45 x 10-17 µm, pouch-like and slightly asymmetric, gradually narrowed from broadly rounded anterior end to short-truncate posterior end (Figs. 1-3, 6). Macronucleus about 7 µm in diameter, in anterior half of cell (Fig. 3). Contractile vacuole in anterior end, with single excretory pore (Figs. 2, 3). Cortex distinctly furrowed transversely by somatic kineties (Figs. 1, 2). On posterior half about 15-20 acontractile processes (tentacles) 2-3 µm long with distal end inconspicuously knobbed (Figs. 1-4, 6, 7). Moves slowly and clumsily with narrowed posterior end ahead. About 13 transverse ciliary girdles, forming about 17 longitudinal ciliary rows, commence at posterior end of body and extend anteriorly leaving pole region free of cilia (Figs. 5, 7). Silverline system finely and irregularly meshed (Fig. 5).

Adult cells, not described by Augustin and Foissner (1992), were recognized in protargol stains only. They are globular with a diameter of 15-20 µm and have short tentacles in the body half opposed to the contractile vacuole (Fig. 29). No stalk is recognizable in the stained cells and may in fact be absent as no scopuloid

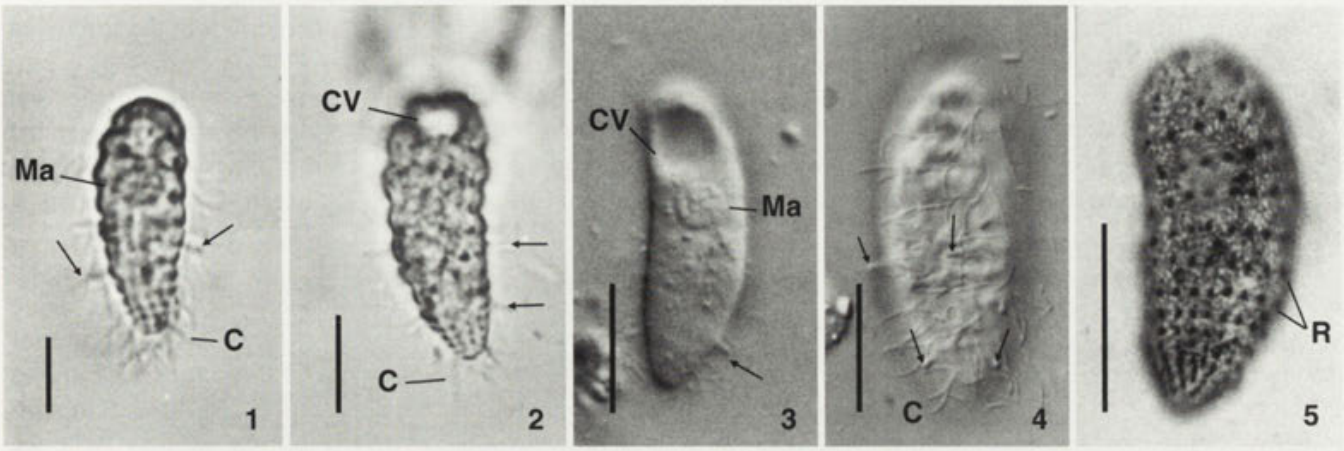

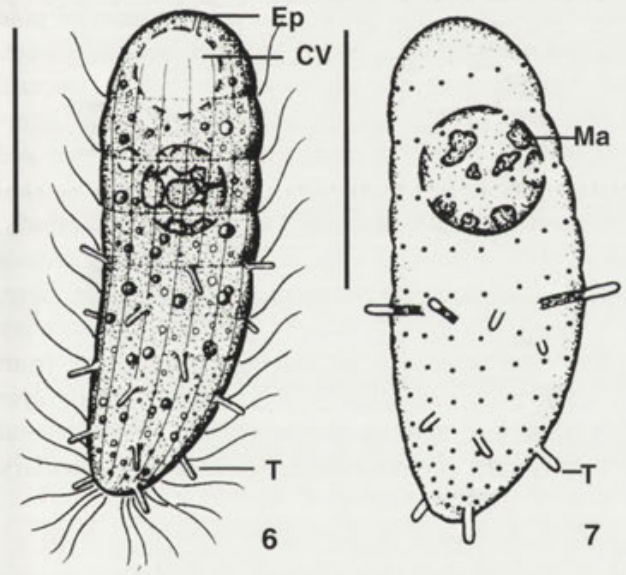

Figs. 1 - 7. *Enchelyomorpha vermicularis* from life (1-4, 6) and after dry silver nitrate (5) and protargol (7) impregnation. Figures 3-7 are from Augustin and Foissner (1992). 1, 2, 3, 4 - bright field (1, 2) and interference contrast (3, 4) light micrographs of typical specimens with many small tentacles (arrows) and distinctly furrowed body; 5, 7 - the ciliary rows form a longitudinal and circular pattern, and a very fine-meshed silverline system extends throughout the cortex; 6 - slightly schematic drawing showing general organization of cell. C - cilia, CV - contractile vacuole, Ep - excretory pore of contractile vacuole, Ma - macronucleus, R - ciliary rows, T - tentacles. Bars 15 µm

could be identified in the swarmer, i.e. in *E. vermicularis*.

Electron microscopic description of *E. vermicularis*

Morphometric data shown in Table 1 are not repeated in this section.

Cortex: The cortex of *E. vermicularis* is about 54 nm thick and of usual structure, i.e. has a cell membrane followed by alveoli, which are very flat and small, and a thin layer of finely granular epiplasm (Fig. 23). The alveolar content is strongly osmiophilic and slightly thickened at the triangular alveolar junctions, which contain finely granular material, possibly epiplasm or a substance to which silver nitrate adheres, producing the silverline system (Fig. 5). As in other suctorians, there are small (about 160 x 130 nm) pits in the cortex covered only by the cell membrane and some epiplasm (Fig. 10). These pores strongly resemble the parasomal sacs around the cilia and are distinguishable from these only in the anterior pole region of the cell where no cilia occur.

Tentacles: The short cortical processes in the posterior half of the body each contain a slightly elliptical axoneme composed of two concentric microtubule cores (Figs. 1, 3, 6, 13; Table 1). The axonemes, which are not associated with barren basal bodies but often located near somatic cilia, originate deep in the cytoplasm and extend almost to the distal end of the tentacles where haptocysts are anchored (Figs. 16, 18). The microtubules of the outer core are linked to each other and to those of the inner core by strands of fibrogranular material. The microtubules of the inner core are very close together and carry distinct projections (arms) on the concave side of the axoneme, facing the lumen of the tentacle which is filled with cytoplasm containing dumb-bell shaped membranous structures (Figs. 12-16). The distal end of the tentacles, the knob, is covered by the cell membrane and the cortical alveoli which becomes evident in transverse sections (Fig. 11).

Three regions can be distinguished along the axoneme. Its distal portion is slightly conically dilated and shows five widely separate microtubule lamellae each in the outer and inner core (Fig. 12). In the middle region of the axoneme the number of microtubules increases slightly and those of the outer core become fairly evenly spaced. Those of the inner core remain

grouped to five lamellae, each composed of seven microtubules and parallel to the outer core (Figs. 13, 14; Table 1). However, their lamellar arrangement becomes inconspicuous in the proximal region of the axoneme, where the microtubules are almost as evenly spaced as those of the outer core (Fig. 15). No specializations were found around and at the base of the axoneme.

Haptocysts: These organelles are found mainly in the distalmost portion of the tentacles (Figs. 11-13, 18) but also within the axoneme (Fig. 19) and in the cytoplasm (Fig. 17). The cylindroid shaft is rounded anteriorly and composed of a finely granular coat, which is apparently continuous with the granular substance composing the barrel-shaped posterior bulb, and a heavily osmiophilic tube separated from the bulb by a strongly osmiophilic granulum (Figs. 17-19, Table 1). Very likely, radial structures project from the shaft and the bulb into the cytoplasm (arrows in Figs. 11, 17, 19), as described by Mogensen and Butler (1984) in *Trichophrya rotunda*.

Kinetids: In contrast to the tentacle axonemes, which were well preserved by the method used, the basal bodies and their fibrillar associates were not. However, the quality of the material was sufficient to analyze the kinetids in some detail. They are rotated 90° counterclockwise to the kinety axis (see discussion), i.e. the ciliary rows extend transversely to the longitudinal body axis, which must be taken into account in the following description.

The cilia and basal bodies are of usual structure and size (Figs. 20, 21; Table 1). Each kinetid has associated 2-3 postciliary microtubules at triplet 9, a kinetodesmal fibre at triplets 6 and 5, a transverse fibre at triplet 3, and 2 parasomal sacs (Figs. 20-22, 24).

The postciliary microtubules are slightly convergent and extend horizontally into the intrakinetal ridge, where they curve sharply backwards to the narrowed posterior end of the cell. They are rather long and several bundles thus overlap to form a loose array of 8-19 microtubules bridging 3-6 ciliary rows (Figs. 21, 22, 24; Table 1). Those of the last kinetids extend on the posterior pole area, where they form a dense, rather irregular sheet. The flattened kinetodesmal fibre is of usual structure and extends steeply upward to the centre of the interkinetal ridge, where its distal end becomes frayed and anchored to the epiplasm (Fig. 20). The kinetodesmal fibre is about 1300 nm long and extends anteriorly, seemingly connecting the kinetids of neighbouring rows (Fig. 22), as does the inconspicuous transverse fibre, however, in posterior direction. The parasomal sacs are at the posterior end of the kinetid, rather distant from the basal body and slightly oblique to the transverse body axis. The anterior sac is near the kinetodesmal fibre, while the posterior sac is between the postciliary

Table 1

Electron microscopic morphometric characteristics of *Enchelyomorpha vermicularis*[*]

Character	$\bar{x}$	M	SD	$SD_{\bar{x}}$	CV	Min	Max	n
Axoneme, diameter long axis	452.6	469.0	40.6	9.8	9.0	375	500	17
Axoneme, diameter short axis	413.7	417.0	40.2	9.8	9.7	344	469	17
Axoneme, number of microtubules in outer core	30.0	30.0	0.0	0.0	0.0	30	30	16
Axoneme, number of microtubules in inner core	35.0	35.0	-	-	-	34	35	18
Axoneme, number of microtubule ribbons in inner core	5.0	5.0	0.0	0.0	0.0	5	5	16
Axoneme, number of microtubules in ribbon of inner core	7.0	7.0	-	-	-	6	7	18
Cortex, thickness (with epiplasm)	52.0	54.0	9.0	2.7	17.4	31	63	11
Epiplasm, thickness	14.5	13.0	2.3	0.7	16.1	12	20	11
Basal body, length	334.8	344.0	17.8	5.4	5.3	313	366	11
Basal body, diameter	198.3	195.0	12.1	3.6	6.1	188	218	11
Parasomal sac, deepness	178.2	187.0	39.6	13.2	22.2	122	250	9
Parasomal sac, diameter	144.2	150.0	20.0	6.7	13.9	122	172	9
Postciliary microtubules, number per bundle in cortical ridges	12.9	12.0	3.7	1.4	28.8	8	19	7
Haptocyst, length	327.4	322.0	13.7	4.8	4.2	312	346	8
Haptocyst, width	135.4	135.5	13.8	4.9	10.2	122	154	8
Hydrogenosome, long axis	1249.0	1109.5	523.9	102.7	41.9	667	2688	26
Hydrogenosome, short axis	937.8	938.0	265.5	52.1	28.3	437	1344	26
Autophagous vacuole, long axis	743.7	703.0	214.1	36.7	28.8	437	1437	34
Autophagous vacuole, short axis	690.6	640.5	203.9	35.0	29.5	406	1437	34

* All data based on ultrathin sections of 4 cells fixed with glutaraldehyde and osmium tetroxide. Measurements in nm. Abbreviations: CV - coefficient of variation in %, M - median, Max - maximum, Min - minimum, SD - standard deviation, $SD_{\bar{x}}$- standard deviation of the mean, $\bar{x}$ - arithmetic mean

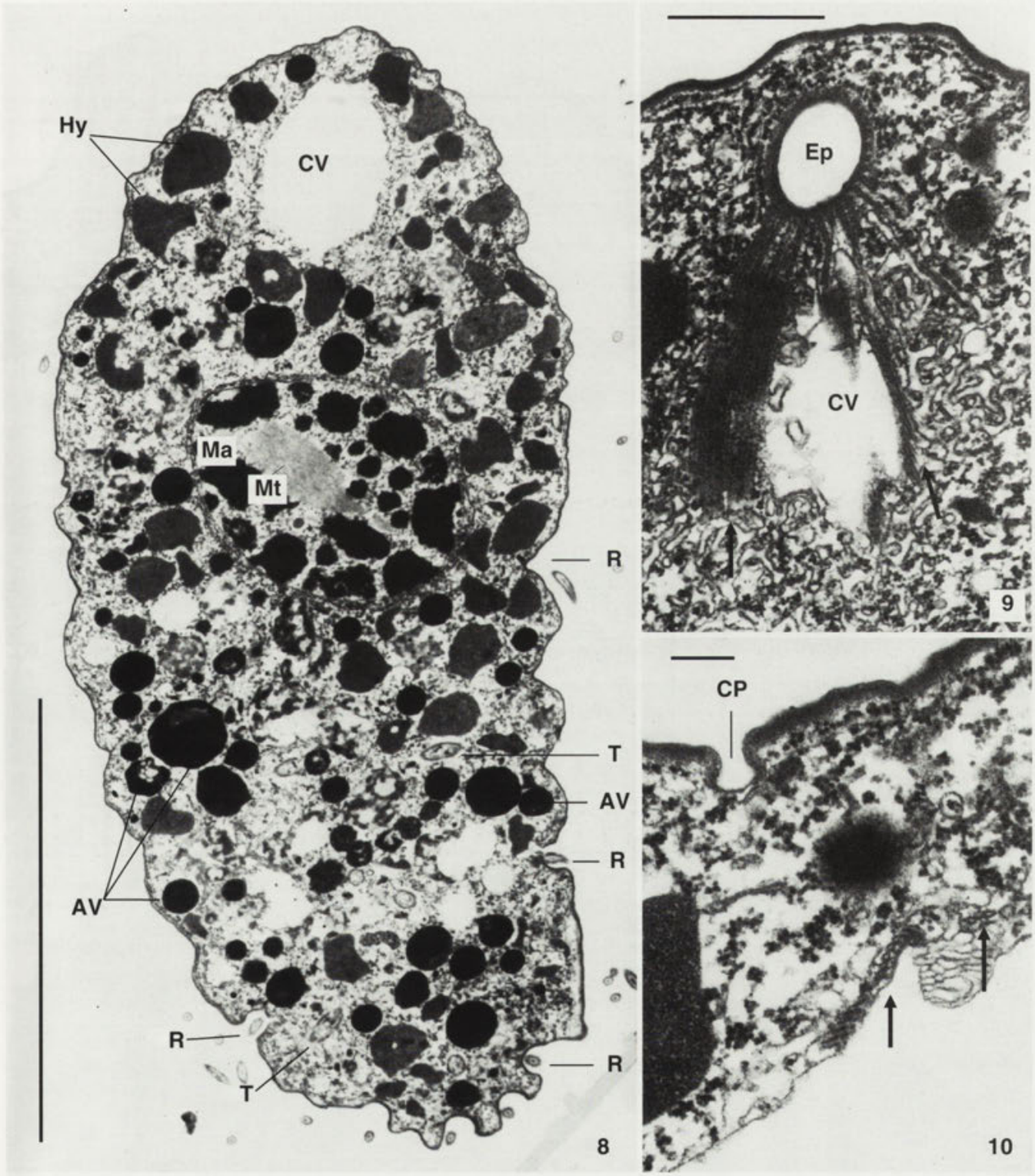

Figs. 8 - 10. Electron micrographs of the general organization and the contractile vacuole of *E. vermicularis*. 8 - longitudinal section showing the macronucleus (Ma) with a distinct microtubule bundle (Mt) inside, the contractile vacuole (CV) in the anterior end, transversely extending ciliary rows (R), tentacle axonemes (T), hydrogenosomes (Hy) and autophagous vacuoles (AV); 9, 10 - longitudinal sections through the anterior end showing a cortical pit (CP) and many microtubule bundles (arrows) originating at the excretory pore (Ep) and surrounding the contractile vacuole (CV) which is embeded in spongious cytoplasm. Bars - 10 μm (Fig. 8), 200 nm (Fig. 9), 1 μm (Fig. 10)

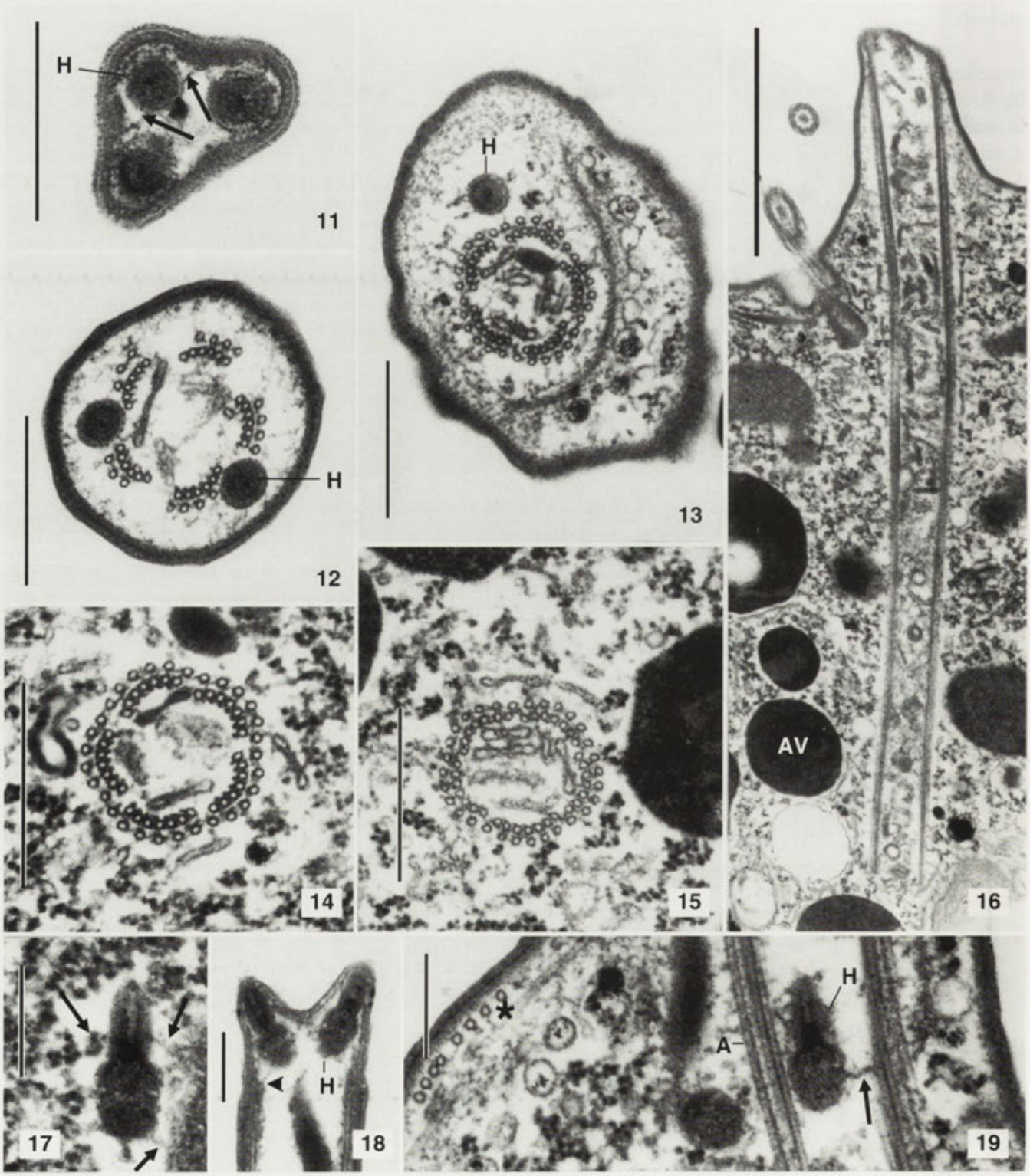

Figs. 11 - 19. Electron micrographs of the tentacles and haptocysts of *E. vermicularis*. 11, 12, 13, 14, 15 - transverse sections of tentacles arranged from the distal to the proximal end. The tentacles contain haptocysts (H) with radial projections (arrows) and a conspicuous axoneme composed of two concentric microtubule cores (Bars - 500 nm); 16 - longitudinal section of a tentacle filled with granular and membranous material. Some dark-stained autophagous vacuoles (AV) are recognizable in the cytoplasm (Bar - 1500 nm); 17, 18, 19 - haptocysts (H) occur in the cytoplasm and axoneme (A) and have a barrel-shaped posterior bulb. The arrows mark radial projections of the haptocysts, the arrowhead points to the distal end of the axoneme, and the asterisk marks transversely sectioned postciliary microtubules of the somatic kinetids. Bars 250 nm

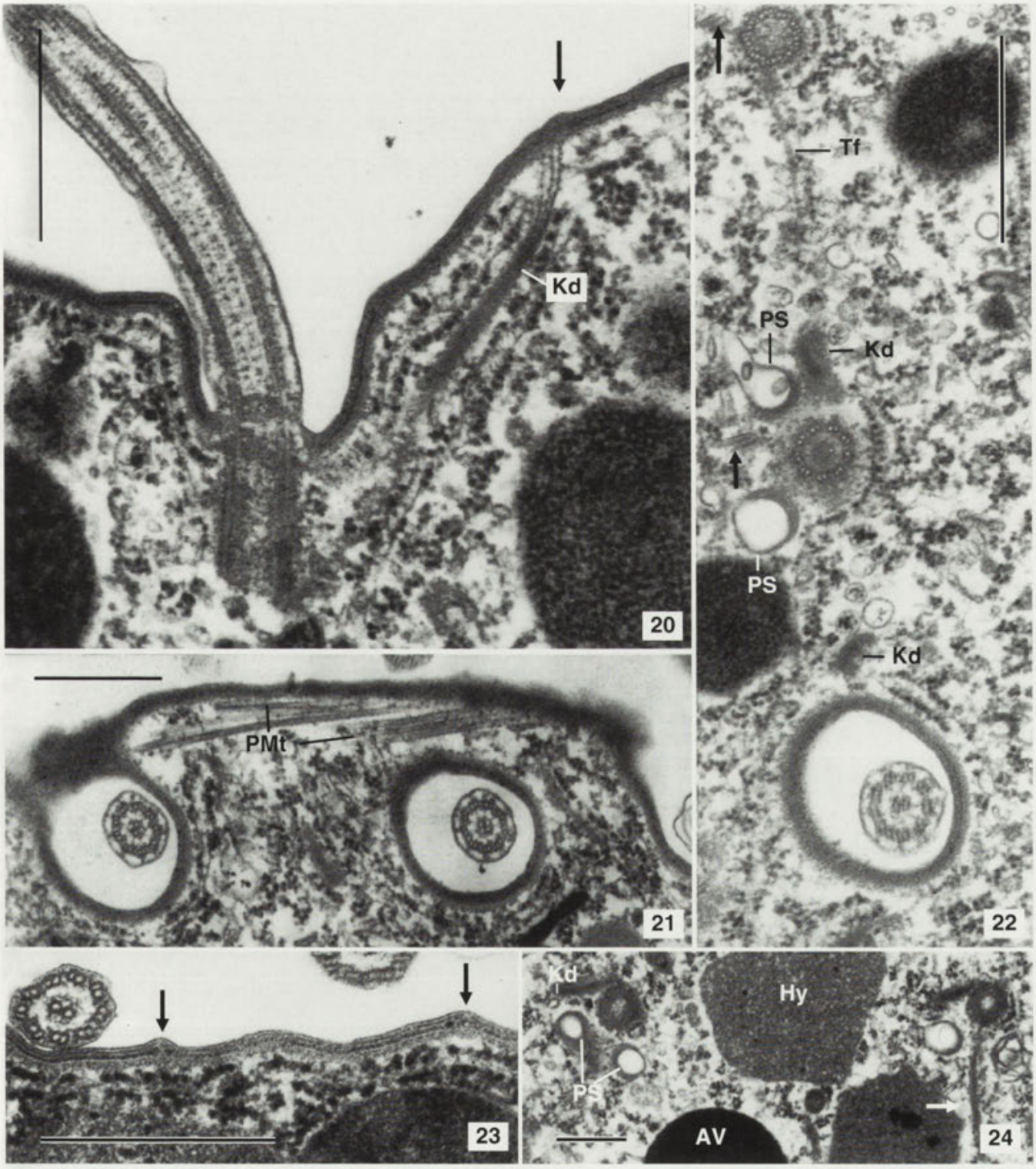

Figs. 20 - 24. Electron micrographs of the somatic kinetids and the cortex of *E. vermicularis*. 20 - longitudinal section of a kinetid showing the frayed distal end of the kinetodesmal fibre (Kd) anchored to the epiplasm (arrow); 21 - oblique section showing postciliary microtubule ribbons (PMt) extending into an interkinetal ridge; 22, 24 - transverse sections of somatic kinetids showing kinetodesmal fibers (Kd), a transverse fibre (Tf), postciliary microtubule ribbons (arrows) extending between the parasomal sacs (PS), hydrogenosomes (Hy) and autophagous vacuoles (AV); 23 - transverse section showing alveolar junctions in the cortex (arrows). Bars - 500 nm

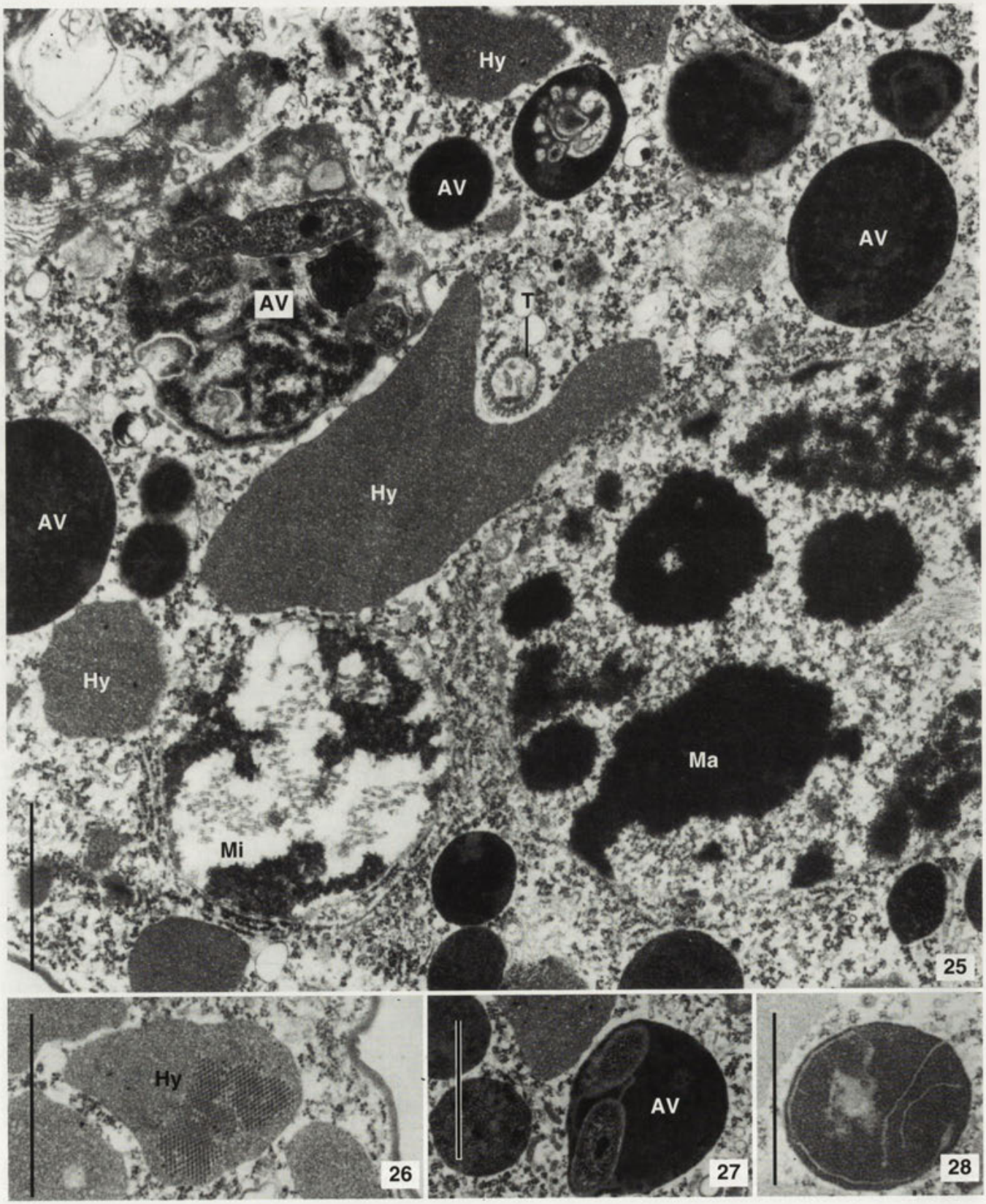

Figs. 25 - 28. Electron micrographs of *E. vermicularis* showing cytoplasmic inclusions, viz. the macronucleus (Ma), micronucleus (Mi), a tentacle axoneme (T), autophagous vacuoles (AV) and hydrogenosomes (Hy) which sometimes have crystalline inclusions (Fig. 26). Bars 1000 nm

ribbon and the transverse fibre. Thus, the proximal portion of the postciliary microtubule ribbon extends between the parasomal sacs, causing a characteristic kinetid pattern (Figs. 22, 24).

No subkinetal microtubules or barren basal bodies were found.

Nuclear apparatus: *E. vermicularis* has a roundish macronucleus (Figs. 1, 2, 6, 7) and an ellipsoid micronucleus which is difficult to recognize in the light microscope but prominent in the electron microscope due to many loosely arranged microtubules extending in its main axis (Fig. 25). Likewise, the macronucleus contains microtubules which are, however, more densely packed than those in the micronucleus (Figs. 8, 25). Both nuclei are surrounded by about four layers of rough endoplasmic reticulum and their ultrastructure appears similar to that known from other suctorian swarmers (e.g. Bardele 1969, Hauser 1970).

Contractile vacuole: *E. vermicularis* has a single contractile vacuole with a prominent excretory pore near the centre of the anterior pole (Figs. 2, 3, 6, 8-10). The vacuole is surrounded by spongious cytoplasm and a basket of microtubules which originate at the excretory pore and form distinct posteriorly extending ribbons (Figs. 9, 10).

Cytoplasmic inclusions: Two types of cytoplasmic inclusions were found which clearly differ in size and structure. The first type, probably hydrogenosomes, is rather irregularly shaped and has an average size of 1109 x 938 nm (Table 1). It is surrounded by at least one unit membrane and contains lightly stained, homogenously distributed, finely granular material (Figs. 24, 25). In two cells some of these bodies contained highly ordered inclusions, possibly protein crystals or virus particles (Fig. 26).

The second type of inclusion is more regularely shaped and smaller than type one, viz. has an average size of 703 x 640 nm (Table 1). These bodies are heavily stained and often contain a variety of inclusions, some of which are highly reminiscent of bacteria (Figs. 16, 24, 25, 27). Several stages of condensation can be clearly recognized in Fig. 25, suggesting that these inclusions are degenerating food vacuoles and/or autophagous vacuoles.

Morphogenesis

Swarmer formation commences by proliferation of basal bodies in small areas, one each to the right and left of the contractile vacuole (Fig. 29). These fields enlarge and become convex, while a distinct bundle of microtubules (?) appears in the centre of the macronucleus (Fig. 30). By continued growth and enfolding the distances between the basal bodies are increased and the margins of each ciliary field become connected, producing two ellipsoid swarmers within an adult (Fig. 31). Only one swarmer was observed in about 10% of the morphogenetic active cells.

Unfortunately, the slides did not contain stages showing either the division of the macronucleus, which is one of the latest events in embryogenesis (Bardele 1970), or the release of the swarmers.

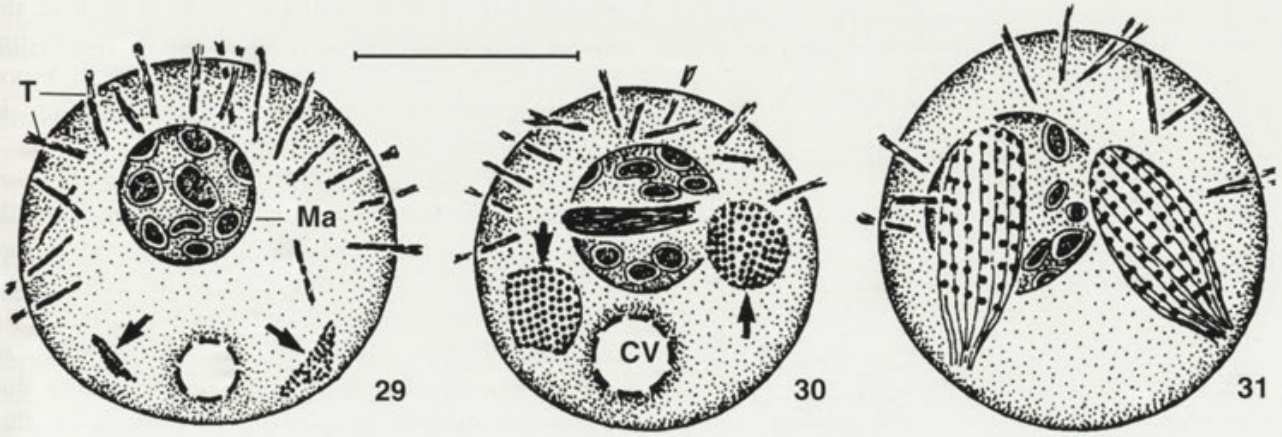

Figs. 29 - 31. Early and middle stages of swarmer formation in *E. vermicularis*. Usually, two swarmers (arrows) are produced, one each to the right and left of the contractile vacuole. CV - contractile vacuole, Ma - macronucleus, T - tentacles. Bar - 10 µm

DISCUSSION

Enchelyomorpha, a "good" suctorian

Lynn and Foissner (1994) reviewed the distribution of tentacle and tentacle-like structures in ciliates. This compilation shows that suctorians are unique in having two concentric microtubule cores in their tentacles. The outer core may or may not be complete and the inner core is always composed of ribbons of arm-bearing microtubules. The axonemes of *E. vermicularis* match this pattern perfectly (Figs. 12-16), leaving no doubt as to its suctorian relationship. This is supported by the occurrence of haptocysts, a type of extrusome as yet found only in this group of ciliates (Batisse 1994), and also by its mode of reproduction, viz. endogenous budding.

The position of *Enchelyomorpha* within the Suctoria

Classification of taxa within the suctorians is mainly according to the mode of swarmer production, which is polygemmic and internal in *Enchelyomorpha* (Figs. 29-31). Thus, *Enchelyomorpha* belongs to the Entotropida or Endogenina, depending on the classification preferred (Batisse 1994, Corliss 1979). It is just this order which contains two other peculiar suctorians, viz. *Allantosoma*, living in the cecum and colon of horses, and *Cyathodinium*, inhabiting the cecum of domestic pigs (Batisse 1994). Batisse (1994) uses details of the swarmer formation for subordinal classification. Unfortunately, such details are not known for *Enchelyomorpha*. However, data are sufficient to discuss some affinities. A relationship of *Enchelyomorpha* with the Acinetina is indicated by the fine structure of the tentacles and the general organization and ciliature of the swarmer, whereas swarmer production resembles *Cyathodinium* in the suborder Discophryina.

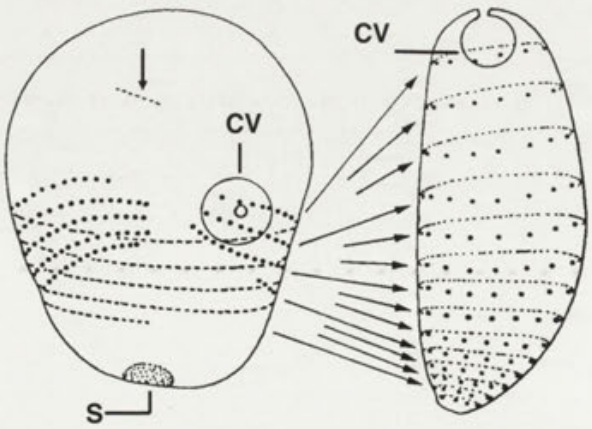

Fig. 32. The enchelyomorphid swarmer can be derived from a tokophryid bud simply by increasing the number and spreading of its circular-transverse ciliary rows. The arrow marks a short, oblique ciliary row lacking in *E. vermicularis*. CV - contractile vacuole, S - scopuloid. Based on figures by Augustin and Foissner (1989, 1992)

As concerns the tentacle axonemes, those of *Acineta* (Bardele and Grell 1967), *Tokophrya* (Rudzinska 1967, 1970), *Cyathodinium* (Paulin and Corliss 1969) and *Enchelyomorpha* (Figs. 12-16) are extremely similar not only in the number of microtubules comprising the axonemes but also in that the lamellae of the inner core are only slightly curved and thus almost parallel to the outer microtubule core. Unfortunately, other members of the Acinetidae and Tokophryidae have tentacle axonemes which look rather dissimilar to those of *Enchelyomorpha*. Their lamellae are distinctly curved and often composed of hundreds of microtubules, e.g. in *Acinetopsis* (Grell and Meister 1982a), *Trematosoma* (Batisse 1972), *Choanophrya* (Hitchen and Butler 1973a), and *Rhyncheta* (Hitchen and Butler 1974). The fine structure of the tentacle axoneme is thus very likely a weak character for establishing phylogenetic relationships.

We thus place more weight on the symmetry and ciliature of the swarmer. Both *Tokophrya* and *Enchelyomorpha* have monaxone, oblong swarmers and possess circular-transverse ciliary rows. It is easy to imagine how an enchelyomorphid swarmer originates from a tokophryid swarmer simply by increasing the number of ciliary rows (Fig. 32). Unfortunately, this attractive hypothesis has some shortcomings. In contrast to *Enchelyomorpha*, *Tokophrya* and *Acineta* swarmers typically have a short, oblique ciliary row near the inflated anterior end and lack tentacles in the free-swimming (larval) stage. Furthermore, the typical brood pouch of the Acinetina is apparently lacking in *Enchelyomorpha* (Figs. 29-31).

There is a striking similarity between *Enchelyomorpha* and *Cyathodinium* during the early and middle stages of swarmer production: both develop two swarmer anlagen at opposite sites of the adult (Figs. 29-31; Cunha and Freitas 1940, Lucas 1932, Nie 1950). Unfortunately, we did not find late dividers of *Enchelyomorpha*, but there is a fair probability that they look similar to those of *Cyathodinium*, i.e. that budding is evaginative and *Enchelyomorpha* thus belongs to the Discophryina.

Enchelyomorpha obviously has a highly distinct combination of characters which suggests maintenance of the family Enchelyomorphidae Augustin and

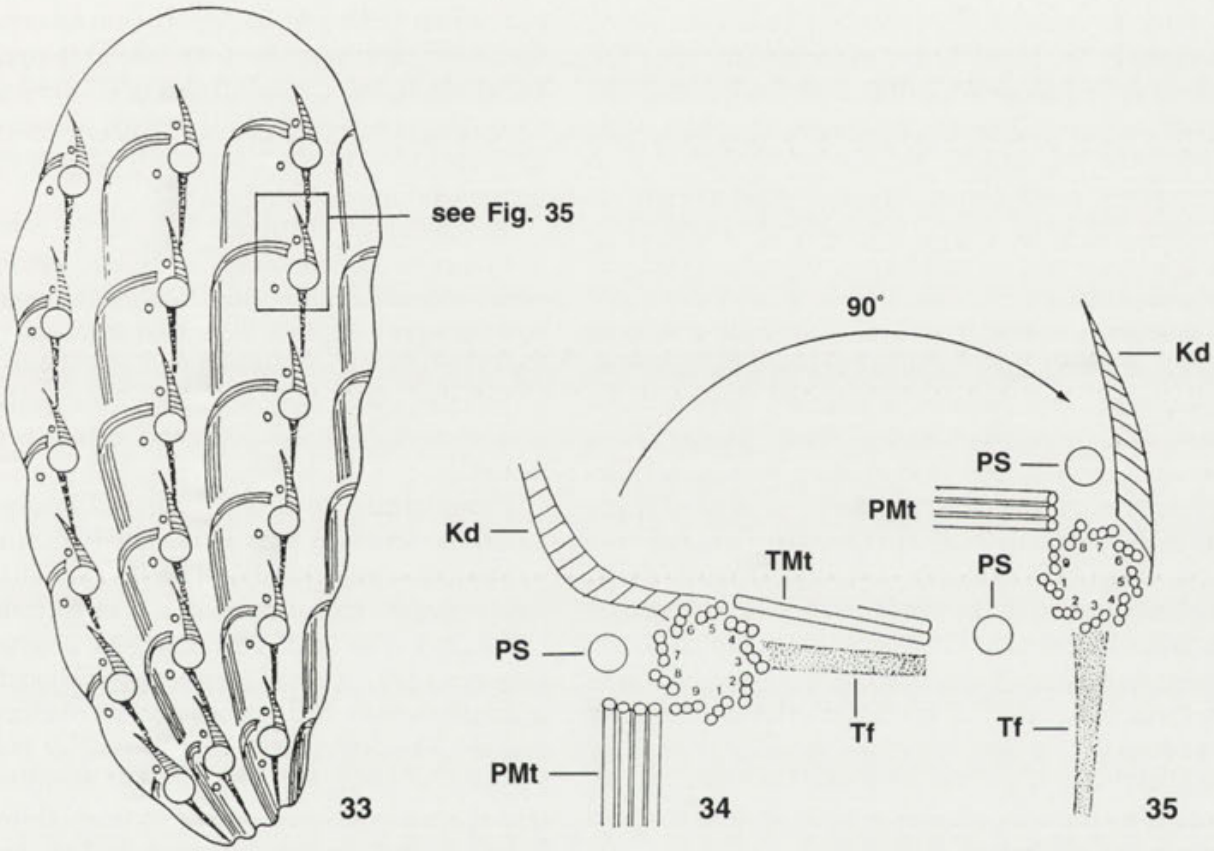

Figs. 33 - 35. Schemes of the cortical fine structure of *E. vermicularis* (33, 35) and *Trithigmostoma steini* [34; from Hofmann and Bardele (1987), subkinetal microtubules omitted]. The typical kinetid pattern of *Enchelyomorpha* can be modelled by a 90° rotation of the *Trithigmostoma* kinetid, if it is assumed that the narrowed portion of *Enchelyomorpha* is its posterior end. Kd - kinetodesmal fibre, PMt - postciliary microtubule ribbon, PS - parasomal sac, TMt - transverse microtubule ribbon, Tf - transverse fibre. Numbers designate triplets of basal body

Foissner, 1992. This is strengthened by the lack of mitochondria, i.e. its anaerobic mode of life.

Fine structural comparison

Having shown that *E. vermicularis* is a suctorian swarmer, a more detailed comparison of its structure with related taxa seems appropriate. However, most electron microscopic data on suctoria are from adult cells (Batisse 1994), while our investigations on *Enchelyomorpha* concern the swarmer only. This limits a fruitful comparison considerably and it is quite possible that, for instance, the simple tentacle structure of *Enchelyomorpha* is a juvenile character. We thus restrict the comparison to a few main structures, namely the tentacles, the somatic kinetids and the cytoplasmic inclusions.

Tentacles and haptocysts: The tentacles of *Enchelyomorpha* appear simple when compared to those of many other suctorians, e.g. *Trichophrya rotunda* (Mogensen and Butler 1984), *Rhyncheta cyclopum* (Hitchen and Butler 1974), *Discophrya* (Curry and Butler 1976), *Acinetopsis rara* (Grell and Meister 1982a), and *Ephelota gemmipara* (Grell and Benwitz 1984a). The most remarkable feature concerns the distal end, i.e. the tip containing the haptocysts, which is very likely sealed by the full set of cortical membranes, whereas it is covered solely by the cell membrane in other species. However, this might be a juvenile feature, because the tip of the growing tentacles of *Choanophrya infundibulifera* is also covered by the cell membrane and the cortical alveoli (Hitchen and Butler 1973b). Growing suctorian tentacles are usually associated with a non-ciliated basal body which possibly acts as an organizing centre for the microtubules of the axoneme [see Hitchen and Butler (1973b) for short review]. No barren basal bodies have been observed in *E. vermicularis* which

matches results by Grell and Benwitz (1984b) on *Ephelota gemmipara* and *E. plana*.

The haptocysts of *E. vermicularis* look rather simple compared with those of other suctorians (Batisse 1994, Jurand and Bomford 1965, Mogensen and Butler 1984). Specifically, the proximal portion of the shaft is not dilated and the granular material in the bulb appears homogenous. Furthermore, the bulb is not globular, as is usual, but barrel-shaped. Similar haptocysts occur in *Ephelota* spp. according to the micrographs in Grell and Benwitz (1984a).

Somatic kinetids: The pioneering study of Batisse (1972) showed a basic similarity between the suctorian, cyrtophorid and rhynchodid kinetids. It provided a strong argument for uniting these groups in a monophyletic taxon, the class Phyllopharyngea (Puytorac et al. 1974), which is still recognized (Lynn 1991, Puytorac et al. 1993). This view has not been contradicted by later studies (Grell and Benwitz 1984a, b, Mogensen and Butler 1984) and is also supported by our investigations. In fact, the enchelyomorphid kinetid pattern can be easily modelled by a simple rotation of the cyrtophorid kinetid (Figs. 33-35). However, detailed studies on the fine structure of the suctorian kinetids are not available, and our own study also has shortcomings. Thus a substantial comparison is difficult and should await more detailed investigations.

Enchelyomorpha vermicularis has a holotrichous ciliature with basal bodies so regularly arranged that the ciliary rows can be interpreted as extending longitudinally or transversely with respect to the swarmer axes (Figs. 5, 7). The electron microscopic investigations showed that the proximal portion of the postciliary microtubule ribbon extends in the transverse axis of the swarmer, while the longer distal portion curves backwards to the narrowed end of the cell. Accordingly, the kinetodesmal and transverse fibres extend along the main body axis. If it is accepted that the postciliary microtubules and the kinetodesmal fibres define the orientation of the kinetid, then the ciliary rows extend transversely and the kinetids are rotated 90° counterclockwise with respect to the longitudinal body axis and the cyrtophorid kinetid pattern. This interpretation appears reasonable because most suctorian swarmers, especially those of the Acinetina to which *Enchelyomorpha* possibly belongs, have circular-transverse ciliary rows with ends almost touching each other (Batisse 1994, Grell and Benwitz 1984b, Guilcher 1951).

In *Trematosoma bocqueti* two parasomal sacs occur in the posterior area of the kinetid (Batisse 1972), whereas *Acinetopsis rara* has only one sac at the right side of the basal body near the kinetodesmal fibre (Grell and Meister 1982b). In *Trichophrya rotunda* a parasomal sac occurs on either side of the kinetid (Mogensen and Butler 1984). The parasomal sacs of *E. vermicularis* are located as in *T. bocqueti*, if it is taken into account that the ciliary rows extend transversely to the longitudinal body axis (Figs. 22, 24, 33, 35).

A remarkable difference between *E. vermicularis* and other suctorians concerns the kinetodesmal fibre which not only extends close beneath the epiplasm but definitely contacts it *via* the frayed distal end (Fig. 20). This resembles some colpodid ciliates (Lynn 1976).

Whether subkinetal microtubules are really lacking in *E. vermicularis* needs confirmation from better fixed material.

Cytoplasmic inclusions: *Enchelyomorpha vermicularis* definitely lacks structures which could be interpreted as mitochondria. This is in accordance with most faunistic records, showing it to be restricted to microaerobic or anaerobic biotopes (Augustin and Foissner 1992). Thus, *E. vermicularis* should possess hydrogenosomes and endosymbiotic (methanogenic) bacteria like other anaerobic ciliates [for review see Fenchel and Finlay (1991)]. We could not identify such organelles unequivocally in the sections. However, the lightly stained, rather irregular bodies distributed throughout the cytoplasm closely resemble hydrogenosomes known from, e.g. *Trimyema* (Finlay et al. 1993), *Plagiopyla* (Berger and Lynn 1992) and an anaerobic suctorian, *Cyathodinium* (Paulin 1973), living in the cecum of pigs, although we could not identify a double membrane surrounding them which might, however, be due to inadequate fixation (Paul et al. 1990).

Structures resembling bacteria (methanogens) were not found in the cytoplasm but often in the dark globules interpreted as autophagosomes (Figs. 25, 27, 28). Likewise, stalk (scopuloid) granules and scopular pores as described in several suctorian swarmers (Bardele 1970, Grell and Benwitz 1984b, Grell and Meister 1982b, Hascall and Rudzinska 1970, Mignot and Puytorac 1968) are apparently lacking in *E. vermicularis*. In fact, we could not identify any structure reminiscent of a scopuloid. The adult of *E. vermicularis* is thus very likely stalkless.

Acknowledgements. Supported by the Austrian FWF (Project PO8924-BIO). The technical assistance of Dr. Eva Herzog, Maria Waldhör, Andreas Zankl and Mag. Eric Strobl is greatly acknowledged. Special thanks to Prof. A. Batisse (Univ. Paris) who draws our attention to *Cyathodinium*.

REFERENCES

Augustin H., Foissner W. (1989) Morphologie einiger Ciliaten (Protozoa: Ciliophora) aus dem Belebtschlamm. *Lauterbornia* **1**: 38-59

Augustin H., Foissner W. (1992) Morphologie und Ökologie einiger Ciliaten (Protozoa: Ciliophora) aus dem Belebtschlamm. *Arch. Prostistenk.* **141**: 243-283

Bardele C. F. (1969) *Acineta tuberosa* II. Die Verteilung der Mikrotubuli im Makronucleus während der ungeschlechtlichen Fortpflanzung. *Z. Zellforsch.* **93**: 93-104

Bardele C. F. (1970) Budding and metamorphosis in *Acineta tuberosa*. An electron microscopic study on morphogenesis in suctoria. *J. Protozool.* **17**: 51-70

Bardele C. F. (1989) From ciliate ontogeny to ciliate phylogeny: a program. *Boll. Zool.* **56**: 235-244

Bardele C. F., Grell K. G. (1967) Elektronenmikroskopische Beobachtungen zur Nahrungsaufnahme bei dem Suktor *Acineta tuberosa* Ehrenberg. *Z. Zellforsch.* **80**: 108-123

Batisse A. (1972) Premières observations sur l'ultrastructure de *Trematosoma bocqueti* (Guilcher), Batisse (Ciliata, Suctorida). *Protistologica* **8**: 477-495

Batisse A. (1994) Sous-classe des Suctoria Claparède et Lachmann, 1958. *Traité de Zoologie* **2**(2): 493-563

Berger J., Lynn D. H. (1992) Hydrogenosome-methanogen assemblages in the echinoid endocommensal plagiopylid ciliates, *Lechriopyla mystax* Lynch, 1930 and *Plagiopyla minuta* Powers, 1993. *J. Protozool.* **39**: 4-8

Blatterer H., Foissner W. (1988) Beitrag zur terricolen Ciliatenfauna (Protozoa: Ciliophora) Australiens. *Stapfia*, Linz **17**: 1-84

Collin B. (1912) Étude monographique sur les acinétiens II. Morphologie, physiologie, systématique. *Archs Zool. exp. gèn.* **51**: 1-457

Corliss J. O. (1979) The Ciliated Protozoa. Characterization, Classification and Guide to the Literature. 2 ed. Pergamon Press, Oxford, New York, Toronto, Sydney, Paris, Frankfurt

Cunha A.M. da, Freitas G. (1940) Ensaio monográfico da familia Cyathodiniidae. *Mem. Inst. Osw. Cruz* **35**: 457-494 (in Portuguese with English summary)

Curry A., Butler R. D. (1976) The ultrastructure, function and morphogenesis of the tentacle in *Discophrya* sp. (Suctorida) Cileatea. *J. Ultrastruct. Res.* **56**: 164-176

Fenchel T., Finlay B. J. (1991) The biology of free-living anaerobic ciliates. *Europ. J. Protistol.* **26**: 201-215

Finlay B. J., Embley T. M., Fenchel T. (1993) A new polymorphic methanogen, closely related to *Methanocorpusculum parvum*, living in stable symbiosis within the anaerobic ciliate *Trimyema* sp. *J. gen. Microbiol.* **139:** 371-378

Foissner W., Blatterer H., Foissner I. (1988) The Hemimastigophora (*Hemimastix amphikineta* nov. gen., nov. spec.), a new protistan phylum from Gondwanian soils. *Europ. J. Protistol.* **23**: 361-383

Grell K. G., Benwitz G. (1984a) Die Ultrastruktur von *Ephelota gemmipara* Hertwig und *E. plana* Wailes (Suctoria): Ein Vergleich I. Die adulte Form. *Protistologica* **20**: 205-233

Grell K. G., Benwitz G. (1984b) Die Ultrastruktur von *Ephelota gemmipara* Hertwig und *E. plana* Wailes (Suctoria): Ein Vergleich II. Der Schwärmer. *Protistologica* **20**: 437-461

Grell K. G., Meister A. (1982a) Die Ultrastruktur von *Acinetopsis rara* Robin (Suctoria) I. Tentakeln und Nahrungsaufnahme. *Protistologica* **18**: 67-84

Grell K. G., Meister A. (1982b) Die Ultrastruktur von *Acinetopsis rara* Robin (Suctoria) II. Zellbau und Schwärmerbildung. *Protistologica* **18**: 403-421

Guilcher Y. (1951) Contribution a l'étude des ciliés gemmipares, chonotriches et tentaculifères. *Annls. Sci. nat. (Zool.)* **13**: 33-133

Hascall G. K., Rudzinska M. A. (1970) Metamorphosis in *Tokophrya infusionum*; an electron-microscope study. *J. Protozool.* **17**: 311-323

Hauser M. (1970) Elektronenmikroskopische Untersuchung an dem Suktor *Paracineta limbata* Maupas. *Z. Zellforsch.* **106**: 584-614

Hitchen E. T., Butler R. D. (1973a) Ultrastructural studies of the commensal suctorian, *Choanophrya infundibulifera* Hartog I. Tentacle structure, movement and feeding. *Z. Zellforsch.* **144**: 37-57

Hitchen E. T., Butler R. D. (1973b) Ultrastructural studies of the commensal suctorian, *Choanophrya infundibulifera* Hartog II. Tentacle morphogenesis. *Z. Zellforsch.* **144**: 59-73

Hitchen E. T., Butler R. D. (1974) The ultrastructure and function of the tentacle in *Rhyncheta cyclopum* Zenker (Ciliatea, Suctorida). *J. Ultrastruct. Res.* **46**: 279-295

Hofmann A. H., Bardele C. F. (1987) Stomatogenesis in cyrtophorid ciliates I. *Trithigmostoma steini* (Blochmann, 1895): from somatic kineties to oral kineties. *Europ. J. Protistol.* **23**: 2-17

Jurand A., Bomford R. (1965) The fine structure of the parasitic suctorian *Podophrya parameciorum*. *J. Microscopie* **4**: 509-522

Kahl A. (1926) Neue und wenig bekannte Formen der holotrichen und heterotrichen Ciliaten. *Arch. Protistenk.* **55**: 197-438

Kahl A. (1930) Urtiere oder Protozoa I: Wimpertiere oder Ciliata (Infusoria) 1. Allgemeiner Teil und Prostomata. *Tierwelt Dtl.* **18**: 1-180

Kahl A. (1931) Über die verwandtschaftlichen Beziehungen der Suctorien zu den prostomen Infusorien. *Arch. Protistenk.* **73**: 423-481

Kent W. S. (1880-1882) A Manual of the Infusoria: Including a Description of All Known Flagellate, Ciliate, and Tentaculiferous Protozoa British and Foreign, and an Account of the Organization and Affinities of the Sponges. Vols. I-III. David Bogue, London, 913pp. (Vol. I 1880: 1-432; Vol. II 1881: 433-720, 1882: 721-913; Vol. III 1882: Plates)

Kormos J., Kormos J. (1957) Die entwicklungsgeschichtlichen Grundlagen des Systems der Suctorien I. *Acta zool. hung.* **3**: 147-162

Liebmann H. (1936) Die Ciliatenfauna der Emscherbrunnen. *Z. Hyg. InfektKrankh.* **118**: 555-573

Lucas M.S. (1932) The cytoplasmatic phases of rejuvenescence and fission in *Cyathodinium piriforme*. II. A type of fission heretofore undescribed for ciliates. *Arch. Protistenk.* **77**: 407-423

Lynn D. H. (1976) Comparative ultrastructure and systematics of the Colpodida. Fine structural specializations associated with large body size in *Tillina magna* Gruber, 1880. *Protistologica* **12**: 629-648

Lynn D. H. (1981) The organization and evolution of microtubular organelles in ciliated protozoa. *Biol. Rev.* **56**: 243-292

Lynn D. H. (1991) The implications of recent descriptions of kinetid structure to the systematics of the ciliated protists. *Protoplasma.* **164**: 123-142

Lynn D. H., Foissner W. (1994) The feet of *Pseudochlamydonellopsis plurivacuolata* (Ciliophora, Cyrtophorida) and a brief review of tentacle-like structures of ciliates. *Europ. J. Protistol.* **30**: 423-430

Matthes D. (1988) Suctoria (Sauginfusorien). *Protozoenfauna* **7/1**: 1-226

Mignot J-P., Puytorac P. de (1968) Sur la structure et la formation du style chez l'acinétien *Discophrya piriformis* Guilcher. *C. r. hebd. Séanc. Acad. Sci., Paris* **266**: 593-595

Mogensen M. M., Butler R. D. (1984) Cytological studies of *Trichophrya rotunda* (Hentschel). *J. Protozool.* **31**: 101-111

Nie D. (1950) Morphology and taxonomy of the intestinal protozoa of the guinea-pig, *Cavia porcella*. *J. Morph.* **86**: 381-493

Paul R. G.,Williams A. G., Butler R. D. (1990) Hydrogenosomes in the rumen entodiniomorphid ciliate *Polyplastron multivesiculatum*. *J. gen. Microbiol.* **136:** 1981-1989

Paulin J. J.(1973) The resorption of cilia in *Cyathodinium piriforme*. *J. Protozool.* **20**: 281-285

Paulin J. J., Corliss J. O. (1969) Ultrastructural and other observations which suggest suctorian affinities for the taxonomically enigmatic ciliate *Cyathodinium*. *J. Protozool.* **16**: 216-223

Puytorac P. de, Batisse A., Bohatier J., Corliss J. O., Deroux G., Didier P., Dragesco J., Fryd-Versavel G., Grain J., Grolière C.,

Hovasse R., Iftode F., Laval M., Roque M., Savoie A., Tuffrau M. (1974) Proposition d'une classification du phylum Ciliophora Doflein, 1901 (réunion de systématique, Clermont-Ferrand). C. r. hebd. Séanc. Acad. Sci., Paris **278**: 2799-2802

Puytorac P. de, Batisse A., Deroux G., Fleury A., Grain J., Laval-Peuto M., Tuffrau M. (1993) Proposition d'une nouvelle classification du phylum des protozoaires Ciliophora Doflein, 1901. *C. r. hebd. Séanc. Acad. Sci., Paris* **316**: 716-720

Rudzinska M. A. (1967) Ultrastructures involved in the feeding mechanism of suctoria. *Trans. N. Y. Acad. Sci.* **29**: 512-525

Rudzinska M. A. (1970) The mechanism of food intake in *Tokophrya infusionum* and ultrastructural changes in food vacuoles during digestion. *J. Protozool.* **17**: 626-641

Smith J. C. (1899) Notices of some undescribed infusoria, from the infusorial fauna of Louisiana. *Trans. Am. microsc. Soc.* **20**: 51-56

Received on 6th May, 1994; accepted on 1st September, 1994

ACTA
PROTOZOOLOGICA

Acta Protozoologica (1995) 34: 35 - 44

Ultrastructural Examination of Virus-like Particles in a Marine Rhizopod (Sarcodina, Protista)

Diana L. LIPSCOMB and Gavin P. RIORDAN

Department of Biological Sciences, George Washington University, Washington D.C., USA

Summary. Recent research indicates that bacteriophages are abundant and important for controlling populations in prokaryote microbial communities. The number and role of viruses in eukaryotic microbial communities is less well known. This report demonstrates the presence of polyhedral virus-like particles infecting a free-living, marine rhizopod. The virus-like particle appears to cause cell damage and possibly death. It is able to replicate within the protist and may be able to spread to other members of the population. A survey of the literature indicates that viruses and virus-like particles are present in other protists, perhaps more commonly than usually reported. If viruses are widely dispersed in eukaryote microbial populations, they could contribute significantly to cycling in aquatic food webs and have implications for gene transfer between marine organisms.

Key words. Viruses of protists, *Corythionella*, marine microbiology, electron microscopy.

INTRODUCTION

Within the last few years it has become apparent that bacteriophages are abundant in aquatic habitats (Bergh et al. 1989, Børsheim et al. 1990) where they play an important role in microbial food webs both as prey (Gonzalez and Suttle 1993) and in releasing significant amounts of bacterial carbon to the dissolved organic carbon pool by lysing bacterial cells (Bratbak et al. 1990, Thingstad et al. 1993). Furthermore, viruses play a significant role in regulating bacteria and cyanobacteria populations (Proctor and Fuhrman 1990, Suttle et al. 1990). Although reports of viruses infecting protists are relatively rare, because they are also subject to infection and lysis it is likely that viral parasitism plays an important, but poorly understood, ecological role in eukaryotic microbial communities (Laybourn-Parry 1992).

This study documents the presence of a virus-like particle (VLP) similar in morphology to a herpes virus in a marine rhizopod and reviews what is known about viral infection in protists.

MATERIALS AND METHODS

The rhizopod, *Corythionella* sp. Golemansky, 1974 (Euglyphidae, Gromiida), was collected from the upper 5 mm layer of sand from marine water of Rehoboth Bay, Delaware. For electron microscopy, the amoebae were transferred to beem capsule baskets (Hayunga 1977) in petri dishes containing 2.5% v/v glutaraldehyde in 0.05M sodium cacodylate buffer with 0.7M sucrose and 2mM MgCl. They were fixed at room temperature for one hour, rinsed with the buffer solution and postfixed in 2% buffered OsO_4 for 30 min. Cells were dehydrated and

Address for correspondence: D. L. Lipscomb, Department of Biological Sciences, George Washington University, Washington D.C. 20052, USA; Fax (202) 994-6100; E-mail:biodl@gwuvm.gwu.edu

embedded in Epon 812. Ultrathin sections were stained with 4% uranyl acetate followed by 0.2% lead citrate. The sections were examined and photographed with a Zeiss-10 electron microscope. It was not possible to establish a culture of *Corythionella* in the laboratory and, therefore, not possible to examine the molecular biology or transmission of the virus-like particles.

RESULTS

Virus-like particles (VLPs) are seen within the nucleus and cytoplasm of *Corythionella* (Fig. 1). Unlike some other viruses or VLPs reported from protists, none were seen in any of the other cytoplasmic organelles or food vacuoles. Profiles of the VLPs were either hexagonal or pentagonal in section (Fig. 2). In an icosahedron, a section perpendicular to the 3-fold axis of rotational symmetry is hexagonal and, if perpendicular to the 5-fold axes, is pentagonal. Therefore, the VLPs of *Corythionella* are probably icosahedral. The VLPs are 80±5 nm in diameter with the wall of the capsid measuring approximately 5 nm thick and the core 70-75 nm in diameter. No tail, filaments, or injection tubes were seen in thin sections.

Within the nucleus, the VLPs are evenly distributed and not packed into paracrystalline arrays (Figs. 1, 2, 4). Depending on the plane of section, the core varies in density from apparently empty particles, to those containing a peripheral ring of electron dense material, to those filled with darkly staining material (Fig. 2). The cytoplasmic VLPs are in a localized area of ribosome-free cytoplasm adjacent to the nucleus (Fig. 3). The core of the cytoplasmic VLPs are filled with darkly staining material and each is surrounded by a membrane. The cytoplasmic VLPs are not packed into paracrystalline arrays nor surrounded by a common membrane. The morphology of the VLPs is thus consistent with those viruses that replicate and are encapsulated in the nucleus, then bud through the nuclear membrane (acquiring individual membranes), and accumulating in the cytoplasm of their host cells.

The cell organelles of the infected rhizopod show some cytopathenogenic characteristics. The nucleus of the rhizopod is normally spherical with evenly distributed chromatin. In infected cells, the nucleus shows some lobulation and the chromatin is found around the peripheral margin under the nuclear envelope (Fig. 4). The nucleus otherwise appears normal - there are no multiple lamellae of the nuclear membrane nor granular or fibrillar inclusions as are seen in some virally infected cells. The organelles of the cytoplasm do not appear healthy: the endoplasmic reticulum is swollen and the mitochondrial cristae have degenerated (Figs. 1, 4). The mode of infection of the amoeba by the VLP is unknown. A ciliate, *Chaenea teres*, that was isolated from the same habitat was not infected (Lipscomb and Riordan 1990).

DISCUSSION

Comparison of the Virus-like Particles from *Corythionella* to Known Viruses

Ultrastructural examination of cells is often used as a direct and accurate means for diagnosing many virus infections (Doane and Anderson 1987, Grimley and Henson 1981). Based on morphological criteria, we believe the VLPs found in *Corythionella* are most like herpes viruses, although transmissibility has not been demonstrated. This assumption is based on their general appearance, size, geometry, and their location in both the nucleus and cytoplasm. Furthermore, the cytopathogenic effects on *Corythionella* are characteristic of viral infection. The reasons for this conclusion are explained here in more detail. Using ultrastructural examination, virus families can be distinguished in part by shape and size of the capsid and the presence or absence of an envelope (Doane and Anderson 1987, Grimley and Henson 1981). The capsomeres of eukaryote viruses have either a rod-like, spherical or polyhedral geometry. Polyhedral capsomeres, such as are seen in the VLP described here, may be packed together so that the resulting capsid is an icosahedron. There are four DNA virus families with icosahedral capsids that infect eukaryotes: parvovirus, papovavirus, adenovirus, and herpes virus. There are three RNA virus families with icosahedral capsids that infect eukaryotes: reovirus, picornavirus, and togavirus. The rhizopod virus described here has an icosahedral capsid and, unless it is a previously undescribed type of virus, must belong to one of these seven groups.

The size of any virion is relatively uniform throughout each family. The VLP described here is 805 nm in diameter. This means it is far too large to be a parvovirus, papovavirus, picornavirus, or togavirus. Its size is compatible with that reported for adenovirus, herpes virus, and reovirus. The rhizopod VLPs in the cytoplasm of the host cell are surrounded by individual membrane envelopes. Adenoviruses and reoviruses

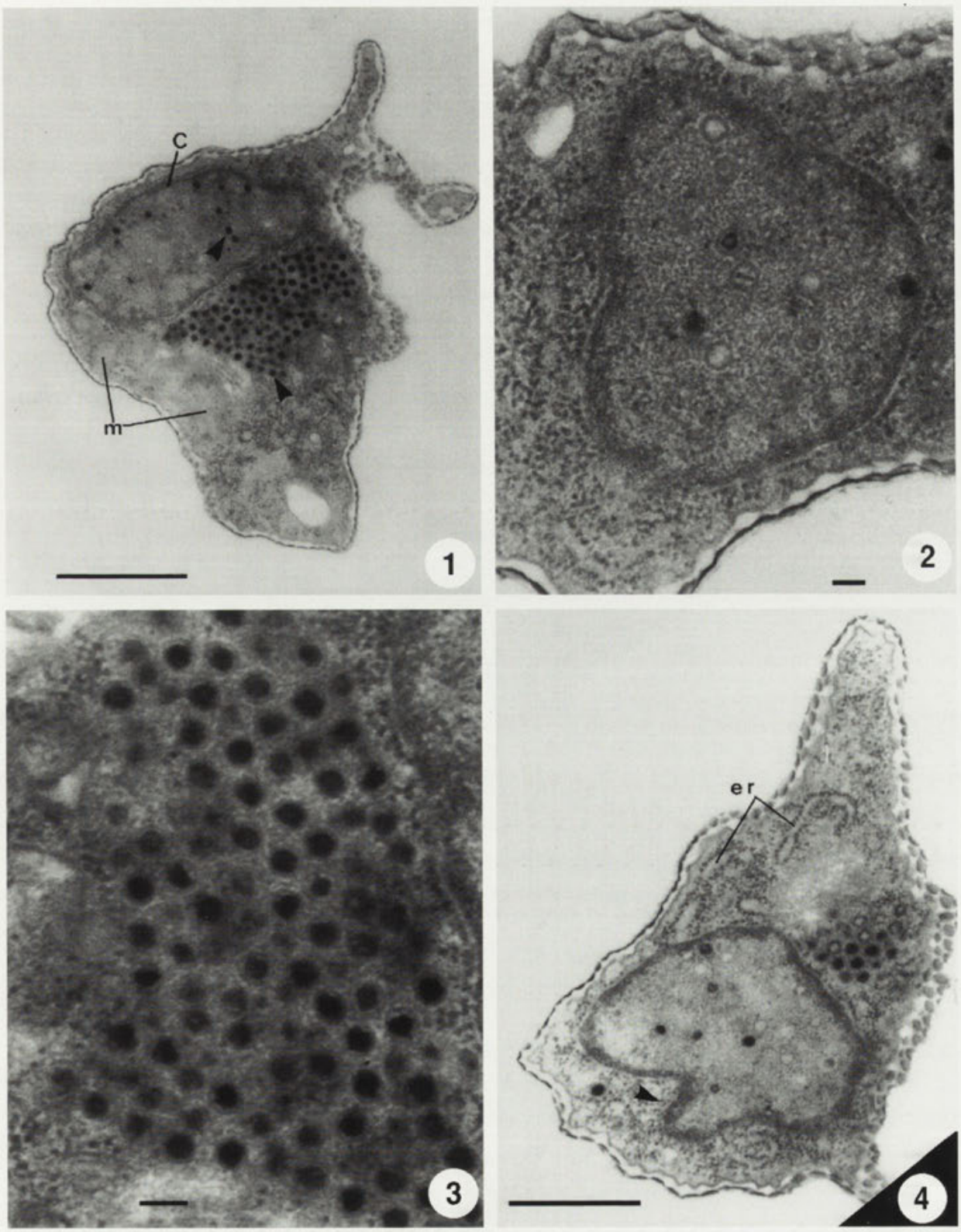

Fig. 1-4. 1 - the virus particles infecting the nucleus and cytoplasm (arrows) are clearly seen in thin sections. In the nucleus, the chromatin (C) is marginally displaced. In the cytoplasm, the mitochondria (m) are degenerating. The amoeba is within a flexible test. Bar -1 µm. 2 - virus particles are evenly distributed in the nucleus. Bar - 0.1 µm. 3 - viruses in the cytoplasm are not surrounded by a single common membrane but are individually surrounded by a membrane. Bar - 0.1 µm. 4 - the nucleus of *Corythionella* shows lobulation (arrow) and the endoplasmic reticulum (er) is swollen. Bar - 1 µm

Table 1

Viruses and virus-like particles (VLPs) of unicellular protists

Host	Location [Cytoplasmic (C), Nuclear (N)]	Type or morphological features	Habitat of host	Reference
CILIOPHORA				
Ignotocoma sabellarium	C	50 X 75 nm tubes	peristome of polychaetes	Lom and Kozloff (1969)
Ichthyophthirius multifilis	food vacuole	30 nm polyhedron	goldfish (*Carassius auratus*)	Lobo-da-Cunha and Azevedo (1992)
Tetrahymena pyriformis	C	vaccina virus	F	Perez-Prieto and Garcia-Gancedo (1981)
Onchodromus acuminatus	food vacuole	vaccina virus	F	Jareño (1987)
Hyalophysa chattoni	food vacuole	90 nm spheres	grass shrimp	Kucera (1992)
ACRASEA				
Guttulinopsis vulgaris	N	55-65 nm polyhedron	moist dung	Erdos (1981)
RHIZOPODEA				
Entamoeba histolytica	1. C	1. 40 nm	intestine of humans	1. Miller and Schwartzwelder (1960)
	2. C	2. 75-80 nm polyhedron		2. Diamond et al. (1972)
	3. N	3. 7 nm filaments		3. Mattern et al. (1972)
	4. N	4. 17 nm spheres		4. Mattern et al. (1974)
E. invadens	C	Rhabdovirus	mammal	Bird and McCaul (1976)
Pelomyxa sp.	N	50 nm spheres	anaerobic F	Daniels and Breyer (1973)
Naegleria gruberi	C	70 nm polyhedron	soil	Dunnebacke and Schuster(1971); Schuster (1969); Schuster and Dunnebacke (1971)
Corythionella sp.	N and C	80 nm polyhedron	M	Lipscomb and Riordan (this study)
GRANULORETICULOSEA				
Elphidium excavatum clavatum	C	100 nm microcrystalline arrays	M	Heeger (1988)
APICOMPLEXA				
Plasmodium gallinaceum	C	35-55 nm	*Gallus gallus*	Terzakis (1969)
Eimeria necatrix	C	Newcastle disease	*Gallus gallus*	Ellis and Revets (1990); Mihajlovic et al. (1980)
Eimeria tenella	C	Newcastle disease	*Gallus gallus*	Sibalic et al. (1980)
Eimeria stiedae	C	35 nm RNA virus (icosahedral)	*Gallus gallus*	Revets et al. (1989)
Babesia bovis	C	35 nm RNA virus (icosahedral)	cow	Johnston et al.(1990)
Perkinsus atlanticus	C	polyhedron	mollusca	Azevedo (1990)

Table 1 (cont.)

MICROSPORIDIA				
Noesema apis	C	isomeric virus	*Apis mellifera* (bee)	Liu (1984)
Thelohaniidae sp.	C	isomeric virus	diptera	Larsson (1988)
DIPLOMONADIDA				
Giardia muris	C	60 nm polyhedron	mammal	Feely et al. (1988)
G. lamblia	C	double-stranded RNA	mammal	Wang and Wang (1986b); Miller et al.(1988a,b); Teras and Kesa (1988)
Giardia sp.	C	double-stranded RNA	*Cavia porcellus* and *Felis catus*	De Jonckheere and Gordts (1987)
TRICHOMONADIDA				
Trichomonas vaginalis	C	double-stranded RNA	reproductive tract of mammals	Wang and Wang(1985,1986a); Flegr et al. (1988)
KINETOPLASTIDA				
Trypanosoma melaophagium				Molyneux and Heywood (1984)
Leishmania hertigi	C	55-60 nm clustered in paracrystals		Croft and Molyneux (1979); Eley et al. (1987)
L. braziliensis	C	32 nm spheres	mammals	Molyneux (1974); Tarr et al. (1988); Widmer et al. (1989, 1990)
DINOFLAGELLIDA				
Blastodinium sp.	N	20 nm spheres	intestine of crustacea	Soyer (1978)
Gyrodinium resplendens	C	30 nm tubes	M	Franca (1976)
Gymnodinium uberrium	C	385 nm polyhedron	F	Sicko-Goad and Walker (1979)
CRYPTOMONADIDAE				
Cryptomonas sp.	N and C	1. 99 nm polyhedron 2. 120 nm with stalk and surrounded by membrane	M	Pienaar (1976)
PRYMNESIIDA				
Chrysochromulina sp.	unknown	22 nm polyhedron	M	Manton and Leadbeater (1974)
Hymenomonas carterae	1. N 2. C	1. 63 nm polyhedron 2. 400 nm polyhedron	M	1. Pienaar (1976) 2. Sherman and Brown (1978)
CHRYSOMONADIDA				
Dinobryon sp.	C	100 nm polyhedron	F	Sherman and Brown (1978)
Hydrurus foetiolus	C	52-59 nm polyhedron	F	Hoffman (1978)
Chromophysomes cornuta	C	1. 50-60 nm polyhedron 2. 150-180 nm polyhedron	F	Preisig and Hibberd (1984)
Paraphysomas bourrelli	C	1. 50-60 nm polyhedron 2. 150-180 nm polyhedron	F	Preisig and Hibberd (1984)
P. caelifrica	C	150-180 nm polyhedron	F	Preisig and Hibberd (1984)

Table 1 (cont.)

P. corynephora	C	1. 50-60 nm polyhedron 2. 150-180 nm polyhedron 3. 270-300 polyhedron	F	Preisig and Hibberd (1984)
Aureococcus anofagefferens	C	polyhedron	M	Sieburth et al. (1988)
Mallomonas sp.	C	385 nm polyhedron	F	Sicko-Goad and Walker (1979)
EUSTIGMATOPHYCEAE				
Monodus sp.	N	400 nm polyhedron	F	Sherman and Brown (1978)
CHLOROMONADIDA				
Chlorella pyrenoidosa	C	41-42 nm polyhedron with short tail	F	Kawakami and Kawakami (1978)
Chlorella sp.	C	several types	*Paramecium bursaria*	See review in Van Etten et al. (1987, 1988, 1991)
Aulacomonas sp.	C	200-230 nm polyhedron with 150-200 nm tail	F	Swale and Belcher (1973)
PRASINOMONADIDA				
Platymonas sp.	N	51-58 nm polyhedron	M	Pearson and Norris (1974)
Micromonas pusilla	C	130-135 nm polyhedron		Mayer (1979), Mayer and Taylor (1979), Pienaar (1976), Waters and Chan (1982)
Pyraminomonas orientalis	1. N 2. N	1. 60 nm polyhedron 2. 200 nm polyhedron	F	Moestrup and Thomsen (1974)
Heteromastix sp.	N	320 nm polyhedron	M	
Mesostigma viridae	C	130 nm polyhedron	F	Melkonian (1982)
RHODOPHYTA				
Porphyridium	N and C	40 nm polyhedron	F	Chapman and Lang (1973)
CHYTRIDIOMYCOTA				
Allomyces arbuscula	C	40 nm spheres	soil	Khandjian et al. (1974)
Aphelidium sp.	C	200 nm polyhedron	fin green algae (*Acenedesmus armatus*)	Schnepf et al. (1970)
LABYRINTHOMORPHA				
Labyrinthomyxa manna (=*Dermocystidium marinum*)	N and C	46-53 polyhedron	M	Perkins (1969)
Thraustochytrium sp.	N and C	110 nm polyhedron with envelope (herpes-like virus)	M	Kazama and Schornstein (1972, 1973)
Schizochytrium aggregatum	N and C	110 nm polyhedron with envelope (herpes-like virus)	M	Perkins (1976)

lack an envelope, but herpes viruses in the cytoplasm of host cells are surrounded by individual membrane envelopes. Furthermore, a fiber is found attached to pentons of the adenovirus capsid and this is not seen in the rhizopod VLP described here. Based on all of these features we have concluded that this rhizopod VLP is most like the viruses of the herpes virus family.

Information on the VLP replication in *Corythionella* provides additional evidence supporting this conclusion. Icosahedral DNA viruses replicate within the nucleus, while icosahedral RNA viruses replicate in the cytoplasm. After replication, viral nucleic acid becomes tightly coiled and enclosed in a capsid. Encapsidation typically occurs in the same location as the virus nucleic

acid replication (Grimley and Henson 1981). The rhizopod VLP capsid is seen in the nucleus, thus suggesting that it replicated there and is a DNA virus. Of the DNA isocohedral viruses, most nucleocapsids assembled in the nucleus accumulate there and are liberated by cell lysis. The exception is the herpes virus in which nucleocapsids condense in the nucleoplasm but bud through the nuclear membrane, thus acquiring an envelope, and accumulate in the cytoplasm. This appears to be the case in the rhizopod VLP: virus capsids are seen in the nucleus and also in the cytoplasm where they are surrounded by an individual membrane envelope.

The final similarity between the VLP and a herpes virus comes from the cytopathogenic affect of the virus on the protist. Although non-infected cells have spherical nuclei with evenly distributed chromatin, *Corythionella* infected with VLPs have distorted nuclei with the chromatin just under the nuclear membrane. Nuclear shape changes and nucleochromatin margination are characteristic effects of herpes viruses on their host cell (Doane and Anderson 1987, Grimley and Henson 1981).

Confirmation that the VLP from *Corythionella* is a herpes virus and its exact classification must be based on a combination of growth characteristics in culture, immunogenic specificities, vectors of transmission, peptide analysis, oligotide fingerprinting, and heteroduplex mapping. These molecular analyses were not possible at this time because pure preparations of virions could not be obtained. Nevertheless, strong circumstantial evidence exists that the VLP in *Corythionella* is a herpes-like virus.

The only other instance of herpes-like viruses found in unicellular eukaryotes occurs in the labyrinthulids (slime nets) (Kazama and Schornstein 1972, 1973; Perkins 1969, 1976). These viruses are similar to the VLP from *Corythionella* except that they are slightly larger and cytoplasmic particles are surrounded by two, not one, membrane envelopes.

Viruses in Unicellular Protists

The presence of prokaryotic and eukaryotic symbionts living within single-celled protists is well documented and has been reviewed many times (e.g., Corliss 1985, Görtz 1983, Taylor 1990). The occurrence of viruses in unicellular eukaryotes, on the other hand, has only rarely been mentioned in such reviews despite the fact that there are actually a variety of viruses and virus-like particles in unicellular eukaryotes (Lemke 1976, Table 1). Therefore, we offer here a brief review of viruses and VLPs in protists.

Viruses from protists which are themselves symbionts in other organisms are best known. The molecular characterization of various RNA viruses in parasitic protozoa, for example, are some of the most thorough studies of viral systems in protists (see reviews by Patterson 1990; Wang and Wang 1988, 1990, 1991). Interestingly, the viruses of *Babesia bovis* (Johnston et al. 1990), *Eimeria stiedae* (Revets et al. 1989), *Giardia lamblia* (Wang and Wang 1986a), *Leishmania braziliensis* (Tarr et al. 1988, Widmer et al. 1989), and *Trichomonas vaginalis* (Khoshman and Alderete 1994; Wang and Wang 1985, 1986b) share many features with yeast dsRNA killer viruses. All are double-stranded RNA viruses with nonsegmented genomes approximately 5-7 kb in length. All appear to be either spherical or icosahedral and usually 30-40 nm in diameter (Patterson 1990, Wang and Wang 1991).

Viruses that infect *Chlorella*-like green algae that reside in *Paramecium bursaria* have also been well characterized (see review by Van Etten et al. 1987, 1988, 1991). Over 30 types of viruses have been isolated from *Chlorella* species of North America. These are large (150-190 nm in diameter) polyhedral, dsDNA containing (at least 300 kb), plaque-forming viruses (Schuster et al. 1986; Van Etten et al. 1987, 1988, 1991). These viruses were placed into 11 groups on the basis of plaque size, reaction with an antibody, resistance of the virus DNAs to restriction endonucleases, and the nature and abundance of methylated bases (Schuster et al. 1986). Viruses from *Chlorella* from Europe are similar in size, genome size, presence of methylated bases, structural proteins, and sensitivity to chloroform. Because they do not react with the same antibody and their DNA hybridizes poorly with that from the North American strains, they have been placed in a closely related, but different, taxon.

Viruses and VLPs of other symbiotic protists are known primarily from electron microscopy (e.g., *Entamoeba* - Bird and McCaul 1976; Diamond et al. 1972; Mattern et al. 1972, 1974; Miller and Schwartzwelder 1960; *Noesema* - Lui 1984; *Thelohaniidae* - Larsson 1988; *Blastodinium* - Soyer 1978; *Ignotocoma* - Lom and Kozloff 1969; *Hyalophysa* - Kucera 1992). These viruses and VLPs include a variety of forms with different shapes, sizes, and locations within the host cell (Table 1). The reason viruses are often found in protists that are themselves obligatory symbionts is not clear. Possibly these viruses play a pivotal role in the delicate balance of the host-parasite interaction (Wang and Wang 1991). Or it may simply be due to the fact that parasitic

protozoa are the subject of more research attention than free-living forms. It may only be a matter of time before viruses are discovered in all protist groups.

Viruses or VLPs have not been reported from the Euglenida (=Euglenophyceaae), Bacillariophyta (diatoms), bicoecids, choanoflagellates, Opalinata, Proteromonadida, Parabasilia, Retortamonadida, or Actinopoda, but many types of free-living protists can have viruses (Table 1). The consequences of the presence of viruses in free-living protists is not clear. Some authors have suggested that protists act as vectors or reservoir hosts of viruses that attack multicellular plants and animals (Porter 1990, Teras et al. 1981). Although there is some evidence that parasitic protists may serve as vectors of viruses (Mihajlovic et al. 1980, Sibalic et al. 1980), transmission of particles from free-living protists to other eukaryotes has not been observed. Other authors have hypothesized that the pathogenicity of some free-living rhizopods that have pathogenic and nonpathogenic forms may be triggered by the presence of viruses (Teras and Kesa 1988, but see Olivier et al. 1984).

The role of naturally occurring virus infections in regulating aquatic populations is just beginning to be investigated, but most of these studies are confined to examination of bacteriophages, not the viruses of eukaryotes (e.g., see Baross et al. 1978, Bergh et al. 1989, Børsheim et al. 1990, Procter and Fuhrman 1990, Sherr 1989). These studies suggest that predation pressure from protozoan grazing may not be the major cause of bacterial mortality. Using improved ultracentrifugation and transmission electron microscopy counting techniques, we now know that viruses are more numerous than earlier estimates suggested. In marine waters densities range from 10^3 to 10^9 ml^{-1} (Bergh et al. 1989, Børsheim et al. 1990, Suttle et al. 1990), while in fresh water lake abundances as high as $254x10^6 ml^{-1}$ have been recorded (Bergh et al. 1989). Because as much as one-third of bacterial or cyanobacterial population may be attacked or infected, phages have a quantitatively important impact on prokaryote population size (Procter and Fuhrman 1990, Bergh et al. 1989). Bacteriophages impact their host's environment in another way. The bacterial cytoplasm and cellular material released during viral-induced cell lysis enters the pool of dissolved organic matter and thus becomes available as a substrate for new bacterial production. Bratbak et al. (1990) suggests that by recycling organic matter in a bacteriophage-dissolved organic material loop, bacterial production may become very high and even exceed primary production.

Although populations of protists are generally thought to be regulated by predation from larger protozoa and microinvertebrates, and by food supply (Fenchel 1987), viral infection is common enough to suggest it may also play a role in maintaining population levels. Furthermore, it is likely that the release of cellular material by cell lysis due to viral infection may dump significant amounts of dissolved carbon by heterotrophic and autotrophic prokaryotes (Laybourn-Parry 1992). These suggestions are strengthened by the observed lysis of the phytoflagellata *Micromonas pusilla*, an important member of the marine nanoplankton, by an iridovirus (Mayer and Taylor 1979) and by the observation of viruses and VLPs in numerous free-living protists (Table 1).

The role of viruses in microbial communities is only beginning to be studied. The discoveries of viruses and VLPs in symbiotic and free-living protists seems to be sufficient evidence that they may be more important in eukaryotic microbial ecosystems than has been previously realized. The role of phages in food webs, in controlling populations and even in facilitating the exchange of genetic material among marine prokaryotes is being examined by ecologists (Sherr 1989). It is necessary to begin to look at whether the viruses infecting eukaryotes play an equally important role. It is hoped that biologists in other fields, whether the intent of their study is morphology, physiology, etc., should take the time to note the presence of virus particles infecting marine microorganisms when they are encountered.

Acknowledgements. NSF grant #DEB 9305925 to D.L. Lipscomb is gratefully acknowledged. We thank Dr. Tom Sawyer for identifying *Corythionella*.

REFERENCES

Azevedo, C. (1990) Virus-like particles in *Perkinsus atlanticus* (Apicomplexa, Perkinsidae). *Dis. Aquat. Org.* **9:** 63-65

Baross J. A., Liston J., Morita R. Y. (1978) Incidence of Vibrio parahaemolyticus bacteriophages and other Vibro bacteriophages in marine samples. *Appl. Environ. Microbiol.* **36**: 492-499

Bergh O., Børsheim K. Y., Bratbak G., Heldal M. (1989) High abundance of viruses found in aquatic environments. *Nature* **340:** 467-468

Bird R.G., McCaul T.F. (1976) The rhabdoviruses of *Entamoeba histolytica* and *Entamoeba invadens*. *Annals Trop. Med. Parasit.* **70:** 81-93

Børsheim K.Y., Bratbak G., Heldal M. (1990) Enumeration and biomass estimation of planktonic bacteria and viruses by transmission electron microscopy. *Appl. Environ. Microbiol.* **56:** 352-356

Bratbak G., Heldal M. Norland S., Thingstad T.F. (1990) Viruses as partners in spring bloom microbial trophodynamics. *Appl. Environ. Microbiol.* **56:** 1400-1405

Chapman R. L., Lang N. (1973) Virus-like particles and nuclear inclusions in the red algae *Porphyridium purpureum* (Bory) Drew et Ross. *J. Phycol.* **9:** 117-122

Corliss J.O. (1985) Concept definition prevalence and host-interactions of xenosomes (cytoplasmic and nuclear endosymbionts). *J .Protozool.* **26:** 373-376

Croft S.L., Molyneux D.H. (1979) Studies on the ultrastructure, virus-like particles and infectivity of *Leishmania hertigi*. *Ann. Trop. Med. Parasitol.* **73:** 213-222

Daniels E. W., Breyer E. P. (1973) Ultrastructure of the giant amoeba *Pelomyxa palustris*. *J. Protozool.* **14:** 169-179

De Jonckheere J. F. , Gordts B. (1987) Occurrence and transfection of a *Giardia* virus. *Mol. Biochem. Parasitol.* **23:** 85-89

Diamond L. S., Mattern C. F. T., Bartgis I. L. (1972) Viruses of *Entamoeba histolytica*. I. Identification of transmissible virus-like agents. *J. Viro.* **9:** 326-341

Doane F. W., Anderson N. (1987) Electron microscopy in diagnostic virology: a practical guide and atlas. Cambridge University Press, Cambridge

Dunnebacke T. H., Schuster F. L. (1971) Infectious agent from a free-living soil amoeba *Naegleria gruberi*. *Science* **174:** 516-518

Eley S.M., Molyneux D.H., Moore N.F. (1987) Investigation of virus-like particles in *Leishmania hertigi*. *Microbios* **51:** 145-149

Ellis J., Revets H. (1990) *Eimeria* species which infect the chicken contain virus-like RNA molecules. *Parasitology* **101:** 163-169

Erdos G.W. (1981) Virus-like particles in the ascrasid cellular slime mold *Guttulinopsis vulgaris*. *Mycologia* **73:** 785-788

Feely D. E., Chase D. G., Hardin E. L., Erlandsen S. L. (1988) Ultrastructural evidence for the presence of bacteria, viral-like particles and mycoplasma-like organisms associated with *Giardia* spp. *J. Protozool.* **35:** 151-158

Fenchel T. (1987) Ecology of Protozoa. Science Tech Inc, Madison

Flegr J., Cerkasov J., Stokrova J. (1988) Multiple populations of double-stranded RNA in two virus-harboring strains of *Trichomonas vaginallis*. *Folia Microbiol.* **33:** 462-465

Franca S. (1976) On the presence of virus-like particles in the dinoflagellate *Gyrodinium resplendens* (Hulbert). *Protistologica* **12:** 422-430

Gonzalez J.M., Suttle C.A. (1993) Grazing by marine nanoflagellates on viruses and virus-sized particles: ingestion and digestion. *Marine Ecology Progress Series* **94:** 1-10

Görtz H. (1983) Endonuclear symbionts in ciliates. *Int. Rev. Cytol.* supp. **14**: 145-176

Grimley R. M., Henson D. E. (1981) Electron microscopy in virus infections. In: Diagnostic Electron Microscopy (Eds. B.F. Trump, R.T. Jones) John Wiley and Sons, New York, 1-68

Hayunga E. G. (1977) A specimen holder for dehydrating and processing very small tissue samples. *Trans. Am. Microsc. Soc.* **96:** 156-158

Heeger T. (1988) Virus-like particles and cytopathological effects in *Elphidium excavatum clavatum*, a benthic foraminiferan. *Dis. Aquat. Org.* **4:** 233-236

Hoffman L.R. (1978) Virus-like particles in *Hydrurus* (Chrysophyceae). *J. Phycol.* **14:** 110-114

Jareño M.A. (1987) Some ultrastructural changes produced by vaccinia virus in *Onychodromus acuminatus* (Ciliata, Hypotricha). *Acta Protozool.* **26:** 9-14

Johnston R.C., Farias N.A.R., Gonzales J.C., Dewes H., Masuda, A. (1990) A putative RNA virus in *Babesia bovis*. *Mol. Biochem. Parasitol.* **45:** 155-158

Kawakami, H., Kawakami, M. (1978) Behavior of a virus in a symbiotic system, *Paramecium bursaria*-zoochlorella. *J. Protozool.* **25:** 217-225

Kazama F.Y., Schornstein K.L. (1972) Herpes-type virus particles associated with a fungus. *Science* **177:** 696-697

Kazama F.Y., Schornstein K.L. (1973) Ultrastructure of a fugus herpes-type virus. *Virology* **52:** 478-487

Khandjian E.W., Roos U.-P., Timberlake W.E., Eder L., Turian G. (1974) RNA virus-like particles in the chytridiomycete *Allomyces arbuscula*. *Arch. Microbiol.* **101:** 351-356

Khoshman A., Alderete J.F. (1994) *Trichomonas vaginalis* with a double-stranded RNA virus has unregulated levels of phenotypically variable immunogen mRNA. *J. Virology* **68:** 4035-4038

Kucera F.P. (1992) Virus-like particles associated with the apostome ciliate *Hyalophysa chattoni*. *Dis. Aquat. Org.* **12:** 151-153

Laybourn-Parry J. (1992) Protozoan plankton ecology. Chapman and Hall, London

Larsson J.I.R. (1988) Isomeric virus-like particles in spores of two microsporidia belonging to the Thelohaniidae. *J. Invertebr. Pathol.* **51:** 163-165

Lemke P.A. (1976) Viruses of eukaryotic microorganisms. *Annu. Rev. Microbiol.* **30:** 105-145

Lipscomb D.L., Riordan G.P. (1990) The ultrastructure of *Chaenea teres* and an analysis of the phylogeny of the haptorid ciliates. *J. Protozool.* **37:** 287-300

Lobo-da-Cunha A., Azevedo C. (1992) Virus-like particles in the fish parasite *Ichthyophirius multifiliis* (Ciliophora). *J. Fish Diseases* **15:** 273-277

Lom J., Kozloff E. N. (1969) Virus-like particles in the ancistrocomid ciliate *Ignotocoma sabellarium* Kosloff. *Protistologica* **5:** 173-192

Lui T.P. (1984) Virus-like cytoplasmic particles associated with lysed spores of *Noesema apis*. *J. Invertebr. Pathol.* **44:** 103-105

Manton I., Leadbeater B.S.C. (1974) Fine-structural observations on six species of *Chrysochromulina* from wild Danish marine nanoplankton, including a description of *C. campanulifera* sp. nov. and a preliminary summary of the nanoplankton as a whole. *Dan. Vidensk. Sel. Biol. Skr.* **20:** 1-26

Mattern C. F. T., Diamond L. S., Daniel W. A. (1972) Viruses of *Entamoeba histolytica* II. Morphogenesis of the polyhedral particles (ABRM2 - HK-9) - HB-301 and the filamentous agent (ABRM)2 - HK-9. *J. Virol.* **9:** 342-358

Mattern C.F.T., Hruska J.F., Diamond L.S. (1974) Viruses of *Entamoeba histolytica*. V. Ultrastructure of the polyhedral virus V_{301} *J. Virol.* **13:** 246-249

Mayer J. A. (1979) Isolation and ultrastructural study of a lytic virus in the small marine phytoflagellate, *Micromonas pusilla* (Prasinophyceae). *Dissert. Abst.* **39:** 5713

Mayer J.A., Taylor F.J.R. (1979) A virus which lyses the marine nanoflagellate *Micromonas pusilla*. *Nature* **281:** 299-301

Melkonian M. (1982) Virus-like particles in the scaly green flagellate *Mesostigma viride*. *British Phyc. Journal* **17:** 63-68

Mihajlovic B., Sibalic S., Tomanovic B., Asanin R. (1980) The possibility of incorporation and transmission of Newcastle disease virus by *Eimeria necatrix*. *Acta Vet.(Beogr.)* **30:** 143-147

Miller J. H., Schwartzwelder J. C. (1960) Virus-like particles in an *Entamoeba histolytica* trophozoite. *J. Parasitol.* **46:** 523-524

Miller R.L., Wang A.L., Wang C.C. (1988a) Purification and characterization of the *Giardia lamblia* double-stranded RNA virus. *Mol. Biochem. Parasitol.* **28:** 189-195

Miller R.L., Wang A.L., Wang C.C. (1988b) Identification of *Giardia lamblia* isolates susceptible and resistant to infection by the double-stranded RNA virus. *Expl Parasitol.* **66:** 118-123

Moestrup O., Thomsen H.A. (1974) An ultrastructural study of the flagellate *Pyramimonas orientalis* with particular emphasis on Golgi apparatus activity and the flagellar apparatus. *Protoplasma* **81:** 247-269

Molyneux D.H. (1974) Virus-like particles in *Leishmania* parasites. *Nature* **249:** 588-589

Molyneux D. H., Heywood P. (1984) Evidence for the incorporation of virus like particles into *Trynaposoma*. *Z. ParasitKde.* **70:** 553-556

Olivier L.R., Lecatsas M., Jackson T.F.H.G., Gthiram V., Simjee A.E., Prozesky O.W. (1984) Viruses and pathogenicity of *Entamoeba histolytica*. *Lancet* **2:** 528

Patterson J.L. (1990) Viruses of protozoan parasites. *Expl Parasitol.* **70:** 111-113

Pearson B.R., Norris R.E. (1974) Intranuclear virus-like particles in the marine alga *Platymonas* sp. (Chlorophyta, Prasinophyceae). *Phycologia* **13:** 5-9

Perez-Prieto S., Garcia-Gancedo A. (1981) Uptake of Vaccina virus by *Tetrahymena pyriformis*. *Microbiologica Esp.* **34:** 29-43

Perkins F. O. (1969) Ultrastructure of vegetative stages in *Labyrinthomyxa marina* (=*Dermocystidium marinum*) a commercially significant oyster pathogen. *J. Invertebr. Pathol.* **32:** 199-222

Perkins F. O. (1976) Fine structure of lower marine and estuarine fungi. In: Recent Advances in Aquatic Mycology (Ed. E.B.G. Jones). John Wiley and Sons, New York, 95-118

Pienaar R.N. (1976) Virus-like particles in three species of phytoplankton from San Juan Island, Washington. *Phycologia* **15:** 185-190

Porter D. (1990) Labyrinthulomycota. In: Handbook of Protoctista (Eds. L. Margulis, J.O. Corliss, M. Melkonian, D. Chapman) Jones and Bartlett, Boston, 388-398

Preisig H.R., Hibberd D.J. (1984) Virus-like particles and endophytic bacteria in *Paraphysomonas* and *Chromophysomonas* (Chrysophyceae). *Nord. J. Bot.* **4:** 279-285

Proctor, L.M., Fuhrman, J.A. (1990) Viral mortality of marine bacteria and cyanobacteria. *Nature* **343:** 60-62

Revets H., Dekegel D., Deleersnijder W., Jonckheere J. De, Peeters J., Leysen E., Hamers R. (1989) Identification of virus-like particles in *Eimeria stiedae*. *Mol. Biochem. Parasitol.* **36:** 209-216

Schnepf E., Soeder C.J., Hegewald E. (1970) Polyhedral virus like particles lysing the aquatic Phycomycete *Aphelidium* sp., a parasite of the green alga *Scenedesmus armatus*. *Virology* **42:** 482-487

Schuster A.M., Burbank D.E., Meister B., Skrdla M.P., Meints R.H., Hattman S., Swinton D., Van Etten J.L. (1986) Characterization of viruses infecting a eukaryotic *Chlorella*-like green algae. *Virology* **150:** 170-177

Schuster F. L. (1969) Intranuclear virus-like bodies in the amoeboflagellate *Naegleria gruberi*. *J. Protozool.* **16:** 724-727

Schuster F.L., Dunnebacke T.H. (1971) Formation of bodies associated with virus-like particles in the amoeboflagellate *Naegleria gruberi*. *J. Ultrastruct. Res.* **36:** 659-668

Sherman L.A., Brown R.M. (1978) Cyanophages and viruses of eukaryotic algae. In: Comprehensive Virology, Vol. 12. (Eds. H. Fraenkel-Conrat and R.R. Wagner) Plenum, New York, 145-234

Sherr E. (1989) And now small is plentiful. *Nature* **340:** 429

Sibalic S., Mihajlovic B., Tomanovic B., Ruzica A. (1980) To-date results of the investigation of incorporation, perpetuation and transmission of the Newcastle virus through some species of parasites. *Veterinaria (Sarajevo)*. **29:** 241-244

Sicko-Goad, L., Walker, G. (1979) Viroplasm and large virus-like particles in the dinoflagellate *Gymnodinium uberrimum*. *Protoplasma* **99:** 203-210

Sieburth J.M., Johnson P.W., Hargraves P.E. (1988) Ultrastructure and ecology of *Aureococcus anophagefferens* gen. et sp. nov. in Narragansett bay, Rhode Island, summer 1985. *J. Phycol.* **24:** 416-425

Soyer M-O. (1978) Particles de type viral et filaments trichocystoides chez les dinoflagelles. *Protistologica* **14:** 53-58

Suttle C.E., Chan A.M., Cottrell M.T. (1990) Infection of phytoplankton by viruses and reduction of primary productivity. *Nature* **347:** 467-469

Swale E.M.F., Belcher J.H. (1973) A light and electron microscope study of the colourless flagellate *Aulacomonas* Skuja. *Arch. Mikrobiol.* **92:** 91-103

Tarr P.I., Aline R.F., Smiley B.L., Scholler J., Keithly J., Stuart K. (1988) LR1: a candidate RNA virus of *Leishmania*. *Proc. Natl. Acad. Sci. USA* **85:** 9572-9575

Taylor F.J.R. (1990) Symbiosis in marine protozoa. In: Ecology of Marine Protozoa, (Ed. G.M. Capriulo) Oxford University Press, New York, 323-340

Teras J., Kesa, L. (1988) The relationship between protozoa and viruses. 2. Virus-like particles and cytopathogenic agent in protozoa. *Proc. Acad. Sci. Est. SSR, Biol.* **37:** 185-194

Teras J.H., Kesa L. P., Kallas E. V. (1981) The experimental study on the relationships between *Tetrahymena pyriformis* and RNA and DNA viruses. 4. On the interaction of *T. pyriformis* with coxsackie B-5 virus after exposure to myxovirus influenza of type A2. *Protozoologiya* **6:** 126-136

Terzakis J. A. (1969) A protozoan virus. *Mil. Med.* **134:** 916-921

Thingstad T.F., Heldal M., Bratbak G., Dundas I. (1993) Are viruses important partners in pelagic food webs? *TREE* **8:** 209-213

Van Etten J.L. van, Xia Y., Meints R.H. (1987) Viruses of a chlorella-like green algae. In: Plant-Microbe Interactions, Vol. 2, (Eds. T. Kosuge and E.W. Nester). MacMillian, New York, 307-325

Van Etten J. L. van, Schuster A. M., Meints R. H. (1988) Viruses in eukaryotic Chlorella-like Algae. In: Viruses of Fungi and Simple Eukaryotes, (Eds. Y. Koltin and M.J. Leibowitz). Marcel Dekker Inc., New York, 411-428

Van Etten J.L. van, Lane L.C., Meints R.H. (1991) Viruses and viruslike particles of eukaryotic algae. *Microbiol. Rev.* **55:** 586-620

Wang A.L., Wang C.C. (1985) A linear double-stranded RNA virus in *Trichomonas vagnalis*. *J. Biol. Chem.* **260:** 3697-3702

Wang A.L., Wang C.C. (1986a) Discovery of a specific double-stranded RNA virus in *Giardia lamblia*. *Mol. Biochem. Parasitol.* **21:** 269-276

Wang A.L., Wang, C.C. (1986b) The double-stranded RNA in *Trichomonas vaginalis* may originate from virus-like particles. *Proc. Natl. Acad. Sci. USA* **83:** 7956-7960

Wang A.L., Wang C.C. (1988) Viruses of parasitic protozoa. In: Molecular Basis of the Action of Drugs and Toxic Substances, (Eds. T.P. Singer, N. Castagnoli. C.C. Wang). de Gruyter, Berlin, 126-137

Wang A.L., Wang C.C. (1990) Viruses of parasitic protozoa. *Parasitology Today* **7:** 76-80

Wang A.L., Wang C.C. (1991) Viruses of protozoa. *Ann. Rev. Microbiol.* **45:** 251-263

Waters R.E., Chan A.T. (1982) *Micromonas pusilla* virus: the virus growth cycle and associated physiological events within the host cells; host range mutation. *J. Gen. Virol.* **63:** 199-206

Widmer G., Comeau A.M., Furlong D.B., Wirth D.F., Patterson J.L. (1989) Characterization of a RNA virus from the parasite *Leishmania*. *Proc. Natl. Acad. Sci. USA* **86:** 5979-5982

Widmer G., Keenan M.C., Patterson J.L. (1990) RNA polymerase activity is associated with viral particles isolated from *Leishmania brazilensis* subsp. *guyanensis*. *J. Virol.* **64:** 3712-3715

Received on 14th July, 1994; accepted 20th October, 1994

Acta Protozoologica (1995) 34: 45 - 56

ACTA
PROTOZOOLOGICA

A Light Microscopic and Ultrastructural Study of *Gurleya legeri* sensu Mackinnon (1911) - with Establishment of the New Species *Gurleya dorisae* sp. n. (Microspora, Gurleyidae)

J. I. Ronny LARSSON

Department of Zoology, University of Lund, Lund, Sweden

Summary. The microsporidium *Gurleya dorisae* sp. n., a parasite of caddis fly larvae of the species *Anabolia nervosa* and *Micropterna lateralis*, is described based on light microscopic and ultrastructural characteristics. All life cycle stages have isolated nuclei. The merogonial reproduction was revealed by small groups of merozoites. The dominant sporogony yields four sporoblasts by rosette-like budding, enclosed in a sporophorous vesicle produced by the sporont. Together with the tetrasporous sporogony production of macrospores in 3-, 2- or 1-sporous vesicles occurs. Spores are pyriform, with pointed anterior pole. Fixed tetraspores from *A. nervosa* measure 3.0-3.5 x 4.6-5.2 µm. The greatest fixed macrospores observed were 10.4 µm long. The spore wall has the normal three subdivisions, including a layered, *ca* 43 nm wide exospore, where the intermediate layer is a double-layer. The polaroplast has two lamellar parts, with the anterior lamellae more closely packed. The polar filament is isofilar, with 20-25 coils in tetraspores, up to 34 coils in macrospores. The coils have approximately identical diameter in tetraspores and macrospores. Granular and tubular inclusions of two kinds appear in the episporontal space. Wide, septate tubules of exospore nature disappear when the spores mature. Narrow, thin-walled tubules persist. Macrospores often exhibit aberrant cytology. In *A. nervosa* the adipose tissue is more or less completely invaded by the parasite. The fat body lobes are not transformed into syncytia. Defense reactions were not observed in this host. Infection in *M. lateralis* was visible as local herds, and nodule formation with incorporation of dark pigment was observed. The species is compared to previously described microsporidia of caddis flies and the generic position is discussed. It is obviously identical to the microsporidium Mackinnon (1911) reported under the name *Gurleya legeri* Hesse, 1903.

Key words. Microspora, *Gurleya dorisae* sp. n., ultrastructure, taxonomy, Trichoptera larvae.

INTRODUCTION

During the years 1909 and 1910 Dr. Doris L. Mackinnon collected parasites from caddis fly larvae, mainly of the genera *Limnephilus* and *Anabolia*, in the neighbourhood of Aberdeen (Mackinnon 1911). Among the four parasites reported together, one is a microsporidium with tetrasporoblastic sporogony, yielding micro- and macrospores in regular arrangement. The species was identified as *Gurleya legeri* Hesse, 1903. The type host of this microsporidium is an insect not related with caddis flies: larvae of the mayfly *Ephemerella ignita*, with provenance from Haute-Saône in France (Hesse 1903).

A microsporidium which is considered identical to the species studied by Mackinnon, appears in streams

Address for correspondence: R. Larsson, Department of Zoology, University of Lund, Helgonavägen 3, S-223 62 Lund, Sweden; FAX +46-46-104541; E-mail: Ronny.Larsson@zool.lu.se

in Scania in southern Sweden. The ultrastructure of the species is briefly described herein. As the microsporidium neither is identical to *Gurleya legeri* Hesse, 1903, even if that was suggested by Mackinnon, nor to any other described species of microsporidia, a new species is established. Some traits on the cytology, the identity of the species and the generic position are briefly discussed.

MATERIALS AND METHODS

The investigation was based on three samples of caddis fly larvae (Trichoptera), from three different streams or rivers in Scania, in the south of Sweden. In the sample collected in Höje å , close to the village of Esarp (Sample 1; July 13, 1987), the host was *Anabolia nervosa* (Curtis, 1834). In the other two samples, from Vege å , close to Knutstorp (Sample 2; July 29, 1987), and from a small stream about 500 m from its affluence into the river Rönneå, at Djupadalsmölla (Sample 3; August 14, 1991), the host was *Micropterna lateralis* (Stephens, 1837).

Fresh squash preparations were made using the agar method of Hostouský and Žizka (1979) and examined using phase contrast microscopy, differential interference phase contrast techniques, or dark field illumination. Permanent squash preparations were air dried lightly and fixed in Bouin-Duboscq-Brasil (BDB) solution or in methanol for at least one hour. For paraffin sectioning infected animals were immersed in BDB or 4 % formaldehyde overnight or longer. After washing and dehydration in a graded series of ethanols, specimens were cleared in butanol and embedded in Paraplast (Lancer, St. Louis, MO, USA). Sections were cut longitudinally at 10 µm. Squash preparations and sections were stained using Giemsa solution, Heidenhains iron haematoxylin, a modification of the polychromatic staining according to Vetterling and Thompson (1972), where the nuclear staining was substituted with Heidenhain's haematoxylin for one hour, or using the modification of Noland's gentian violet by Farley (1965). For details on the general histological techniques used see the manual by Romeis (1968). All permanent preparations were mounted in D.P.X. (BDH Chemicals Ltd., Poole, UK). Measurements were made with an eye-piece micrometer at x 1000.

For transmission electron microscopy, pieces of infected tissue were excised and fixed in 2.5 % (v/v) glutaraldehyde in 0.2 M sodium cacodylate buffer (pH 7.2) at 4°C for 24 or 50 hours. After washing in cacodylate buffer and postfixing in 2 % (w/v) osmium tetroxide in cacodylate buffer for 1 h at 4°C, the tissue samples were stained using uranyl acetate and lead citrate (Reynolds 1963).

RESULTS

Prevalence and pathology

When removed from the cases infected larvae were easily recognized by the white anomalous coloration of the adipose tissue, shining through the semitransparent cuticle. The frequency of the microsporidium appeared normally to be low. Sample 1 contained 35 Limnephilidae larvae, but only three of them, all belonging to the species *Anabolia nervosa* (Curtis, 1834) hosted the parasite. Of additional 7 larvae of Polycentropodidae 3 had *Episeptum inversum* (see Larsson 1986), the only other microsporidium present in the sample.

Sample 2 contained 41 larvae of *Micropterna lateralis* (Stephens, 1837) where only one had the microsporidium, and five healthy specimens of a *Leptocerus* species. No other microsporidia were present in this sample. Sample 3 was small, containing 10 specimens of *M. lateralis*, five of them with the microsporidium, and one larva belonging to the family Rhyacophilidae (not further identified), which was free of microsporidia.

Only the adipose tissue was infected. In *Anabolia nervosa* practically all fat cells were invaded by the microsporidium (Fig. 1). In *Micropterna lateralis* infected cells were dispersed as isles among healthy fat tissue (Fig. 2). The microsporidium remained in close contact with the host cell cytoplasm, without provoking development of a parasitophorous vacuole. Infected cells, and their nuclei, were hypertrophic. The nuclear diameter increased up to threefold following infection. Infected lobes were not degraded to syncytia.

In the single infected *M. lateralis* larva of Sample 2 defense reactions against the microsporidium were seen. Nodules were formed by haemocytes adhering in layers, building an up to 16 µm thick wall (Fig. 2). In addition black pigment, probably melanins, were deposited in the nodules (Fig. 3), which made the nodules distinctly visible to the naked eye. Spores in the nodules were destroyed.

Presporal stages and life cycle

All life cycle stages observed displayed isolated nuclei, and there were no indications of reductional division in the initial phase of the sporogony.

The earliest life cycle stages observed were small groups of merozoites (Fig. 4).They were irregularly shaped, up to 3.9 µm in diameter in sections, and they had a central, up to 1.7 µm wide, irregularly rounded nucleus. The nuclear envelope was of traditional type: two unit membranes with pores and a perinuclear cisterna. The merozoites had an about 8 nm thick plasma membrane of traditional unit membrane structure. The cytoplasm was rich in free ribosomes, but there were only traces of a rough endoplasmic reticulum (Fig. 4). It is unknown if there is more than one sequence of merogonial divisions.

The last, or possibly only, generation of merozoites matured to sporonts. The shape changed to more or less spherical in young sporonts (Fig. 5). The nucleus increased in size, and ribosomes to a greater extent became associated with membranes to a rough endoplasmic reticulum, which surrounded the nucleus in concentrical layers. Aggregations of cytoplasmic vesicles, obviously Golgi apparatuses, became apparent in the proximity of the nucleus from the beginning of the sporogony (Fig. 5).

The plasma membrane of the young sporont was externally reinforced by an approximately 10 nm thick uniform layer of electron-dense secretions, which were generated almost simultaneously over the whole cell. The dense material then lost contact with the plasma membrane, forming protrusions, and became the envelope of a sporophorous vesicle (Fig. 6). Inside the vesicle, a new layer of electron-dense material was generated on the plasma membrane (Fig. 7). This was the primordium of the exospore, and it grew from an 18-20 nm thick layer of uniform electron-dense material to an approximately 27 nm thick, three-layered coat with a more dense layer in the middle.

The episporontal space of the newly formed sporophorous vesicle, had granular and tubular inclusions (Fig. 7). These were later organized to a continuous and regularly arranged tubular or net-like material, uniting the sporont and sporoblasts with the envelope of the sporophorous vesicle (Figs. 8-9). When the sporoblasts were individualized, superfluous plasmodium material generated a second type of tubular inclusions (Fig. 9). They were irregularly shaped and exhibited an about 30 nm thick wall of identical construction to the exospore (Fig. 10). They formed prominent networks of septate tubules (Fig. 10) between the sporoblasts. These tubules disappeared when the sporoblasts matured to spores. The densely packed thin-walled tubular material persisted to a fairly great extent also in vesicles with mature spores (Figs. 13, 20), and due to this material, the sporophorous vesicles were fairly persistent and visible in smears (Figs. 12, 14, 17).

The nucleus of the sporont divided mitotically once or twice, to bi-, tri- or tetranucleate plasmodia before dividing into sporoblasts (Fig. 11). The undivided sporont nucleus measured up to 9.0 µm in diameter, nuclei in binucleate sporonts up to 5.8 µm in diameter, and nuclei in lobed tetranucleate sporogonial plasmodia up to 3.2 µm. In plasmodia with three nuclei one nucleus was larger than the other two (Fig. 11f). The normal sporogony yielded four sporoblasts per mother cell, formed simultaneously (Fig. 11c), but spore yields from one to four were seen (Fig. 12). In Sample 1 (from *A. nervosa*) 1-4-sporous vesicles appeared in the following frequencies: 1 (0.3 %), 2 (2.4 %), 3 (3.3 %), 4 (94.0 %). In sample 3 (from *M. lateralis*) the frequencies were: 1 (0.3 %), 2 (14.5 %), 3 (23.4 %), 4 (61.8 %).There was a distinct size difference between tetraspores and macrospores (Fig. 12), but macrospores in 3-, 2- or 1-sporous vesicles were approximately of the same size. From *A. nervosa* (Sample 1) tetraspores measured 3.5-4.1 x 6.3-7.0 µm in unfixed condition, 3.0-3.5 x 4.6-5.2 µm when fixed and stained. From *M. lateralis* (Sample 2) unfixed tetraspores measured 3.5-4.2 x 6.9-7.4 µm, fixed and stained 3.0-3.5 x 4.6-6.4 µm. Fixed and stained macrospores from *A. nervosa* (Sample 1) measured 4.1-4.9 x 5.8-9.0 µm. From *M. lateralis* (Sample 2) fixed and stained macrospores were 4.1-5.8 x 6.4-10.4 µm great. In vesicles with a reduced number of sporoblasts, anomalous plasmodium fragments were observed (Figs. 11d, 13). Vesicles with one spore were obviously the result of a division where only one of the daughter cells reached to mature to spore, not of a sporont transforming directly into a sporoblast.

The transformation from sporoblast to spore, and the initiation and morphogenesis of the sporal organelles, equalled the normal for microsporidia.

Mature spores

The spores were pyriform with the anterior pole lightly pointed (Figs. 12, 14-16). Some macrospores were more stout and ovoid in shape (Fig. 12). The nuclear area of stained spores was visible in the posterior half as an obliquely directed dark strand (Figs. 11a, f). In carefully squashed sporophorous vesicles spores were occasionally arranged in a regular way, often two and two, and with the narrow poles pointing in the same direction.

The spore wall measured 250-365 nm, except anteriorly where dimensions down to 54 nm were observed. It had the traditional three subdivisions: an approximately 43 nm thick exospore, a wide structureless endospore, which was reduced anteriorly, and an approximately 8 nm thick plasma membrane (Figs. 18, 19, 21). The exospore had three distinct layers of constant thickness: an internal about 26 nm electron-dense layer, which gradually transformed into the endospore layer, a median layer resembling a c. 6 nm thick double membrane, and a c. 11 nm wide moderately dense surface layer (Fig. 21).

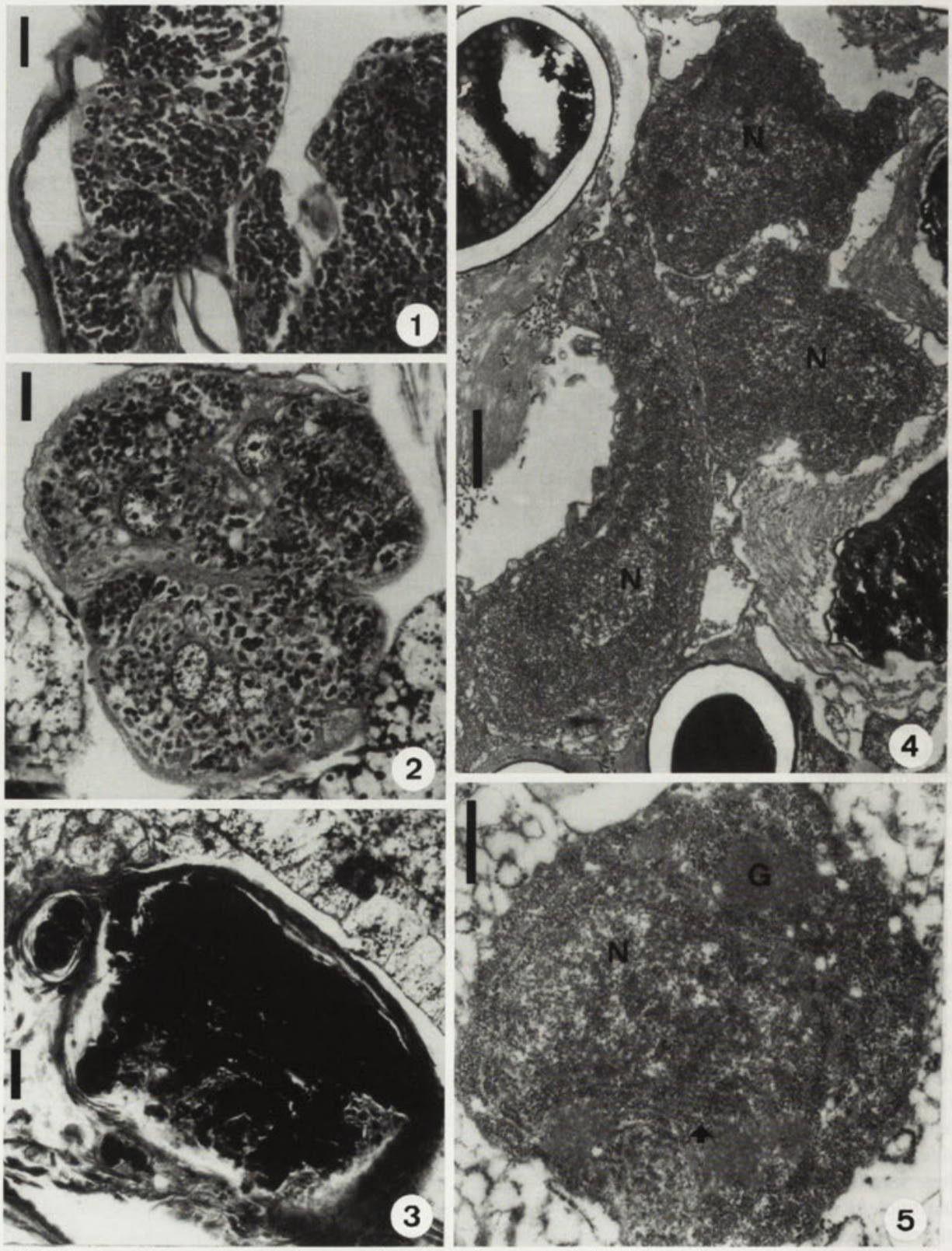

Figs. 1-5. Host-parasite interactions and ultrastructural cytology of the presporal development of *Gurleya dorisae* sp. n. 1 - adipose tissue of an *Anabolia nervosa* larva, completely filled with microsporidia; 2 - local herd of developing microsporidia in a larva of *Micropterna lateralis* with beginning encapsulation; 3 - darkly pigmented nodule formed around a microsporidia-filled fat-body lobe of *M. lateralis*; 4 - associated merozoites; 5 - young sporont, arrow indicates rough endoplasmic reticulum. G - Golgi vesicles, N - nucleus. Bars - 1-2 - 25 µm; 3 - 50 µm; 4 - 1 µm; 5 - 0.5 µm

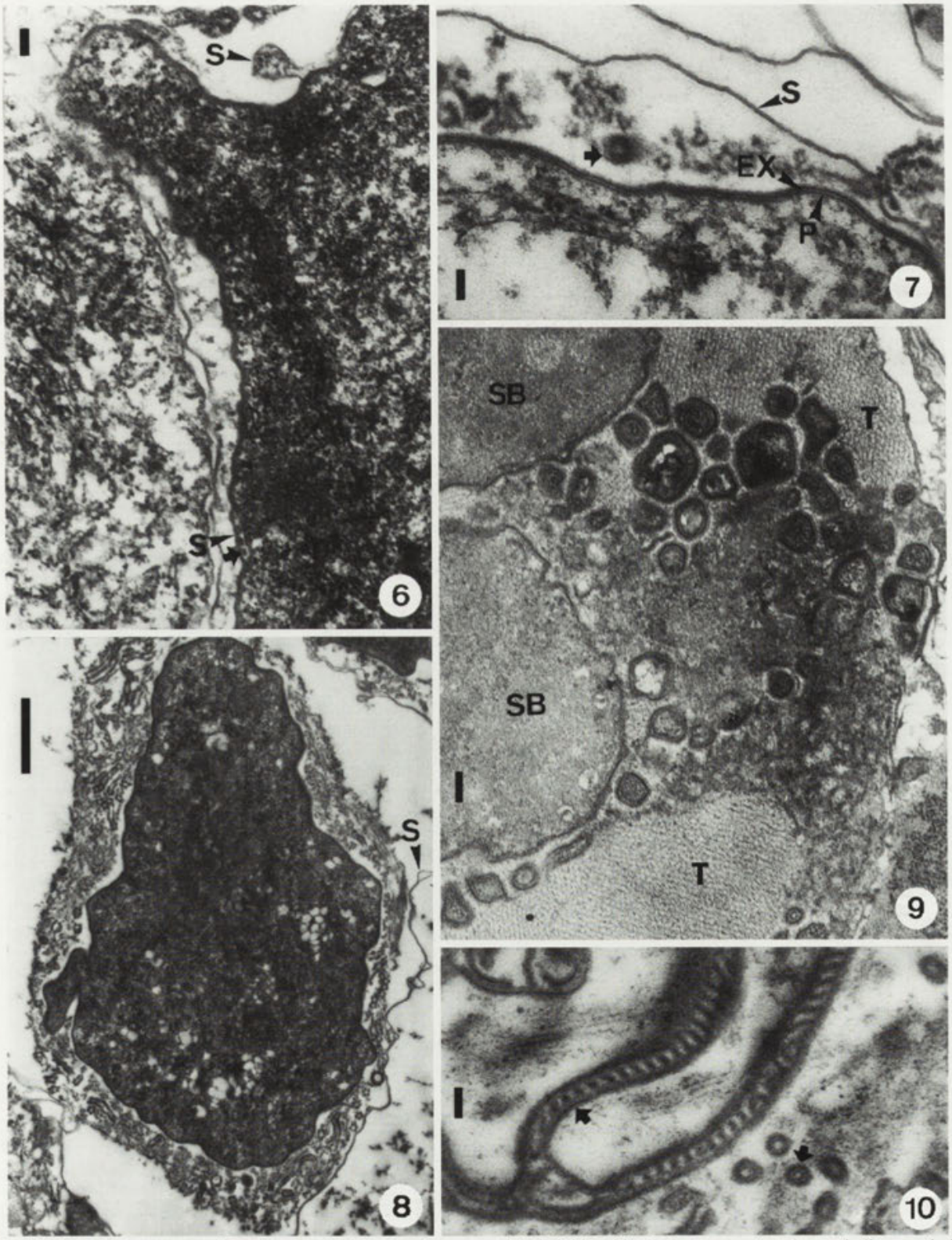

Figs. 6-10. Early sporogony of *G. dorisae*. 6 - the sporophorous vesicle is initiated by the young sporont (arrow indicates tubular inclusions of the episporontal space); 7 - inside the sporophorous vesicle layered electron-dense material (primordium of the exospore) aggregates on the plasma membrane (arrow indicates tubular inclusion); 8 - sporogonial plasmodium in a complete sporophorous vesicle; 9 - sporophorous vesicle at the sporoblast stage, with irregular wide tubular material of exospore nature and areas with closely packed, narrow tubules; 10 - network of septate tubules (arrows) of exospore origin. EX - primordium of the exospore, P - plasma membrane, S - sporophorous vesicle, SB - sporoblast, T - narrow tubules. Bars - 6-7, 9-10 - 100 nm; 8 - 1 µm

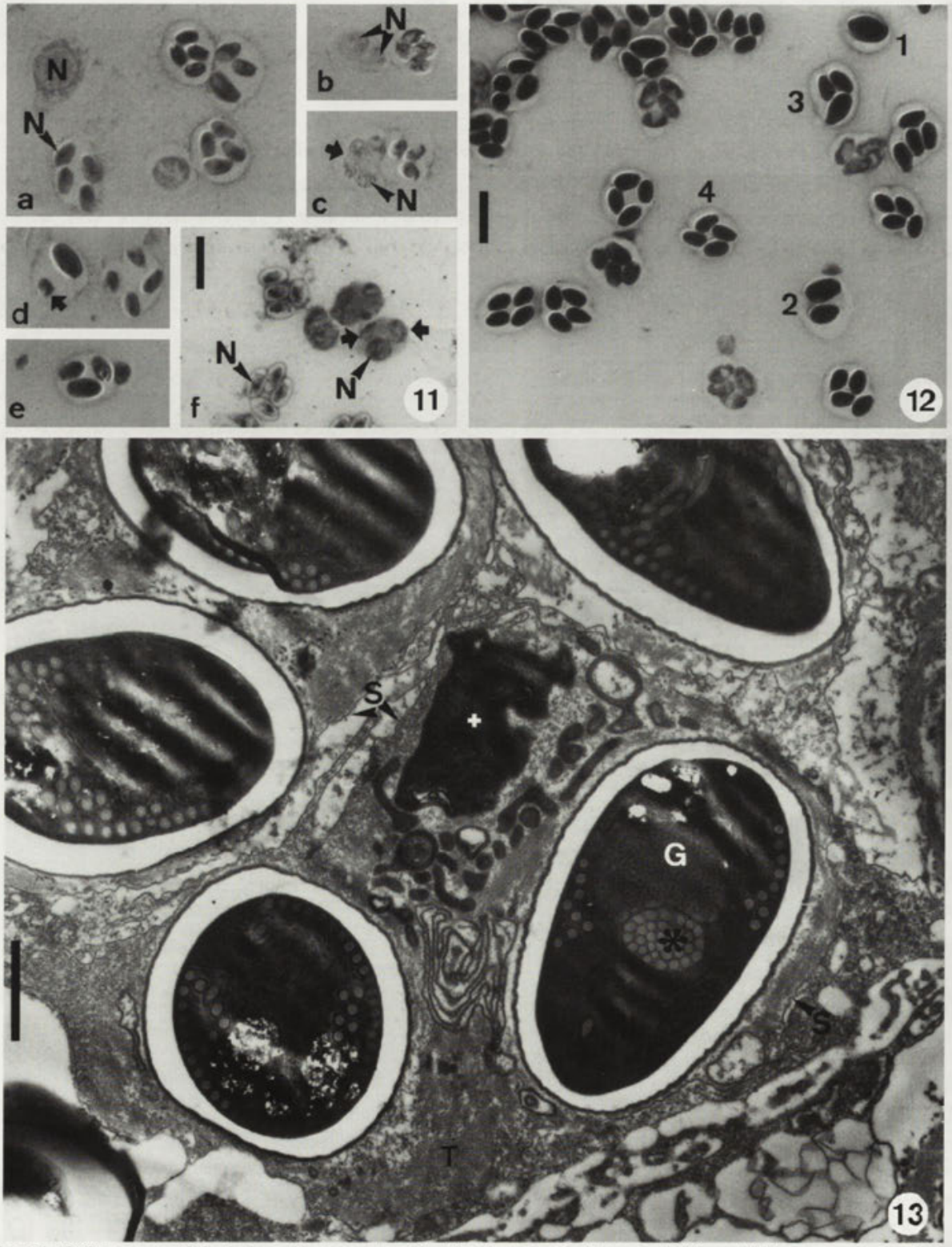

Figs. 11-13. Sporogony of *G. dorisae*. 11 - haematoxylin stained sporogonial stages exhibiting: (a) tetrasporous sporophorous vesicles and an uninucleate sporont, (b) binucleate sporogonial plasmodium, (c) tetranucleate lobed sporogonial plasmodium (arrow), (d) sporophorous vesicle with one macrospore and one sporoblast rudiment (arrow), (e) sporophorous vesicle with one macrospore and two microspores, (f) sporogonial plasmodia (arrows indicate one plasmodium with one large and two smaller nuclei) and tetrasporous sporophorous vesicles; 12 - sporophorous vesicles with 1-4 spores (indicated by numbers); 13 - sporophorous vesicles with macrospores and one sporoblast rudiment (+). G - Golgi vesicles, N - nucleus, S - sporophorous vesicle, T - densely packed, thin-walled tubules. Bars - 11 (common bar on 11f), 12 - 10 µm; 13 - 1 µm

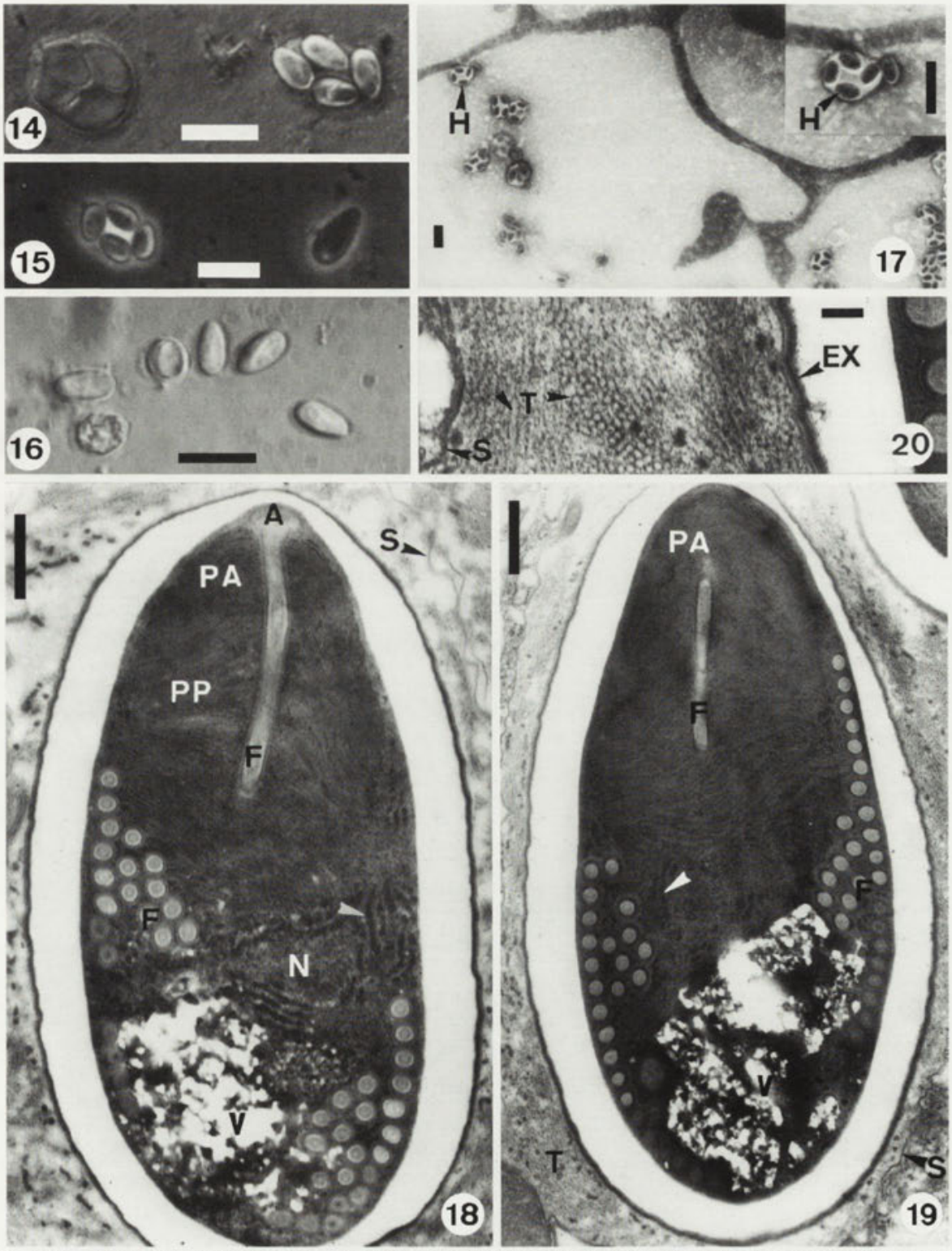

Figs. 14-20. Mature spores of *G. dorisae*. 14 - living tetrasporous sporophorous vesicles with four mature spores and four sporoblasts; 15 - two living sporophorous vesicles: one with a macrospore and one with four microspores; 16 - living mature tetraspores released by squashing; 17 - localization of the holotype (slide No. 870713-E-1 RL); 18 - longitudinally sectioned mature tetraspore; 19 - longitudinally sectioned macrospore; 20 - detail of a sporophorous vesicle with mature spores revealing the closely packed thin-walled tubules. A - anchoring disc, EX - exospore, F - polar filament, H -holotype, N - nucleus, PA - anterior polaroplast region, PP - posterior polaroplast region, S - sporophorous vesicle, T - tubules, V - posterior vacuole. 14 and 16 differential interference phase contrast, 15 phase contrast, 17 haematoxylin staining. Bars -14-17 and inset on 17 - 10 µm; 18-19 - 0.5 µm; 20 - 100nm

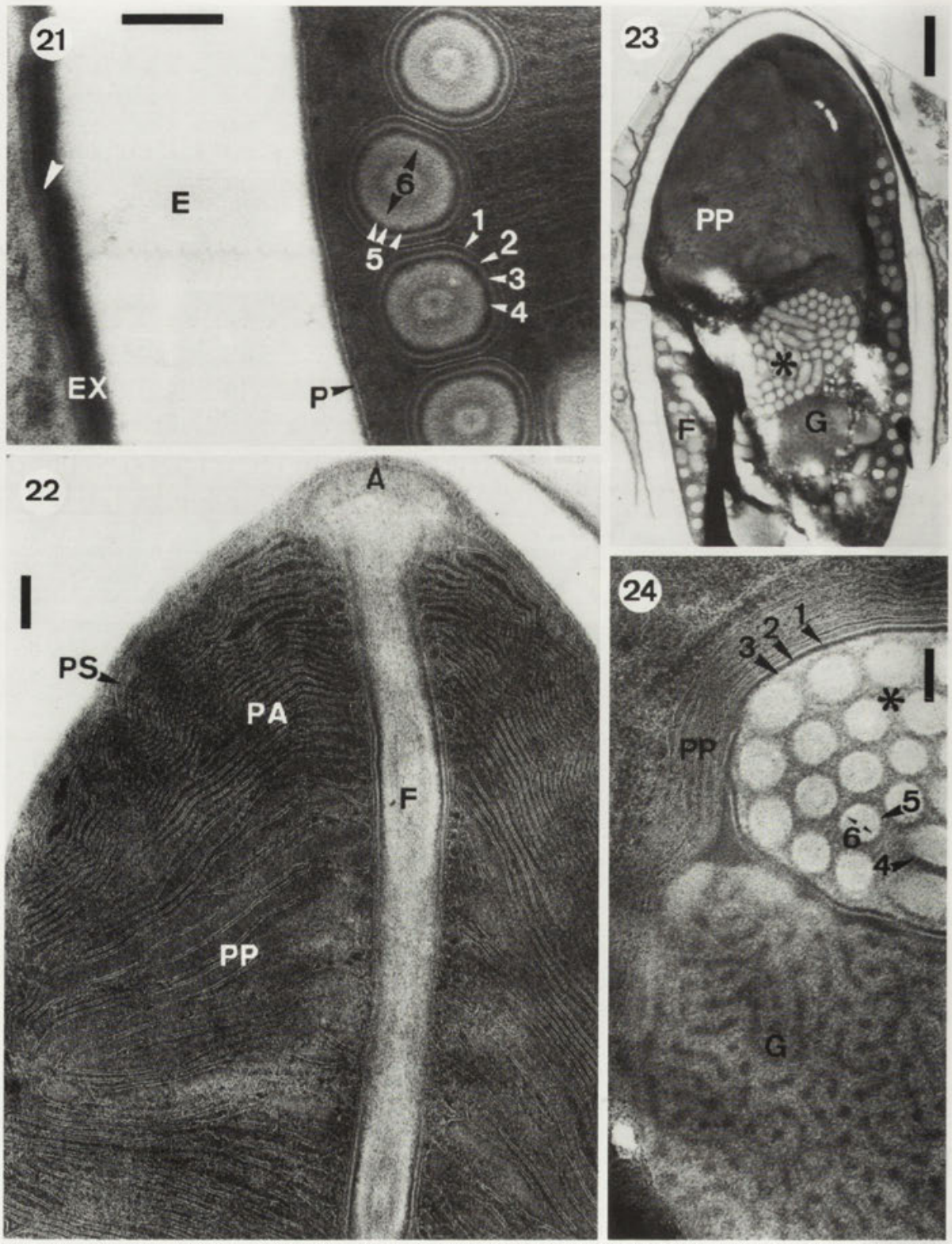

Figs. 21-24. Mature spores of *G. dorisae*. 21 - detail of the spore wall and the polar filament (the layers are numbered 1-6); 22 - detail of the polaroplast and the anterior part of the polar filament; 23 - mature macrospore with anomalous polaroplast and polar filament (*); 24 - detail of an anomalous macrospore, revealing the Golgi vesicles and the final part of the polar filament where the external three layers (1-3) form an envelope around a ball of filament centres (layers 4-6 visible). A - anchoring disc, E - endospore, EX - exospore, F - polar filament, G - Golgi vesicles, P - plasma membrane, PA - anterior polaroplast region, PP - posterior polaroplast region, PS - polar sac. Bars - 21-22, 24 - 100 nm; 23 - 0.5 µm

The polar filament was attached to a layered anchoring disc at the anterior pole of the spore (Figs. 18, 22). The widest sectioned disc of a spore in a 4-sporous sporophorous vesicle measured 346 nm in diameter. Discs of macrospores were up to 369 nm wide. The filament proceeded straight backwards for about one third of the spore length, and the final part was coiled. The anterior coils formed one row of coils close to the spore wall, while the most posterior coils were arranged in one group of coils internally to the row. The angle of tilt of the most anterior coil to the long axis of the spore was about 60°. The row of coils extended for about half of the spore length (Figs. 18-19). Small spores, in 4-sporous sporophorous vesicles, had 20-25 coils, and the number increased in macrospores up to 34 coils. The filament must be characterized as isofilar, even if there were small variations in size between individual coils (Fig. 21). The straight part measured up to 170 nm wide, and the coils were 138-157 nm in diameter. Coils of macrospores were not wider. The transversely sectioned filament exhibited a series of layers with different thickness and electron density, in direction inwards (Fig. 21: 1-6): an approximately 5 nm thick unit membrane cover (1); three narrow (c. 6 nm) layers, electron-dense (2), moderately dense (3), and electron-dense (4); a lucent lightly fibrous, about 16 nm thick layer (5), and the moderately dense centre, of slightly variable size, with diffuse layering, and with dark material in the very centre (6).

The cytology of macrospores was often disturbed, both concerning the polar filament and the polaroplast. The anterior coils of the polar filament were normal, but the terminal part was enlarged, looking like a ball in the centre of the spore (Figs. 13, 23-24). Also this part of the filament was covered like the coils, with the unit membrane (layer 1) and the two narrow external layers (layers 2-3). The bulk of the ball was composed of intertwined filament centres (Fig. 24). Neighbouring the anomalous terminal portion of the filament was a rounded spongious structure (Figs. 13, 23-24), obviously a remainder of the Golgi-apparatus from which the filament was formed.

The polaroplast, which surrounded the uncoiled part of the polar filament, had two regions with regularly arranged, closely packed lamellae, formed by unit membrane folds (Figs. 18, 19, 22): anteriorly narrow (11-32 nm wide), posteriorly wider (27-92 nm wide). The narrow lamellae constituted about 1/4 of the polaroplast. The unit membrane-lined polar sac was a narrow bell-shaped construction, enclosing the anchoring disc and approximately the anterior half of the polaroplast (Fig. 22). The approximately 5 nm thick unit membrane component of the polar filament, the polaroplast lamellae and the polar sac belonged to the same system. Macrospores had often aberrant organisation of the polaroplast lamellae (Fig. 23).

The nucleus, when seen in sectioned spores, was flat and localized approximately to the middle of the spore (Fig. 18). The cytoplasm was electron-dense with prominent strands of polyribosomes in the proximity of the nucleus, filament coils and polaroplast (Figs. 18-19). The posterior vacuole was never well fixed, but could be traced as a spongious, rather lucent area in an oblique position at the posterior pole of the spore (Figs. 18-19).

DISCUSSION

Cytology

The cytology of this microsporidium conforms with the usual for microsporidia, and only two traits need a brief comment: the anomalous cytology of the macrospores and the defense reactions against the microsporidium.

A part of the macrospores contained a ball-like structure in the centre, which by closer study was revealed to be a modification of the polar filament (Figs. 23-24). The surface layers were identical to the surface of a normal filament coil, but the interior was filled with intertwined filament centres. Similar anomalies have been observed previously, for example visible in developing spores of *Edhazardia aedis* (Fig. 50 in Becnel et al. 1989), and in mixed infections of microsporidia and fungi (Larsson et al. 1995).

It is unusual, but not unique, that an infection by microsporidia provokes cellular defense reactions with nodule formation and dark pigmentation like the effects seen here (Figs. 2-3). The most well known case is the nosemosis of the silk moth, caused by *Nosema bombycis*, and known by the name "pébrine" (de Quatrefages 1860). Production of cyst-like structures were observed by Weiser (1956) in larvae of *Ecdyonurus venosus* infected by *Nosema baetis*. Tumorous growths, obviously nodules, with melanization have been reported for *Nosema acridiophagus* in *Melanoplus sanguinipes* by Henry (1969), and nodules with melanization were observed by Brooks (1971) in *Manduca sexta* infected by *Nosema sphingidis*. Jordan

and Noblet (1982) noticed inflammatory responses in *Heliothis zea* artificially infected by *Nosema heliothidis*. The effect was intensified with simultaneous infection by *Vairimorpha necatrix*. Brooks (1971) was of the opinion that defense reactions might be more prevalent in alternate hosts of a protozoan parasite. Much speaks for this interpretation being correct, and if so, the immunological reaction seen in *Micropterna lateralis* could indicate that this is not the primary host of this microsporidium.

Taxonomy

At least 16 species of microsporidia have been reported from Trichoptera. Five of them, *Cougourdella polycentropi* Weiser, 1965, *C. rhyacophilae* Baudoin, 1969, *Episeptum inversum* Larsson, 1986, *Pyrotheca hydropsycheae* Xie and Canning, 1986, and *Gurleya legeri* Hesse, 1903 sensu Mackinnon (1911), exhibit tetrasporoblastic sporogony. The genera *Cougourdella*, *Episeptum* and *Pyrotheca* have distinct cytological characteristics, and it is obvious that the microsporidium treated herein is different from the species assigned to these genera.

The microsporidium Mackinnon (1911) reported from caddisfly larvae, mainly of the genera *Anabolia* and *Limnephilus*, collected in the neighbourhood of Aberdeen, was identified to be *Gurleya legeri* Hesse, 1903. This is a parasite of the mayfly *Ephemerella ignita* (see Hesse 1903). The different orders of hosts and minor differences between the microsporidia, e.g. ovoid versus pyriform spores, suggest that the microsporidia of Hesse and Mackinnon are different species, like stated by Weiser (1961). However, the microsporidium seen by Mackinnon resembles closely the Swedish species. The shape and size of the spores are identical, the infection was seen at the same time of the year (late summer), and the pathological effects on the hosts are the same, except that defense reactions were not noticed by Mackinnon. The hosts were not specified further than that larvae of the genera *Anabolia* and *Limnephilus* were studied. It must be concluded that the species described herein is new to science and obviously identical to the microsporidium Mackinnon (1911) identified as *G. legeri*.

The genus *Gurleya* Doflein, 1898 was established for microsporidia expressing tetrasporoblastic sporogony. The spores of the type species, *G. tetraspora*, were described as oval, having pointed anterior and blunt posterior poles, and the spore surface was striated (Doflein 1898). By the present time the genus contains about 22 named species, approximately half of them parasites of Crustacea. Eight of the species are parasites of insects. The type species, *G. tetraspora* Doflein, 1898, is a parasite of the microcrustacean *Daphnia magna*. This species has not been studied since it was described.

When *Gurleya* was created, the tetrasporoblastic sporogony was a new feature for microsporidia, and it was considered diagnostic for the genus. It took nearly 40 years before a new find made it necessary to establish a second genus for tetrasporoblastic microsporidia (Hesse 1935). It is well known now that tetrasporoblastic sporogony occurs in a number of microsporidia, widely differing in other cytological and life cycle characteristics, and it is obvious that the number of sporoblasts per sporont alone is not sufficient for the identification of the genus. At least 16 genera express tetrasporoblastic sporogony, alone or together with one or two additional sequences of sporogony: *Amblyospora, Auraspora, Baculea, Campanulospora, Cougourdella, Episeptum, Golbergia, Gurleya, Lanatospora,* possibly *Merocinta, Microfilum, Norlevinea, Pyrotheca, Septata, Stempellia,* and *Tetramicra*. It is easy to distinguish the genera established in recent years. The real problem is whether all genera younger than *Gurleya* are distinct genera, or if one of them might by a younger synonym of *Gurleya*. As *G. tetraspora* Doflein, 1898 has not been studied using modern techniques, the characteristics of a *Gurleya* species are unknown.

The microsporidium treated herein expresses a traditional microsporidian cytology, and the regular production of macrospores is not a unique feature. It is easily seen that it cannot be a member of any recently established genus with distinct characteristics, but the genus *Gurleya* remains as a possible solution. There is one remarkable character mentioned in the description of the type species *G. tetraspora*: the presence of striations on the spore wall (Doflein 1898). This is an almost unique observations for a microsporidium, the only other case is *Striatospora chironomi* (see Issi 1986, 1991), and striations have never been observed in microsporidian spores studied using the SEM. However, as striated spore walls are common among the myxosporidia, it cannot be excluded that Doflein's interpretation might have been influenced from his knowledge of these organisms - and the new species appeared in a publication mostly devoted to the myxosporidia (Doflein 1898). As there is reason to doubt that the spore walls of *G. tetraspora* really are striated, we cannot consider this character diagnostic for a *Gurleya* species. There is no firm base for the establishment of a new genus, and the

only remaining genus with a potential to accommodate this microsporidium is *Gurleya.* Therefore the best solution to the genus problem seems to be to use *Gurleya* as a repository for the new species until a new investigation of *G. tetraspora* provides substantial discriminating characters for the genus *Gurleya.*

DESCRIPTION

Gurleya dorisae sp. n.

Synonym: *Gurleya legeri* Hesse, 1903 sensu Mackinnon (1911).

Merogony: only observed as small groups of uninucleate merozoites.

Sporogony: a uninucleate sporont yields a tetranucleate sporogonial plasmodium, which divides rosette-like into four sporoblasts. In addition macrosporos sporogony yielding one, two or three sporoblasts per mother cell occurs.

Spores: pyriform with pointed anterior end. Unfixed tetraspores from the type host measure 3.5-4.1 x 6.3-7.0 µm, fixed and stained 3.0-3.5 x 4.6-5.2 µm. Fixed and stained macrospores from the type host measure 4.1-4.9 x 5.8-9.0 µm. The spore wall is 250-365 nm thick with an approximately 43 nm thick three-layered exospore, where the median layer resembles a double-membrane. The polar filament is isofilar with 20-25, 138-157 nm wide, coils in one row of coils close to the spore wall and one internal group of coils. The row of coils is approximately 1/2 of the spore length. The angle of tilt is about 60°. Macrospores have an increased number of coils (up to 34) of identical diameter to coils of tetraspores. The polaroplast has two regions of lamellae, anterior ones more closely arranged. The polaroplast ends close to the anterior polar filament coil. There is one, rather flat, nucleus in the centre of the spore.

Sporophorous vesicle: rounded to ovoid, persistent. Episporontal space with persistent, densely arranged, narrow, thin-walled tubules. Wider septate tubules, with wall of exospore-material, produced during the sporoblastogenesis, disappear when the spores mature.

Host tissues involved: adipose tissue, induces nuclear hypertrophy but not syncytium formation. Defense reaction with nodule formation observed in other hosts than the type host.

Type host: *Anabolia nervosa* (Curtis, 1834) (Trichoptera, Limnephilidae).

Additional hosts: *Micropterna lateralis* (Stephens, 1837); and reported by Mackinnon (1911): *Limnephilus* sp. and *Anabolia* sp. (Trichoptera, Limnephilidae).

Type locality: the small river Höje å , close to the village of Esarp, Scania, in the south of Sweden.

Types: holotype (Fig. 17) on slide No. 870713-E-1 RL, paratypes on slides No. 870713-E-(1-34) RL.

Deposition of types: the slide with the holotype, and paratype slides, in the International Protozoan Type Slide Collection at Smithsonian Institution (Washington, DC). Paratypes in the collection of Dr. J. Weiser, Prague (Czech Republic) and in the collection of the author.

Etymology: the species name in honour of Dr. Doris L. Mackinnon, Great Britain, who made the first observation of the species.

Acknowledgements. The author is indebted to Mrs. Lina Gefors, Mrs. Inga Jogby, Mrs. Birgitta Klefbohm, Mrs. Inger Norling and Mrs. Inga-Lill Palmquist, all at the Department of Zoology, University of Lund, for excellent technical assistance. The investigation was supported by research grants from the Swedish Natural Science Research Council.

REFERENCES

Becnel J. J., Sprague V., Fukuda, T., Hazard E. I. (1989) Development of *Edhazardia aedis* (Kudo, 1930) n. g., n. comb. (Microsporida: Amblyosporidae) in the mosquito *Aedes aegypti* (L.) (Diptera: Culicidae). *J. Protozool.* **36:** 119-130

Brooks W. M. (1971) The inflammatory response of the Tobacco Hornworm, *Manduca sexta*, to infection by the microsporidian, *Nosema sphingidis*. *J. Invertebr. Pathol.* **17:** 87-93

Doflein F. (1898) Studien zur Naturgeschichte der Protozoen. III .Uber Myxosporidien. *Zool. Jahrb. Abt. Anat.* **11**: 281-350

Farley C. A. (1965) A modification of Noland's stain for permanent smears of protozoan flagella, cilia and spore filaments. *J. Parasit.* **51:** 834

Hesse E. (1903) Sur une nouvelle Microsporidie tétrasporée du genre *Gurleya*. *C. R. Soc. Biol.* **55:** 495-496

Hesse E. (1935) Sur guelgues Microsporidies parasites de *Megacyclops viridis* Jurine. *Arch.Zool. Exp. Gén.* **75**: 651-661

Henry J. E. (1969) Early morphogenesis of tumours induced by *Nosema acridiophagus* in *Melanoplus sanguinipes*. *J. Insect Physiol.* **15:** 391-394

Hostounský Z., Žizka Z. (1979) A modification of the "agar cushion method" for observation and recording microsporidian spores. *J. Protozool.* **46:** 41A-42A

Issi I. V. (1986) Microsporidia as a phylum of parasitic protozoa. *Protozoology (Leningrad)* **10**: 6-136 (in Russian)

Issi I. V. (1991) Microsporidia as a phylum of parasitic protozoa. Translated from Russian by Jerzy J. Lipa. Division on Microsporidia, Society for Invertebrate Pathology

Jordan J. A., Noblet R. (1982) Pathological studies of *Heliothis* infected with *Nosema heliothidis* and *Vairimorpha necatrix*. *J. Georgia Entomol. Soc.* **17:** 183-189

Larsson J. I. R. (1986) Ultracytology of a tetrasporoblastic microsporidium of the caddisfly *Holocentropus picicornis* (Trichoptera, Polycentropodidae), with description of *Episeptum inversum* gen. et sp. nov. (Microspora, Gurleyidae). *Arch. Protistenkd.* **131:** 257-279

Larsson J. I. R., Eilenberg J., Bresciani J. (1995) Ultrastructural study and description of *Cystosporogenes deliaradicae* n. sp. (Microspora, Glugeidae), a microsporidian parasite of the cab-

bage root fly *Delia radicum* (Linnaeus, 1758) (Diptera, Anthomyidae). *Europ. J. Protistol.* (in press)
Mackinnon D. L. (1911) On some more protozoan parasites from Trichoptera. *Parasitology* **4:** 28-38
Quatrefages A., de (1860) Études sur les maladies actuelles du ver à soi. *Mem. Acad. Sci.* **30**: 3-382, 521-638
Reynolds E. S. (1963) The use of lead citrate at high pH as an electron-opaque stain in electron microscopy. *J Cell. Biol.* **17:** 208-212
Romeis B. (1968) Mikroskopische Technik. Oldenbourg Verlag, München-Wien
Vetterling J. M., Thompson D. E. (1972) A polychromatic stain for use in parasitology. *Stain Technol.* **47:** 164-165
Weiser J. (1956) Studie o mikrosporidiích z larev hmyzů našich vod, II. *Čs. parasit.* **3:** 193-202
Weiser J. (1961) Die Mikrosporidien als Parasiten der Insekten. *Monogr. Angew. Entomol.* **17:** 1-149

Received on 20th June, 1994; accepted on 14th October, 1994

ACTA
PROTOZOOLOGICA

Acta Protozoologica (1995) 34: 57 - 60

New Species of Eimeria (Apicomplexa) from Captive Wood Turtles, *Clemmys insculpta* (Testudines: Emydidae), from the Dallas Zoo

Steve J. UPTON[1], Chris T. MCALLISTER[2] and Clay M. GARRETT[3]

[1]Division of Biology, Kansas State University, Manhattan, Kansas; [2]Department of Veterans Affairs Medical Center, Dallas, Texas; and [3]Reptile Department, Dallas Zoo, Dallas, Texas, USA

Summary. A new species of coccidian (Apicomplexa, Eimeriidae) is described from the faeces of captive wood turtles, *Clemmys insculpta*, housed at the Dallas Zoo, USA. Oocysts of *Eimeria lecontei* sp. n. were found in 4 adult turtles and are ellipsoidal, 28.3 x 15.8 (25.6-32.0 x 13.6-17.6) µm, with a thin, delicate wall; shape index (length/width) 1.79 (1.52-2.06). A micropyle was absent but an oocyst residuum and polar granule were present. Sporocysts were elongate, 19.7 x 5.6 (17.6-23.2 x 5.0-6.4) µm, and possessed a Stieda body; shape index 3.59 (2.97-4.15). Each sporozoite had spherical anterior and spherical to ellipsoidal posterior refractile bodies.

Key words. *Clemmys insculpta*, Testudines, *Eimeria lecontei* sp. n., Coccidia, Apicomplexa, Eimeriidae.

INTRODUCTION

The wood turtle, *Clemmys insculpta* (LeConte, 1830), is a mostly terrestrial emydid of North America that ranges from Nova Scotia and eastern Minnesota, south to the Virginias; a disjunct population also occurs in northeastern Iowa (Conant and Collins 1991). The species inhabits woods and farmland meadows, where it can be found in both aquatic and terrestrial environments feeding on earthworms, slugs, insects, tadpoles, and wild fruit. Unfortunately, overcollecting and loss of habitat have contributed to the decline of this species and it is now considered endangered (Lieberman 1993).

Ernst (1972) summarized biological information on *C. insculpta* and Ernst and Ernst (1977) reviewed helminth parasites. However, little is known of the coccidial fauna harbored by this turtle. Wacha and Christiansen (1974) described *Eimeria megalostiedai* from a single *C. insculpta* from Iowa and, more recently, McAllister et al. (1994) reported an *Eimeria pseudemydis*-like coccidian and an undescribed eimerian from captive *C. insculpta* at the Dallas Zoo. Herein we provide a description of this latter eimerian.

MATERIALS AND METHODS

During April and June, 1993, 4 adult (2 males and 2 females, mean±SE carapace length 177.0±15.8, range 148-220 mm) *C. insculpta* housed in an outside enclosure at the Dallas Zoo were examined for coccidia. These animals were donated to the Zoo and, although the exact locality where the turtles originated is not known, they are thought to have been collected somewhere in the northeastern United States. Each turtle was collected from the enclosure and allowed to defecate in glass aquaria, then released back into the enclosure. Oocysts were then concentrated by flotation in an aqueous sucrose

Address for correspondence: S.J. Upton, Division of Biology, Ackert Hall, Kansas State University, Manhattan, KS 66506 USA; FAX (913) 532-6653; E-mail: COCCIDIA@KSUVM.KSU.EDU

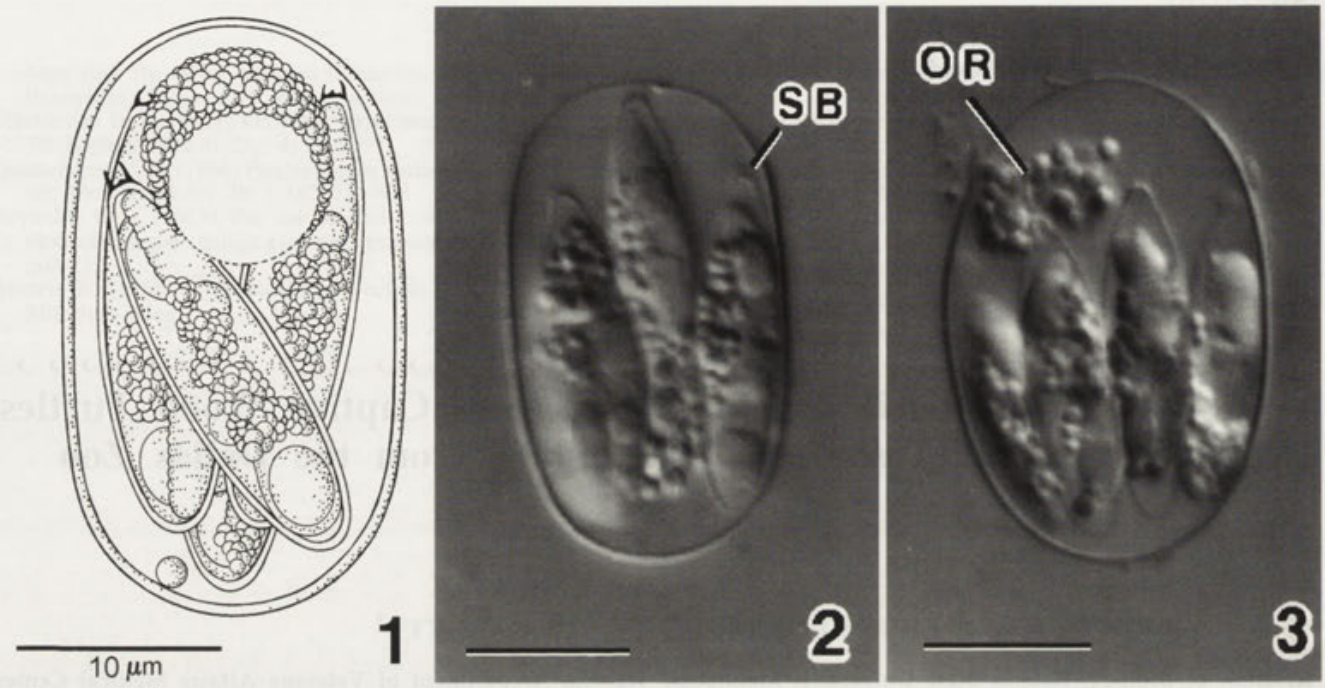

Fig. 1. Composite line drawing of sporulated oocyst of *Eimeria lecontei* sp. n. from *Clemmys insculpta*
Figs. 2-3. Nomarski interference-contrast photomicrographs of sporulated oocysts of *Eimeria lecontei* sp. n. Bars - 10 µm. Abbreviations: OR - oocyst residuum, SB - Stieda body

solution (specific gravity 1.30). Measurements and photomicrographs were taken using Nomarski interference-contrast optics and a calibrated ocular micrometer and are reported in micrometers (µm) as means, followed by the ranges in parentheses. Oocysts were 7 days old when measured.

RESULTS

All 4 turtles were found to be passing unsporulated coccidian oocysts. Upon sporulation, these oocysts were found to represent a previously unreported species, which is described below.

Eimeria lecontei sp. n. (Figs. 1-3)

Description of oocysts: oocysts ellipsoidal, 28.3 x 15.8 (25.6-32.0 x 13.6-17.6) (N=25), with a thin, smooth, delicate wall that appeared to be single-layered; shape index (length/width) 1.79 (1.52-2.06). Micropyle absent; oocyst residuum present, 10.5 x 8.3 (8.0-16.0 x 5.4-11.0) (N=20), composed of coarse granules either scattered or surrounding vacuolar-like structure; polar granule present. Sporocysts elongate, 19.7 x 5.6 (17.6-23.2 x 5.0-6.4) (N=20); shape index 3.59 (2.97-4.15). Stieda body present, blunt with short filaments; substieda body absent. Sporozoites elongate, 15.4 x 2.9 (14.4-16.0 x 2.4-3.4) (N=10) *in situ*, with transverse striations anteriorly. Sporozoites lie lengthwise, in opposite directions in sporocyst. Each sporozoite with spherical anterior refractile body, 2.3 (2.0-2.6) (N=10) and spherical to ellipsoidal posterior refractile body, 3.4 x 2.7 (2.4-5.6 x 2.2-3.2) (N=10). Nucleus located between refractile bodies.

Type-host: *Clemmys insculpta* (LeConte, 1830) "wood turtle" (Chelonia: Emydidae). An 11 years old adult male, carapace length 220 mm, previously housed at the Dallas Zoo, died 26 April 1994. This turtle has been deposited at the University of Texas at Arlington vertebrate collection as No. 938192.

Type locality: Dallas Zoo, Dallas County, Dallas, Texas, USA.

Type specimens: phototypes have been deposited in the U.S. National Helminthological Museum, Beltsville, Maryland as USNM No. 84157.

Site of Infection: unknown. Oocysts recovered from feces.

Sporulation: exogenous. Oocysts were passed unsporulated or partially sporulated and completed development within 5 days at 23°C.

Prevalence: 4/4 turtles housed at the Dallas Zoo were passing oocysts.

Etymology: the specific epithet is given in honor of Major John Eatton LeConte (1784-1860), herpetologist, who described the host in 1830.

DISCUSSION

Although several other species of turtle coccidia possess filaments arising from the Stieda body, none are like those found associated with *E. lecontei* sp. n. Those of *E. trachemydis* from *Trachemys scripta elegans*, *E. filamentifera* from *Chelydra serpentina*, and *E. pallidus* and *E. spinifera* from *Apalone spinifera* are all more elongate and filamentous (McAllister and Upton 1988; McAllister et al. 1990a, b; Wacha and Christiansen 1979) whereas those of *E. somervellensis* in *Pseudemys texana* is singular and stout, and resembles *Die Pickelhaube*, a spike on a German World War I helmet (McAllister and Upton 1992). Filaments of *E. cooteri* in *Pseudemys texana* are also stout, covered by a thin membrane, and possess knob-like structures at their ends (McAllister and Upton 1989).

Acknowledgments. This is Kansas Agricultural Experiment Station Contribution No. 95-75-J.

REFERENCES

Conant R., Collins J.T. (1991) A Field Guide to Reptiles and Amphibians of eastern and central North America. Houghton Mifflon Co., Boston

Ernst C.H. (1972) *Clemmys insculpta*. In: Catalogue of American Amphibians and Reptiles (Ed. G.R. Zug) Society for the Study of Amphibians and Reptiles, New York

Ernst E.M., Ernst C.H. (1977) Synopsis of helminths endoparasitic in native turtles of the United States. *Bull. Maryland Herpetol. Soc.* **13:** 1-75

Liebermann S.S. (1993) Cites amendments strengthen protection for wildlife and plants. *Endangered Species Tech. Bull.* **18**: 7-9

McAllister C.T., Upton S.J. (1988) *Eimeria trachemydis* n. sp. (Apicomplexa: Eimeriidae) and other eimerians from the red-eared slider, *Trachemys scripta elegans* (Reptilia: Testudines), in north-central Texas. *J. Parasitol.* **74:** 1014-1017

McAllister C.T., Upton S.J. (1989) The coccidia (Apicomplexa: Eimeriidae) of Testudines, with descriptions of three new species. *Can. J. Zool.* **67:** 2459-2467

McAllister C.T., Upton S.J. (1992) A new species of *Eimeria* (Apicomplexa: Eimeriidae) from *Pseudemys texana* (Testudines: Emydidae), from North-Central Texas. *Texas J. Sci.* **44:** 37-41

McAllister C.T., Upton S.J., McCaskill L.D. (1990a) Three new species of *Eimeria* (Apicomplexa: Eimeriidae) from *Apalone spinifera pallidus* (Testudines: Trionychidae) in Texas, with a redescription of *E. amydae*. *J. Parasitol.* **76:** 481-486

McAllister C.T., Upton S.J., Trauth S.E. (1990b) Coccidian parasites (Apicomplexa: Eimeriidae) of *Chelydra serpentina* (Testudines: Chelydridae) from Arkansas and Texas, U.S.A., with descriptions of *Isospora chelydrae* sp. nov. and *Eimeria serpentina* sp. nov. *Can. J. Zool.* **68:** 865-868

McAllister C.T., Upton S.J., Trauth S.E. (1994) New host and geographic records for coccidia (Apicomplexa: Eimeriidae) from North American turtles. *J. Parasitol.* **80:** (in press)

Wacha R.S., Christiansen J.L. (1974) *Eimeria megalostiedai* sp. n. (Protozoa: Sporozoa) from the wood turtle, *Clemmys insculpta*, in Iowa. *Proc. Helminthol. Soc. Wash.* **41:** 35-37

Wacha R.S., Christiansen J.L. (1979) *Eimeria filamentifera* sp. n. from the snapping turtle, *Chelydra serpentina* (Linné), in Iowa. *J. Protozool.* **26:** 353-354

Received on 31st August, 1994; accepted on 16th October, 1994

ACTA
PROTOZOOLOGICA

Acta Protozoologica (1995) 34: 61 - 66

Ultrastructural Study of *Nosema omaniae* sp. n. (Microspora, Nosematidae) Parasite of *Omania coleoptrata* (Heteroptera, Omaniidae)

Karamoko DIARRA and Bhen Sikina TOGUEBAYE

Laboratoire de Parasitologie, Département de Biologie Animale, Faculté des Sciences et Techniques, Université Cheikh Anta Diop de Dakar, Dakar, Sénégal

Summary. *Nosema omaniae* (Microsporida, Nosematidae) is being described from *Omania coleoptrata* (Heteroptera, Omaniidae). The microsporidium attacks the adipose and nervous tissues and the muscles. All developmental stages are in direct contact with host cells cytoplasm and their nuclei are diplokaryotic. The meronts are bounded by a thin electron-dense wall and their cytoplasm contains some free ribosomes. The sporonts possess a thick electron-dense envelope and a cytoplasm with abundant ribosomes. The sporoblasts transform directly into diplokaryotic spores. Live mature spores measure 4.4±.2 x 2.3±0.3 µm. Their wall is composed of an electron-dense exospore (45 nm thick), consisting of an inner electron-dense layer and an outer layer that is less dense, and of a clear endospore about 85 nm thick. The polar filament is isofilar with 12 to 13 coils in one rank. The polaroplast possesses an anterior lamellar part and a posterior vesicular part.

Key words. Microspora, *Nosema omaniae* sp.n., ultrastructure, Heteroptera, Senegal.

INTRODUCTION

Explorations undertaken in the Dakar region (Senegal) enabled us to find, in *Omania coleoptrata* (Heteroptera, Omaniidae), a microsporidium belonging to the genus *Nosema* Naegeli, 1857. The heteropteran hosts were collected from temporary pools.

Few *Nosema* of heteroptera have been studied, the species reported so far having been examined by light microscopy only (Lipa 1977, Sprague 1977). The present paper describes, with the aid of electron microscopy, the microsporidium found in *Omania coleoptrata*.

Address for correspondence: B. S. Toguebaye, Laboratoire de Parasitologie, Département de Biologie Animale, Faculté des Sciences et Techniques, Université Cheikh Anta Diop de Dakar, Dakar, Sénégal; Fax (221) 246318

MATERIALS AND METHODS

Thirteen of the 48 adult specimens of *Omania coleoptrata* Horv. collected from temporary pools of Dakar (Senegal, West Africa) were infected with the microsporidium, amounting to a prevalence of 27 %. For electron microscopy, fragment of infected hosts were fixed 12 to 24 h in 2.5 % glutaraldehyde in 0.1 M sodium cacodylate buffer, pH 7.2 at 4°C and then post fixed for 1 h with 1 % osmium tetroxide in the same buffer. After dehydration in ethanol series and propylene oxide, the fragment were embedded in Epon and sectioned with Reichert-Jung ultramicrotome. Sections were stained with uranyl acetate, lead citrate and observed under a JEOL 100 CX II.

RESULTS

Description

Site of infection (Figs. 1-2)

Examination of sections of infected hosts revealed that the microsporidium develops in fat body (Figs. 1-2), nervous tissue and the muscles. These tissues are destroyed and replaced by the developmental stages of the microsporidium.

Meronts and merogony (Figs. 3-4)

Meronts develop in direct contact with the cytoplasm of the host cells and their nuclei are diplokaryotic (Figs. 3-4). They are bounded by a thin electron-dense envelope. The cytoplasm contains some free ribosomes, and saccules of endoplasmic reticulum. The densities of the nucleoplasm and the cytoplasm are similar. Merogony is often binary; two diplokarya are first produced and then, the plasmotomy (Fig. 4) gives rise to two new diplokaryotic meronts.

Sporonts and sporogony (Figs. 5-7)

The beginning of sporogony is marked by the structural transformation of the envelope surrounding the meront; small dense vesicles appear on the outer surface of the envelope (Fig. 5) and form a thick (about 30 nm) electron dense wall. Thus, the sporonts are bounded by a thick electron dense wall (Figs. 6-7) which develops into exospore of the spore wall.

Dividing sporonts are common and their nuclei contain spindle plaques made up of an electron-dense plaque, closely associated with the nuclear membrane which is depressed (Fig. 6). Under this plaque, in the nucleoplasm, electron-dense structure, apparently chromosomes, are present. Each sporont gives rise, by binary fission (Fig. 7), to two diplokaryotic sporoblasts.

Sporoblasts and spores (Figs. 8-14)

The sporoblasts are diplokaryotic (Fig. 8). Fixed, they measure about 4.8 µm in length and 2.4 µm in width. Their surface is irregular and they are more or less elongated. Their cytoplasm becomes opaque and contains cisternae of endoplasmic reticulum, free ribosomes and early stages of the future polar filament. The wall of older sporoblasts is thick and consists of two layers: a thick inner electron-dense layer and an outer layer that is less dense (Fig. 9). The wall of the future exospore of the spore is about 45 nm thick. The sporoblasts evolve directly into diplokaryotic spores.

Young spores (Fig. 10) are elongated. They have an immature polar filament and a thin endospore. The mature fresh spores are ovoid and measure 4.4±0.2 x 2.3±0.3 µm. Their wall (Fig. 14) reaches 130 nm in thickness. It is composed of an exospore (45 nm thick) consisting of an inner electron-dense layer and an outer layer that is less dense, and a transparent endospore of about 85 nm thick. Near the anchoring disc (Fig. 12), the thickness of the endospore decreases to 25 nm. The polar filament is isofilar (Fig. 13) and its diameter is about 100 nm. It is made up of an anterior rectilinear part and of a posterior coiled part with 12 to 13 coils in one rank. The polaroplast (Fig. 13) possesses an anterior lamellar part and a posterior vesicular part. The cytoplasm contains numerous free ribosomes forming sometimes chains arround the diplokaryon.

DISCUSSION

Ultrastructure

The fine structure of various stages of the species described here is typical of other *Nosema* species (Youssef and Hammond 1971, Colley et al. 1975, Toguebaye and Marchand 1984). The only unusual feature observed is the structure of the wall of older sporoblast and the structure of the exospore.

Taxonomy

The microsporidium described here belongs indubitably to the genus *Nosema* Naegeli, 1857 because it is monomorphic, disporous and all its stages are diplokaryotic and in direct contact with the host cytoplasm cell (Sprague 1978, Vavra et al. 1981, Sprague et al. 1992).

To our knowledge, the following seven species of *Nosema* have been described from heteroptera (Lipa 1977, Sprague 1977): *Nosema adiei* Shortt and Swaminath, 1924; *Nosema bialovesiana* Lipa, 1966 ; *Nosema graphosomae* Galli-Valerio, 1924 ; *Nosema leptocoris* Lipa, 1966 ; *Nosema nepae* Lipa, 1966 ; *Nosema pyrrhocoridis* Lipa, 1977 ; *Nosema veliae* Weiser, 1961.

Nosema adiei infects the gut, the Malpighian tubules and the salivary glands of *Cimex rotundatus*. Its spores measure 3 x 1.7 µm (Lipa 1977). *Nosema bialovesiana* infects the midgut and the fat body of *Nepa cinerae* in Poland. Its spores are uninucleate or binucleate and

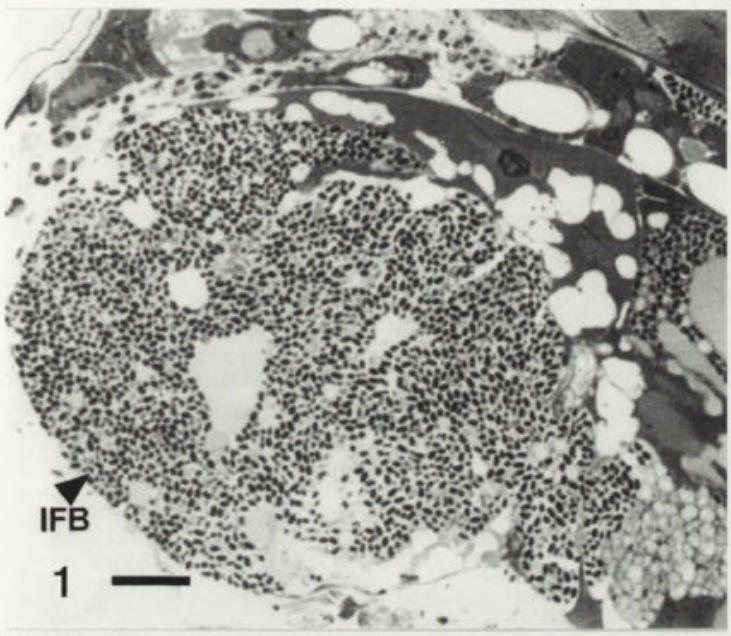

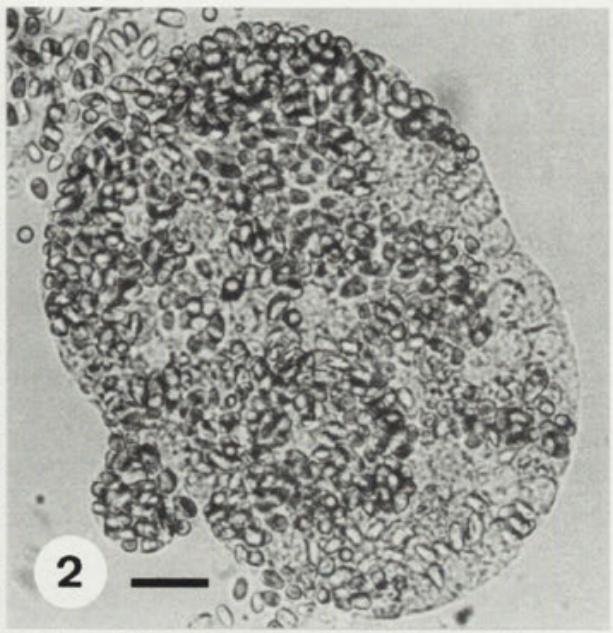

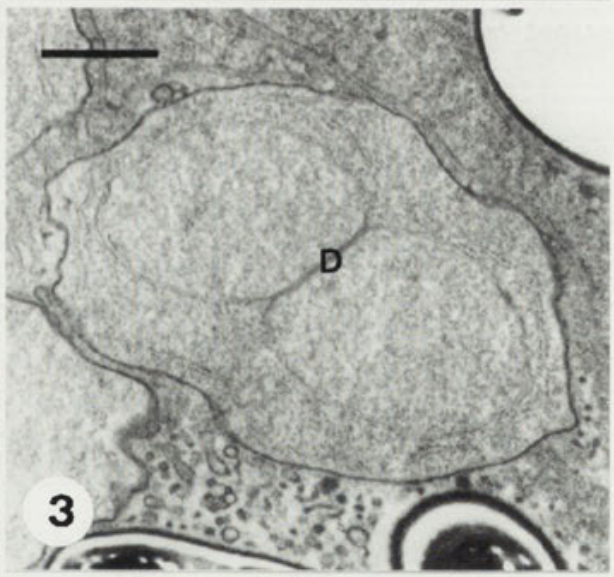

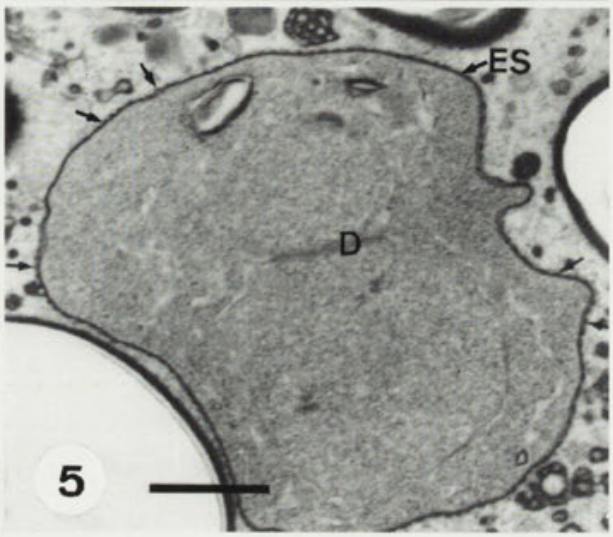

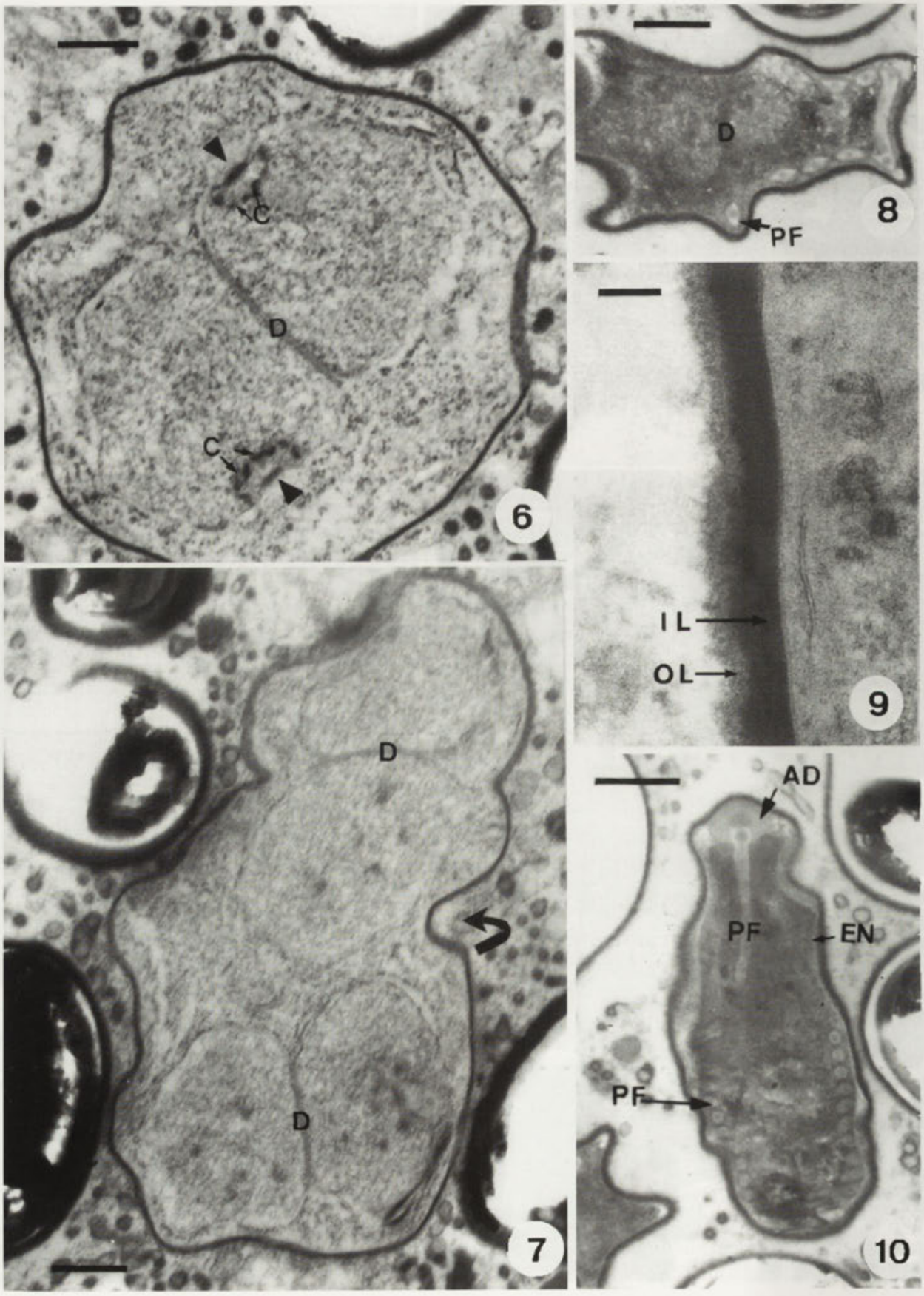

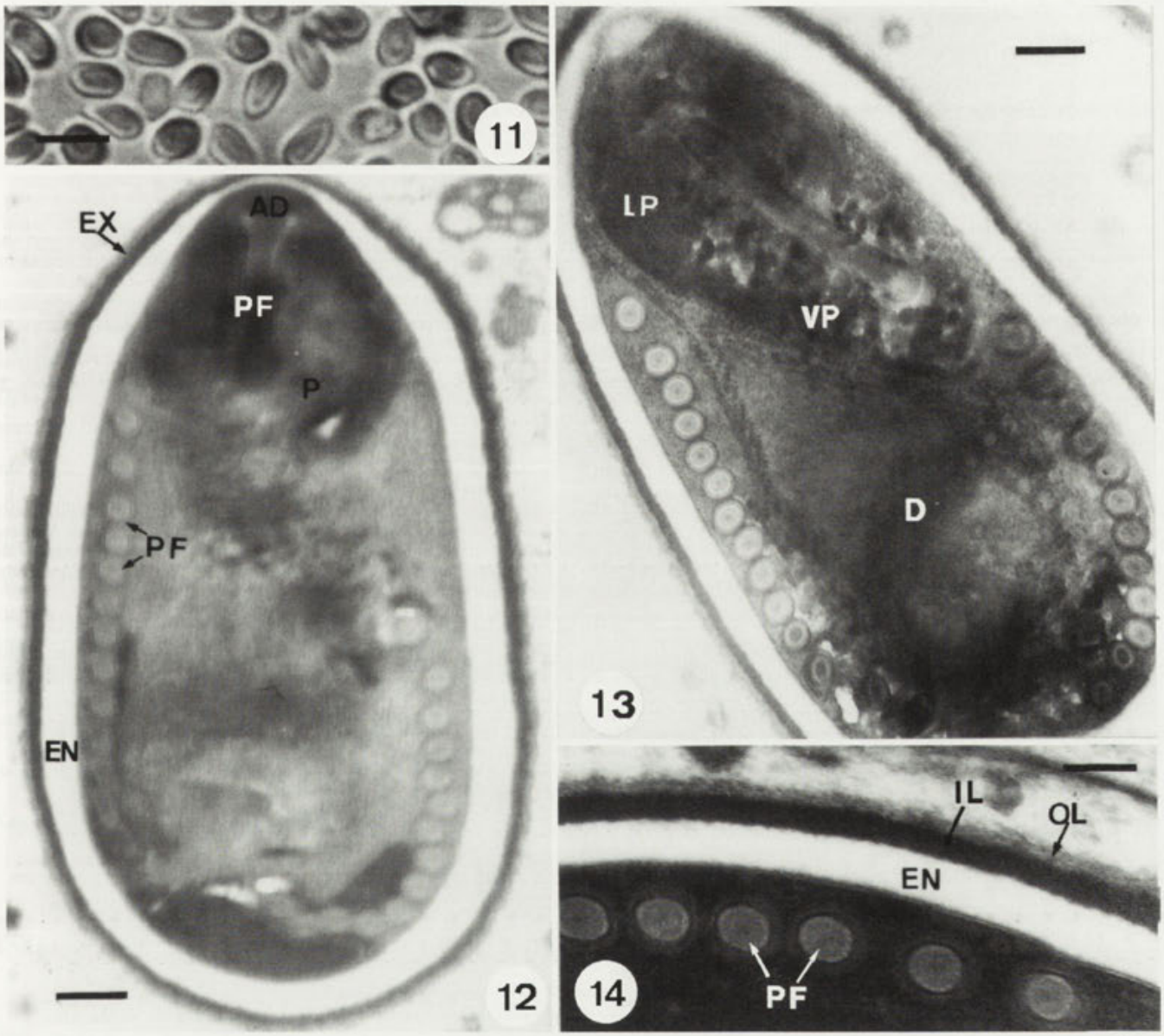

Figs. 1-2. Light microscopic appearance of *Nosema omaniae*. 1 - a sectioned fat body with numerous spores of microsporidium (Bars - 30m); 2 - fat body lobe with spores (Bars - 15 µm)

Figs. 3-4. Merogony. 3 - meront with one diplokaryon (Bar -1µm); 4 - dividing meront (curved arrows) showing two diplokarya (Bar - 1 µm)

Figs. 5-7. Sporogony. 5 - early sporont. The arrows indicate small dense vesicles on the outer surface of the envelope (Bar -1 µm); 6 - diplokaryotic sporont with a thick electron-dense envelope. Spindle plaques (arrowheads) are observed. In the nucleoplasm, chromosomes are present (Bar - 1 µm); 7 - onset of the binary fission (curved arrow) of the sporont with two diplokarya (Bar - 1 µm)

Figs. 8-14. Sporoblasts and spores. 8 - sporoblast with one diplokaryon showing an immature polar filament (Bar - 1 µm); 9 -detail of the wall of older sporoblast showing two layers: an inner electron-dense layer (IL) and an outer layer that is less dense (OL) (Bar - 0,4 µm); 10 - a young spore. It possesses an anchoring disc, an immature polar filament and a thin endospore (Bar - 1 µm); 11 - fresh spores (Bar - 5 µm); 12 - longitudinal section of a mature spore (Bar - 3 µm); 13 - longitudinal section of a mature spore showing the diplokaryon and the detail of the polaroplast (Bar - 3 µm); 14 - detail of the wall of mature spore (Bar - 1 µm)
Abbreviations: AD - anchoring disc, C - chromosomes, D - diplokaron, EN - endospore, ER - endoplasmic reticulum, ES - envelope of the sporont, EX - exospore, IFB - infected fat body, IL - innerelectron-dense layer, LP - lamella polaroplast, OL - outer layer that is less, P - polaroplast, PF - polar filament, VP - vesicular polaroplast

measure 2.8-3.3 x 1.9-2.2 µm. The meronts are uninucleate or binucleate and measure 2-5 µm. The sporonts are elongated and measure 3-4 µm (Lipa 1977, Sprague 1977). *Nosema graphosomae* was reported from *Graphosomae italicum*. Data concerning the infected tissues and the size of spores were not given (Lipa 1977). *Nosema leptocoris* parasitizes the midgut epithelium of *Leptocoris trivattus* of U.S.A. The meronts

measure 24 µm and 1 or 2 nuclei were seen (Sprague 1977). *Nosema nepae* parasitizes the midgut, the fat body and others tissues of *Nepa cinerae* in France and in Poland. The sporonts have a larger nuclei and darker cytoplasm. The spores are polymorphic, either piriform or elongated and measure 5-5.5 x 1.5 µm (Lipa 1977, Sprague 1977). *Nosema pyrrhocoridis* parasitizes the midgut, the Malpighian tubules, the fate body and the hemocytes of *Pyrrhocoris apterus*. The young schizonts are uninucleate and have 2-3 µm in diameter. The sporonts are elongated and their length is up to 8 µm. The spores are diplokaryotic and ovoid. Fixed, they measure 3.0-6.0 x 1.8-3.0 µm (Lipa 1977). *Nosema veliae* parasites *Velia currens* in France. It causes the formation of peri-intestinal cysts, then progressive and massive infection of fat cells and oenocytes, resulting in parasitic castration. The small schizonts measure 1.5 µm and the later larger schizonts measure 2-4 µm. The spores are polymorphic. Those seen at Banyuls (France) are curved and measure 5.5-7 x 3 µm. Those seen at Caen (France) are more regularly ovoid. The macrospore measure 9-11 µm in length (Sprague 1977).

None of these *Nosema* has been described by electron microscopy; it is not possible to compare their fine structural features. The *Nosema* species described here differs from these seven species by three fundamental characteristics: difference in its host organism; size of spores; the absence of monokaryotic stages. We believe that it is a new species and we propose the name *Nosema omaniae* derived from the generic name of its host.

REFERENCES

Colley F.C., Lie K.J., Zaman V., Canning E.U. (1975) Light and electron microscopical study of *Nosema eurytremae*. *J. Invertebr. Pathol.* **26:** 11-20

Lipa J. J. (1977) *Nosema pyrrhocoridis* n. sp., a new microsporidian parasite of red soldier bug (*Pyrrhocoris apterus* L.) (Heteroptera, Pyrrohocoridae). *Acta Protozool.* **16:** 135-140

Sprague V. (1977) Systematics of Microsporidia. In: Comparative Pathobiology. (Eds. L. A. Bulla. Jr., T. C. Cheng), New-York, **2:** 1-510

Sprague V. (1978) Characterization and composition of the genus *Nosema*. *Miscel. Publ. Entomol. Soc. Amer.* **11:** 5-16

Sprague V., Becnel J.J., Hazard E.I. (1992) Taxonomy of phylum microspora. *Critical Rev. Microbiol.* **18:** 285-395

Toguebaye B. S., Marchand B. (1984) Etude ultrastructurale des stades de développement et de la mitose sporogonique de *Nosema henosepilachnae* n. sp. (Microspora, Nosematidae) parasite de *Henosepilachna elaterii* (Rossi 1794) (Coleoptera, Coccinellidae). *Protistologica* **20:** 165-179

Vavra J., Canning E. U., Barker R. J., Desportes I. (1981) Characters of microsporidian genera. *Parasitology* **82:** 131-142

Youssef N. N., Hammond D. M. (1971) The fine structure of the developmental stages of microsporidian *Nosema apis* Zander. *Tissue & Cell* **3:** 283-294

Received on 6th June, 1994; accepted on 13th October, 1994

ACTA
PROTOZOOLOGICA

Acta Protozoologica (1995) 34: 67 - 70

Observations on Two New Myxosporidia (Myxozoa: Myxosporea) from Fishes of Bhery-fishery of West Bengal, India

Nirmal Kumar SARKAR

Department of Zoology, Rishi Bankim Chandra College, Naihati, West Bengal, India

Summary. Two new myxosporidia (Myxozoa: Myxosporea), *Myxobolus labeosus* sp. n. and *Zschokkella cascasiensis* sp. n. are described from the mesentery of *Labeo fimbriatus* and the gallbladder of *Sicamugil cascasia* respectively. The salient features of *Myxobolus labeosus* sp. n. are: small cysts in the mesentery;oval to egg-shaped asymmetrical spore, 8.0-10.0 x 6.5-9.0 µm; two unequal, broadly pyriform polar capsules opening convergedly on one side of the spore at truncate sutural surface, 6.0-6.5 x 2.0- 4.0 µm (large) and 3.5-4.5 x 1.8-2.5 µm (small) and of *Zschokkella cascasiensis* sp. n. are: disporous trophozoites; oval to ellipsoidal spore, 8.0-10.5 x 6.5-8.0 µm; two spherical polar capsules, 3.0-4.0 µm in diam.; coelozoic in the gallbladder.

Key words. Myxosporea, *Myxobolus labeosus* sp.n., mesentery, *Zschokkella cascasiensis* sp.n., gallbladder, Bhery-fishery.

INTRODUCTION

During the investigation of parasitic protozoa of Indian fish, two myxosporean parasites of the genera *Myxobolus* Bütschli, 1882 and *Zschokkella* Auerbach, 1910 (both cited from Lom and Noble 1984) were obtained from two host fish of Bhery-fishery from South 24-parganas, West Bengal, India.

MATERIALS AND METHODS

The host fish were obtained from the Bhery-fishery of South 24-parganas, West Bengal in frozen condition. All autopsies were done on frozen fish in the laboratory. Fresh preparations of parasites were studied from wet smears treated with Lugol's iodine (2%) and also from air-dried smears stained with Giemsa (1:20) after fixation in absolute methanol. Various concentrations of potassium hydroxide (2-10%) solution and saturated urea solution were tested for the extrusion of polar filament. The India-ink method (Lom and Vavra 1963) was employed to detect the presence of mucous envelope associated with the spore. All measurements were made in micrometers (µm). The figures were drawn with the aid of a camera lucida (Mirror type).

Address for correspondence: N. K. Sarkar, Department of Zoology, Rishi Bankim Chandra College, Naihati 743165, West Bengal, India

OBSERVATIONS

Myxobolus labeosus sp. n.

A few small cysts were found in the mesentery near the spleen. No developmental stage was observed in the ruptured cysts except the spores. The mature spores were oval to egg-shaped, asymmetric with rounded ends in valvular view (Figs. 1-5) and lenticular in sutural view (Fig. 6). A few symmetrical spores were also observed

(Fig. 8). The asymmetrical spores were obliquely truncated anterio-laterally which received the openings of both the polar capsules (Figs. 1, 3-5). The suture was broad but not ridged (Fig. 6). The shellvalves were smooth and moderately thick-walled. The two polar capsules were broadly pyriform, unequal in length and width, and maintained posteriorly a distance of about 45 to 90 degree angle between them. The two polar capsules opened very closely side by side at the truncate region of the spore. The two polar capsules never crossed each other. The polar filament of the larger and smaller capsules had five to seven and three to five transverse coils. The extruded polar filaments were unequal and fine, thread-like (Fig. 2). The finely granular binucleate sporoplasm in the form of a crescentic mass filled the extra-capsular cavity. There was no iodinophilous vacuole in the sporoplasm and no mucous envelope around the spores. Measurements (based on twenty fresh spores from one frozen fish; mean values are in parenthesis):

Spore: length - 8.0-10.0 (9.25); width - 6.5-9.0 (7.62)
Polar capsule (large): length - 6.0-6.5 (6.15); width - 2.0-4.0 (2.72)
Polar capsule (small): length - 3.0-4.5 (4.02); width - 1.8-2.5 (2.33)
Infection locus: mesentery associated with spleen
Incidence: 2/13 (15.4%)
Pathogenicity: not apparent
Host: *Labeo fimbriatus*
Period of infection: September to November, 1993
Locality: South 24-parganas, West Bengal, India
Material: syntypes on slide no. MzMxb. - 11, deposited in the Department of Zoology, R.B.C. College, Naihati, West Bengal, India

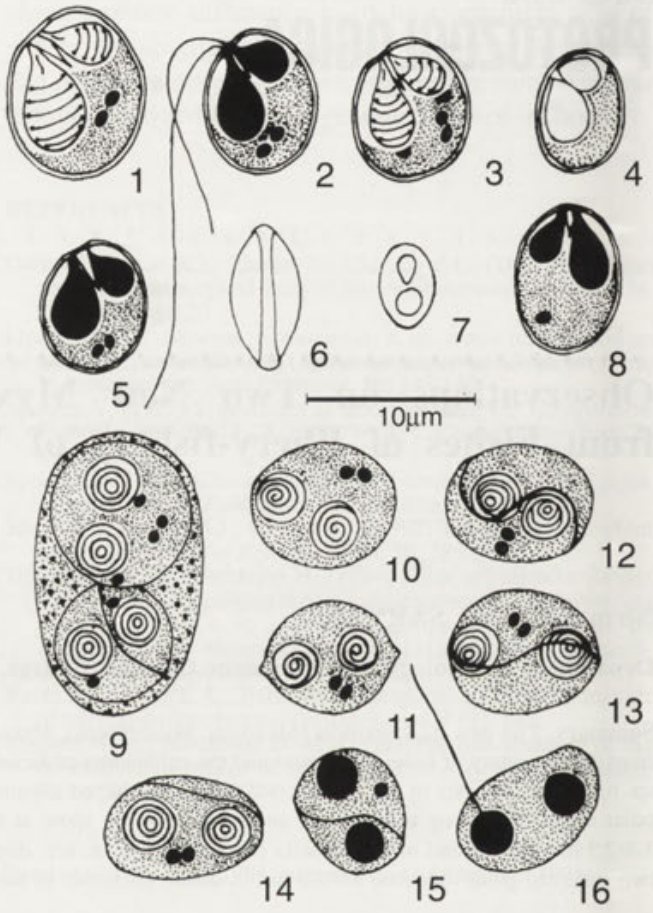

Figs. 1-8. Spores of *Myxobolus labeosus* sp. n.: 1 - fresh spore in valvular view; 2 - spore with extruded polar filaments; 3 - immature fresh spore in valvular view with capsulogenous nuclei; 4 - fresh spore in almost surface view; 5 - spore in valvular view; 6 - fresh spore in sutural view; 7 - fresh spore in top view; 8 - unusual spore in valvular view. 1, 3, 4, 6, 7 - Lugol's iodine; 2, 5, 8 - Giemsa.

Figs. 9-16. Plasmodium and spores of *Zschokkella* cascasiensis sp. n.: 9 - disporous plasmodium; 10-11 - fresh spores in valvular view; 12-14 - fresh spores in sutural view; 15 - spore in sutural view; 16 - spore with extruded polar filament (one). 9-14 - Lugol's iodine; 15-16 - Giemsa

Zschokkella cascasiensis sp. n.

The plasmodia were small, oval to ellipsoidal measuring 20.0 x 16.0 µm (largest). The spore producing plasmodia were disporous with occasional presence of unequal spores in these forms (Fig. 9). The mature spores were spherical to ellipsoidal with rounded ends (Figs. 10, 12-15), rarely with acuminate ends (Fig. 11). The two shellvalves were very thin-walled and smooth. The suture was thin, strongly S-shaped or elongately S-shaped or appeared straight under various views (Figs. 12-15). The two polar capsules were spherical and equal with three to four coils of the filament in each capsule. The extruded polar filament was thick and perpendicular to the axis of the spore (Fig. 16). The extra-capsular cavity was filled with a binucleate (or uninucleate) finely granular mass of sporoplasm. There was no iodinophilous vacuole in the sporoplasm and no mucous envelope around the spore. Measurements (based on twenty five fresh spores from one frozen fish; means are given in parenthesis):

Spore: length - 8.0-10.5 (9,54); width - 6.5-8.0 (7.48)
Polar capsule diameter: 3.0-4.0 (3.36)
Infection locus: gallbladder
Incidence: 2/12 (16.67%)

Pathogenicity: not apparent
Host: *Sicamugil cascasia* (Ham.)
Period of infection: January - February, 1993
Locality: South 24-parganas, West Bengal, India
Material: syntypes on slide No. MxZs - 6, deposited in the Department of Zoology, R. B. C. College, Naihati, West Bengal, India

DISCUSSION

The *Myxobolus* species described in the present study shows similar dimension to *Myxobolus crucifilus* (Qadri, 1962) Landsberg and Lom, 1991 and *M. seshadrii* Lalitha Kumari, 1968 (both of them recorded from *Labeo fimbriatus*). The asymmetrical spore and a pair of unequal polar capsules of the first species are different from the symmetrical spore and equal polar capsules of the last two species. Among other *Myxobolus* spp., the spore of *Myxobolus asymmetricus* (Parisi, 1912) Landsberg and Lom, 1991 agrees with the present species in having an asymmetrical spore. However, the two polar capsules of *M. asymmetricus* are parallel contrary to the strongly converging polar capsules of the present species. Moreover, the surface at which the two polar capsules of *M. asymmetricus* open is round, while the surface is truncate in the myxosporean spore of this study. The present *Myxobolus* species also resembles *M. artus* Akhmerov, 1960 (cited from Shulman 1966) in shape. However, the anterior openings of the two polar capsules, a few posterior sutural folds and the shape (equilateral triangle) of the sporoplasm of the latter species are different from the anterio-lateral openings of the two unequal polar capsules, absence of any sutural fold, almost crescent-like sporoplasm and absence of the iodinophilous vacuole in the former myxosporean species. *Myxobolus transovalis* Gurley, 1893 and *M. orbiculatus* Kudo, 1919 also show similarities with the present species in the shape of the spores. The spore of *M. transovalis* is much smaller (6.0-7.0 µm in length) and its spore has two equal polar capsules. The spore of *M. orbiculatus* is narrower (6.5-7.0 µm) and has two equal polar capsules which differentiate the present species from *M. orbiculatus*. Furthermore, *M. mesentericus* Kudo, 1919 and *M. anili* Sarkar, 1989 which have a similar infection locus and thus demands comparison with the present *Myxobolus* species. The spores of *M. mesentericus* and *M. anili* have different shape, larger dimensions (10.0-11.5 x 8.5-9.5 µm and 10.74 x 8.69 µm respectively) and equal, pyriform and smaller polar capsules (4.75 x 1.5-2.0 µm and 4.82 x 3.03 µm respectively) which are dissimilar to the present species. Taking into account these differences with the related species, the present myxosporean species is considered as a new species and designated as *Myxobolus labeosus* sp. n. after the name of its host.

The other species of the present study has a disporous plasmodium, rounded ends of the spore both in valvular and sutural views, spherical polar capsules and extruded polar filament perpendicular to the axis of the spore, which warrant its inclusion in the genus *Zschokkella* Auerbach, 1910. This species resembles either in shape or size *Zschokkella nova* Klokacewa, 1914 (cited from Kudo, 1919), *Z. globulosa* Davis, 1917, *Z. parasiluri* Fujita, 1927 (cited from Shulman 1966), *Z. fossilae* Chakravarty, 1943, *L. ilishae* Chakravarty, 1943, *Z. labeonis* Lalitha Kumari, 1969, *Z. embiotocidis* Moser and Haldorson, 1976, *Z. kudoi* Moser and Noble, 1977, *Z. mugili* Chen and Hsieh, 1984, *Z. chunshanensis* Chen and Hsieh, 1984, *Z. yangkiangensis* Chen and Hsieh, 1984, *Z. platistomusi* Sarkar, 1987, *Z. gobidiensis* Sarkar and Ghosh, 1991 and *Z. glossogobi* Kalavati and Vaidehi 1991, Among these *Zschokkella* spp., spores of *Z. labeonis, Z. kudoi, Z. mugili* and *Z. chunshanensis* have striated shellvalves and are, therefore, different from the present species which has smooth shellvalves. Moreover, the spore of *Z. labeonis* has one end round and the other end pointed and the extruded polar filament is parallel to its longitudinal axis while the spore of the present species usually has rounded ends and the extruded polar filament is perpendicular to its longitudinal axis. The spore of *Z. kudoi* is much larger (12.0-17.0 x 7.0-11.0 µm) and its sutural line does not extend end to end while the spore of the present myxosporean has smaller dimension and its sutural line extends end to end. The spore of *Z. mugili* is constricted in the middle which is not found in the spore of the present species. The spore of *Z. chungshanensis* is narrower (6.0 µm in width) than the spore of the present species. Of the other *Zschokkella* spp., faint striations are present on the shellvalves of *Z. nova* and *Z. ilishae*. Moreover, the spore of *Z. nova* has a constriction in the middle, slightly larger but narrower in dimension (8.0-12.0 x 5.0-7.0 µm) than the present species while *Z. ilishae* has a disc-shaped plasmodium and a larger but narrower spore (12.36 x 6.18 µm) and larger polar capsule (4.26 µm in diameter) in addition to the different shape of the spore. Besids, the spore of *Z. parasiluri* (11.0-15.0 µm), *Z. yangkiangensis* (12.0-14.0 x 8.4-10.8 µm), *L. gobidiensis* (10.0-13.5 x 6.0-9.0 µm) and *Z. platistomusi* (10.5-12.5 µm) have larger dimensions than the spore of the myxosporean in study. Moreover, *Z. parasiluri* is polysporous, *Z.*

yangkiangensis has fusiform spore, *L. gobidiensis* has spore with thick suture and *Z. platistomusi* has dumbbell-shaped to fusiform spore while the present species is disporous and its spore is spherical to ellipsoidal with thin sutural line. Of the other above mentioned species, *Z. globulosa, Z. fossilae* and *Z. embitocidis* more closely resemble the present species in having a disporous plasmodium and S-shaped suture of the spores. The spore of *Z. embiotocidis* however, is much larger (13.0-17.0 µm x 9.5-13.0 µm) and possesses pyriform polar capsules which are different from the smaller dimension of spore and the spherical polar capsule of the present species. The spores of *Z. globulosa, Z. fossilae* and *Z. glossogobi* show almost similar mensural data of spores of the present myxosporean. But the flattened capsular side of the spore, twisted suture on the longitudinal axis and smaller polar capsule (3.0 µm in diameter) of *Z. globulosa* are different from the present myxozoan. Similarly, the semicircular, narrow spore (4.12-5.18 µm) of *Z. fossilae* is different from the oval to ellipsoidal, wider spore of the present species. The spore of *Z. glossogobi* is rectangular. Its thick-walled shellvalves and smaller polar capsules (1.4-2.4 µm in diameter) are distinct from the present myxosporean in study. Considering the differences with the related *Zschokkella* spp., the present myxozoan is recorded as a new species and designated as *Zschokkella cascasiensis* sp. n. after the name of its host.

Acknowledgements. Sincere thanks are expressed to Dr. A. K. Roy, Teacher-in-Charge of this College and Prof. A. K. Pramanik, Head of the Department of Zoology of this College for providing laboratory facilities.

REFERENCES

Akhmerov A. K. (1960) Myxosporidia of fishes of the Amur River Basin. *Ryb. Koz. Ven.* **5:** 239-308 (In Russian)

Auerbach M. (1910) Die Cnidosporidien (Myxosporidien, Actinomyxidien, Microsporidien), Eine monographische Studie. Verlag von Dr. Werner Klinkhardt, Leipzig

Bütschli O. (1882) Myxosporidia. In: Protozoa (Ed. H.G. Bronn) *Klassen und Ordung des Thiers-Reiches*, **1:** 590-603

Chakravarty M. (1943) Studies on Myxosporidia from the common food fishes of Bengal. *Proc. Indian Acad, Sci.* **18B:** 21-35

Chen C.-L., Hsieh S.-R. (1984) New Myxosporidia from fresh water fishes of China. Ed. by Institute of Hydrobiology, Acad. Sin. Beijing 99-104

Davis H. S. (1917) Myxosporidia of the Beaufort region. A systematic and biologic study. *Bull. Bur. Fish.* **35:** 201-243

Fujita T. (1927) Studies on Myxosporidia of Japan. 5. On myxosporidia in fishes of Lake Biwa. *J. Coll. Agric. Hokkaido Imp. Univ.* **16:** 229-247

Gurley H. R. (1893) On the classification of Myxosporidia, a group of Protozoan parasites infecting fishes. *Bull. US Fish. Comm.* **11:** 407-420

Kalavati C., Vaidehi J. (1991) Two new species of Myxosporidians from fishes of Chilka Lake: Genus *Sphaeromyxa* Thelohan and *Zschokkella* Auerbach Uttar Pradesh *J. Zool.* **11:** 146-150

Klokacewa S. (1914) Uber die Myxosporidien der karausche. *Zool. Anz.* **44:** 182-186

Kudo R. (1919) Studies on Myxosporidia. A synopsis of genera and species of myxosporidia. *Ill. Biol. Monogr.* **5:** 1-265

Lalitha Kumari P. S. (1968) On a new species (Protozoa: Myxosporidia) from an Indian freshwater fish *Labeo fimbriatus*. *Riv. Parasitol.* **29:** 161-164

Lalitha Kumari P. S. (1969) Studies on parasitic protozoa (Myxosporidia) of freshwater fishes of Andhra Pradesh, India. *Riv. Parasitol.* **30:** 153-226

Landsberg J. H., Lom J. (1991) Taxonomy of the genera of *Myxobolus/Myxosoma* group (Myxobolidae: Myxosporea), current listing of species and revision of synonyms. *Syst. Parasitol.* **18:** 165-186

Lom J., Noble E. R. (1984) Revised classification of the class Myxosporea Bütschli 1881. *Folia Parasitol.* **31:** 193-205

Lom J., Vavra J. (1963) Mucous envelope of spores of the subphylum Cnidospora (Doflein, 1901). *Vest. Cs. Spol. Zool.* **27:** 4-6

Moser M., Haldorson L. (1976) *Zschokkella embiotocidis* sp. n. (Protozoa, Myxosporida) from California pile perch *Damalichthys vacca* and striped perch *Embiotoca lateralis*. *Can. J. Zool.* **54:** 1403-1405

Moser M., Noble E. R. (1977) *Zschokkella* (Protozoa: Myxosporida) in Macrourid fishes. *Int. J. Parasitol.* **7:** 97-100

Parisi B. (1912) Primo contributo alla distribuzione geografica dei missosporidi in Italia. *Al. Soc. Ital. Sci. Nat.* **50:** 183-291

Qadri S. S. (1962) New myxosporidia from Indian freshwater fish *Labeo fimbriatus* I. *Gyrospora crucifila* gen. n., sp. n. *Z. Parasitkd.* **21:** 513-516

Sarkar N. K. (1987) Studies on Myxosporidian parasites (Myxozoa: Myxosporea) from marine fishes in West Bengal, India. II. Description of two new species from *Tachysurus platystomus* (Day). *Arch. Protistenkd.* **133:** 151-155

Sarkar N. K. (1989) *Myxobolus anili* sp. n. (Myxozoa: Myxosporea) from a marine teleost *Rhinomugil corsula* Hamilton. *Proc. Zool. Soc. Calcutta.* **42:** 71-74

Sarkar N. K., Ghosh S. (1991) Two new Myxosporidia (Myxozoa: Myxosporea) from fresh water fishes of West Bengal, India. *Uttar Pradesh J. Zool.* **11:** 54-58

Shulman S. S. (1966) Myxosporidian fauna o f the U S S R. Nauka, Moscow, Leningrad. (English translation)

Received on 6th June, 1994; accepted on 3rd November, 1994

ACTA
PROTOZOOLOGICA

Acta Protozoologica (1995) 34: 71 -73

Taxonomic Revision of some Cephaline Gregarines (Apicomplexa: Eugregarinida) Recorded from Odonate Insects (Arthropoda)

Nirmal Kumar SARKAR

Department of Zoology, Rishi Bankim Chandra College, Naihati, West Bengal, India

Summary. Based on author's own observations and on literature, the genus *Menospora* Léger, 1892 is emended, and the genus *Levineia* Kori and Amoji, 1986 is proposed to be a junior synonym of *Menospora* Léger, 1892. Two new genera *Rodgiella* gen.n. and *Hoshideia* gen.n. are also proposed to accommodate *Ancyrophora ceriagrioni* Nazeer Ahamed and Narasimhamurti, 1979 and *Odonaticola polyhamatus* (K. Hoshide, 1977) Amoji and Kori, 1992.

Key words. Revision, *Menospora* emend. n., *Rodgiella* gen. n., *Hoshideia* gen. n., Odonata, Zygoptera.

Menospora Léger, 1892 emend.n.

Léger (1892) instituted the genus *Menospora* to accommodate a cephaline gregarine *Menospora polyacantha* from the midgut of the larvae of *Agrion puella*. Later, *M. polyacantha* has been recorded from several odonates (Geus 1969) without the description of its oocyst. The diagnostic features of the genus *Menospora* as recorded by Léger (1892) are as follows: (1) epimerite a large cup bordered with hooks (2) long neck (3) sporadin solitary (4) dehiscence of gametocyst by simple rupture (5) oocyst smooth, crescentic.

Type species: *Menospora polyacantha*

Recently, Sarkar and Haldar (1980) 1982 described two new species of *Menospora* Léger, 1892 namely *M. enallagmae* and *M. coenagrii* having exactly similar features of *Menospora* Léger except the shape of the oocyst which is cylindro-biconical without emending the generic character like oocyst smooth, crescentic or cylindro-biconical. Later, Kori and Amoji (1986) created a new genus *Levineia* with its type species *Levineia agriocnema* and suggested the following diagnostic characters for *Levineia*: (1) epimerite cup-like with many peripheral sucker-tipped digitate processes (2) neck short (3) sporadin solitary (4) gametocyst dehisces by simple rupture (5) oocyst cylindro-biconical.

The reexamination of the diagnostic features of the two genera *Menospora* Léger and *Levineia* Kori and Amoji, 1986, reveals the only difference in the shape of the oocyst. I, therefore, propose emendation of the generic character of *Menospora* Léger i.e. oocyst smooth, crescentic or cylindro-biconical. This amendment is also expressed by Théodorids (1993, personal communication). This emendation leads to the perfect taxonomic placement of *M. enallagmae* and *M. coenagrii* and removes the unnecessary creation of new genus. As a result, *Levineia* Kori

Address for correspondence: N. K. Sarkar, Department of Zoology, Rishi Bankim Chandra College, Naihati 743165, West Bengal, India

and Amoji, 1986 becomes junior synonym of *Menospora* Léger, 1892 and the genus *Menospora* Léger is now consisting of the following species:

(1) *Menospora polyacantha* Léger, 1892
(2) *M. enallagmae* Sarkar and Haldar, (1980) 1982
(3) *M. coenagrii* Sarkar and Haldar, (1980) 1982
(4) *M. agriocnema* (Kori and Amoji, 1986) nov. comb.
(5) *M. gulbargaensis* (Amoji and Kori, 1991) nov. comb.

Diagnosis: *Menospora* Léger, 1892 emend. n.

Synonym: *Levineia* Kori and Amoji, 1986

Epimerite a large cup or bell bordered with many recurvate digitate processes; neck long or short; sporadin solitary; gametocyst dehisces by simple rupture; oocyst smooth, crescentic or cylindro-biconical; gut parasites of Damsel fly (Odonata: Zygoptera).

Type species: *Menospora polyacantha* Léger, 1892

Type host: larva of *Agrion puella* (Odonata: Zygoptera). The genus includes five species.

***Rodgiella* gen. n.**

Nazeer Ahamed and Narasimhamurti (1979) described a cephaline gregarine *Ancyrophora ceriagrioni* from the midgut of a zygopteran odonate *Ceriagrion coromandelianum* (Fabr.). The epimerite of this species is a shallow cup placed directly on the sumit of the protomerite. Its margin is provided with many inwardly directed digitate processes (discoid or globular epimerite with digitate processes in *Ancyrophora* Léger, 1892) which is slightly similar with the epimerite of *Menospora* Léger, 1892. Further, the oocyst of this species is biconical with two spines at each pole and four equatorial spines two on each side of the oocyst (six uniformly distributed equatorial spines in *Ancyrophora* Léger, 1892 and smooth oocyst in *Menospora* Léger, 1892). Thus, this oocyst is unlike of *Ancyrophora* or *Menospora*. Therefore, a new genus *Rodgiella* gen. n. (after the name of Prof. Rodgi of Gulbarga University) is proposed to accommodate this cephaline gregarine and designated as *Rodgiella ceriagrioni* (Nazeer Ahamed and Narasimhamurti, 1979) nom. n.

Diagnosis: *Rodgiella* gen. n.

Epimerite a shallow cup; its margin produced into many inwardly directed digitate processes; sessile; sporadin solitary; gametocyst dehisces by simple rupture; oocyst biconical with two pairs of polar spines and two pairs of equatorial spines - one pair on each side; gut parasite of Damsel fly (Odonata: Zygoptera).

Type species: *Rodgiella ceriagrioni* (Nazeer Ahamed and Narasimhamurti, 1979)

Type host: *Ceriagrion coromandelianum* (Fabr.) (Odonata: Zygoptera). It includes one species.

***Hoshideia* gen. n.**

Hoshide (1977) described a cephaline gregarine *Hoplorhynchus polyhamatus* from the midgut of an odonate *Munais strigata* Selys. While reviewing the genus *Odonaticola* Sarkar and Haldar, 1981, Amoji and Kori (1992) transferred *H. polyhamatus* to the genus *Odonaticola* Sarkar and Haldar, 1981. However, reexamination of the original description and illustrations reveal that the epimerite of *H. polyhamatus* is a crown being placed on a very short neck. The crown is crenelated below in the form of calyx and a short, upwardly directed digitate part instead of inverted cup with petaloid spines of *Odonaticola*. Moreover, the oocyst of *H. polyhamatus* is tetrahedral in nature instead of boat-shaped oocyst in *Odonaticola* and biconical in *Hoplorhynchus*. *H. polyhamatus* is, therefore, neither a member of *Odonaticola* nor a member of *Hoplorhynchus* Carus, 1863. I, therefore, propose a new genus *Hoshideia* gen. n. to accommodate this species as *Hoshideia polyhamatus* (K. Hoshide, 1977) nom. n. The name of the genus is derived from the name of Dr. H. Hoshide.

Diagnosis: *Hoshideia* gen. n.

Epimerite a complex crown consisting of upwardly directed digitate part and crenelated posterior part in the form of many calyx; sporadin solitary; gametocyst dehisces by simple rupture; oocyst tetrahedral; gut parasite of Damsel fly (Odonata: Zygoptera).

Type species: *Hoshideia polyhamatus* (K. Hoshide, 1977)

Type host: *Munais strigata* Selys (Odonata: Zygoptera). It includes one species.

REFERENCES

Amoji S. D., Kori S. S. (1991) *Levineia gulbargaensis* sp. nov. a new actinocephalid gregarine parasite of an odonate insect. *Ind. Zool.* **15:** 41-44

Amoji S. D., Kori S. S.(1992) Revision of the genus *Odonaticola* Sarkar and Haldar, 1981 (Apicomplexa: Sporozoasida: Gregarinasina). *Acta Protozool.* **31:** 169-171

Carus J. V. (1863) Protozoa. In: Handbuch der Zoologie (Eds. W. Ch. Peters, J. V. Carus, A. Gerstaeker), **2:** 1-421

Geus A. (1969) Sporentierchen, Sporozoa. Die Gregarinida der land- und susswasserbewohnenden Arthropoden Mitteleuropas. In: Die Tierwelt Deutschlands und der angrenzenden Meeresteile nach ihren Merkmalen und nach ihrer Lebensweise, Teil 57, (Eds. F. Dahl, M. Dahl, F. Peus) Fisher, Jena

Hoshide K. (1977) Notes on the gregarines in Japan. VIII. Three new species of eugregarines from Odonata. *Bull. Fac. Educ. Yamaguchi Univ.* **27:** 33-125

Kori S. S., Amoji S. D. (1986) An actinicephalid gregarine *Levineia agriocnema* n. gen. n. sp. from an odonate insect, *Agriocnemis pygmaea* (Rambur). *Riv. Parasitol.* **47:** 343-347

Léger L. (1892) Recherches sur les grégarines. *Tabl. Zool.* **3:** 1-183

Nazeer Ahamed S., Narasimhamurti C. C. (1979) Two new septate gregarines *Dendrorhynchus keilini* sp. n. and *Ancyrophora ceriagrioni* sp. n. from the midgut of the Damsel fly *Ceriagrion coromandelianum* (Fabr.). *Acta Protozool.* **18:** 441-450

Sarkar N. K., Haldar D. P.(1981) Observations on four new species of actinocephalid gregarines (Protozoa: Sporozoea) under a new genus *Odonaticola* from odonate insects. *Arch. Protistenkd.* **124:** 288-302

Sarkar N. K., Haldar D. P. (1980, 1982) Observations on two new species of cephaline gregarines (Protozoa: Sporozoa) from odonates in West Bengal. *Proc. Zool. Soc., Calcutta.* **33:** 17-27

Received on 4th May, 1994; accepted on 13th October, 1994

INSTRUCTIONS FOR AUTHORS

ACTA PROTOZOOLOGICA publishes original papers embodying the results of experimental or theoretical research in all fields of protistology, with the exception of faunistic notices of local character and purely clinical reports. Short (rapid) communications are acceptable as long review articles. The papers should be as concise as possible, be written in English. Submission of a manuscript to ACTA PROTOZOOLOGICA implies that it has not been submitted for publication elsewhere and that it contains unpublished, new information. There are no page charges. Authors should submit papers to:

Miss Małgorzata Woronowicz
Managing Editor of ACTA PROTOZOOLOGICA
Nencki Institute of Experimental Biology,
ul. Pasteura 3
02-093 Warszawa, Poland
Fax: (48) 22 225342

Organization of Manuscripts

Submissions

Please enclose three copies of the text, one set of original line drawings (without lettering!) and three sets of copies with lettering, four sets of photographs (one without lettering). In the case of photographs arranged in plate form, please submit one set of original photographs unmounted and without lettering, and three sets of plates with lettering.

ACTA PROTOZOOLOGICA prefers to use the author's word-processor disk copy (3.5"and 5.25" format IBM or IBM compatible, and MacIntosh 6 or 7 system on 3.5" 1.44 MB disk only) of manuscripts instead of rekeying articles. If available, please send a copy of the disk with your manuscript. Disks will be returned with galley proof of accepted article at the same time. Please observe the following instructions:

1. Label the disk with your name: the word processor/computer used, e.g. IBM; the printer used, e.g. Laserwriter; the name of the program, e.g. Wordperfect 5.1; and any special characters used, and how you obtained them (i.e. dedicated key pressed or printer control codes used directly).
2. Send the manuscript as a single file; do not split it into smaller files.
3. Give the file a name which is no longer than 8 characters.
4. Create and /or edit your manuscript, using the document mode (or equivalent) in the word-processor program.
5. If necessary, use only italic, bold, underline, subscript and superscript. Multiple font, style or ruler changes, or graphics inserted the text, reduce the usefulness of the disc.
6. Do not right-justify and use a hyphen at the end of the line.
7. Avoid the use of footnotes.
8. Distinguish the numerals 0 and 1 from the letters O and l.

Text (three copies)

The text must be typewritten, doublespaced, with numbered pages. The manuscript should be organized into Summary, Introduction, Materials and Methods, Results, Discussion, Acknowledgments, References, Tables and Figure Legends. The Title Page should include the full title of the article, first name(s) in full and surname(s) of author(s), the address(es) where the work was carried out, page heading of up to 40 characters, and up to 6 Key Words. The present address for correspondence, telephone, FAX, and E-mail numbers should also be given.

Each table must be on a separate page. Figure legends must be in a single series at the end of the manuscript. References must be listed alphabetically, abbreviated according to the World List of Scientific Periodicals, 4th ed. (1963). Nomenclature of genera and species names must agree with the International Code of Zoological Nomenclature, third edition, London (1985) or International Code of Botanical Nomenclature, adopted by XIV International Botanical Congress, Berlin, 1987. SI units are preferred.

Examples for bibliographic arrangement of references:

Journals:

Häder D-P., Reinecke E. (1991) Phototactic and polarotactic responses of the photosynthetic flagellate, *Euglena gracilis. Acta Protozool.* **30:** 13-18

Books:

Wichterman R. (1986) The Biology of Paramecium. 2 ed. Plenum Press, New York

Articles from books:

Allen R. D. (1988) Cytology. In: Paramecium, (Ed. H.-D. Görtz). Springer-Verlag, Berlin, 4-40

Zeuthen E., Rasmussen L. (1972) Synchronized cell division in protozoa. In: Research in Protozoology, (Ed. T.T. Chen). Pergamon Press, Oxford, **4:** 9-145

Illustrations

All line drawings and photographs should be labelled with the first author's name written on the back. Figures should be numbered in the text as arabic numerals (e.g. Fig. 1). Illustrations must fit within either one column (86 x 231 mm) or the full width and length of the page (177 x 231 mm). Figures and legends should fit on the same page. Lettering will be inserted by the printers and should be indicated on a tracing-paper overlay or duplicate copy.

Line drawings (three copies + one copy without lettering)

Line drawings should preferably be drawn about twice as large as the desired final size, and be suitable for reproduction in the form of well-defined line drawings and should have a white background. Avoid fine stippling or shading. Computer printouts of laser printer quality may be accepted, however *.TIF, *.PCX, *.BMP graphic formats on disk are preferred.

Photographs (three copies + one copy without lettering)

Photographs at final size should be sharp, gloss finished, bromide prints. Photographs grouped as plates (in size not exceeding 177 x 231 mm including legend) must be trimmed at right angles accurately with edges touching and mounted on firm board. The engraver will then cut a fine line of separation between figures. Magnification should be indicated. There is a page charge for colour illustration.

Proof sheets and offprints

Authors will receive one set of page proofs for correction and are asked to return these to the Editor within 48-hours. Fifty reprints will be furnished free of charge. Orders for additional reprints must be submitted with the proofs.

Indexed in Current Contents in CABS, Chemical Abstracts Service and in Protozoological Abstracts.

ACTA
PROTOZOOLOGICA

REVIEW ARTICLE

S. Fabczak and H. Fabczak: Phototransduction in *Blepharisma* and *Stentor* 1

ORIGINAL ARTICLES

S. Gerber and D.-P. Häder: Effects of artificial UV-B and simulated solar radiation on the flagellate *Euglena gracilis*: physiological, spectroscopical and biochemical investigations 13

W. Foissner and I. Foissner: Fine structure and systematic position of *Enchelyomorpha vermicularis* (Smith, 1899) Kahl, 1930, an anaerobic ciliate (Protozoa, Ciliophora) from domestic sewage 21

D. L. Lipscomb and G. P. Riordan: Ultrastructural examination of virus-like particles in a marine rhizopod (Sarcodina, Protista) 35

J. I. R. Larsson: A light microscopic and ultrastructural study of *Gurleya legeri* sensu Mackinnon (1911) - with establishment of the new species *Gurleya dorisae* sp. n. (Microspora, Gurleyidae) 45

S. J. Upton, C. T. McAllister and C. M. Garrett: New species od Eimeria (Apicomplexa) from captive wood turtles, *Clemmys insculpta* (Testudines: Emydidae), from the Dallas Zoo 57

K. Diarra and B. S. Toguebaye: Ultrastructural study of *Nosema omaniae* sp. n. (Microspora, Nosematidae) parasite of *Omania coleoptrata* (Heteroptera, Omaniidae) 61

N. K. Sarkar: Observations on two new Myxosporidia (Myxozoa: Myxosporea) from fishes of Bhery-fishery of West Bengal, India 67

N. K. Sarkar: Taxonomic revision of some cephaline Gregarines (Apicomplexa: Eugregarinida) recorded from odonate insects (Arthropoda) 71

1995 FEBRUARY
VOLUME 34 NUMBER 1